Biological fabrication of silica-based hybrid materials using silica-polymerizing enzymes

A dissertation submitted in partial fulfillment of the requirements

for the degree of Doctorate of Engineering

By

MAHEEM BANADARA MUDIYANSELAGE

KASUN SHAMEERA GODIGAMUWA

Laboratory of Biotechnology for Resources Engineering,

Division of Sustainable Resources Engineering,

Graduate School of Engineering,

Hokkaido University, Japan

September 2021

ACKNOWLEDGEMENT

Undertaking the doctoral course at the Graduate School of Engineering, Hokkaido University has been an amazing life-changing experience for me. It would not have been possible to complete successfully without the guidance and assistance that received from loving people around me.

First, I would like to express my greatest gratitude to my supervisor Associate Professor, Kazunori Nakashima for his continuous guidance and motivation during the three years of the study period. This thesis would not have been made possible without his excellent guidance and precious suggestions. He provided immense supervision and guided me in the proper direction. Moreover, I would like to extend my gratitude to Professor, Satoru Kawasaki for offering useful suggestions, encouragement, and support during the entire study period. Additionally, my thank goes to Mrs. Hitomi Tada for her friendly cooperation and support throughout this period.

My dreams became true when I received the acceptance from Graduate School of Engineering, Hokkaido University. Therefore, I am very grateful to the English Engineering Education Program (e3) provided by Hokkaido University and the financial support from Uehara Memorial Foundation for making it all possible to study in Japan.

My deepest appreciation goes to my master course supervisor Professor, Namal Priyantha, Department of Chemistry, University of Peradeniya, Sri Lanka for the encouragement to study abroad and for pushing me for the correct path.

I am indebted to all my friends who study and studied with me in the Laboratory of Biotechnology for Resources Engineering, Division of Sustainable Resources

Engineering, Hokkaido University, for their kind help always given to me throughout the past three years. A very special thank you to Mr. Junnosuke Okamoto and Mr. Sota Tsujitani for helping me to get stabilized in Sapporo and in the laboratory. During these years, their help given to me and effort to translate Japanese to English or English to Japanese are priceless.

I would like to extend my deepest appreciation to my loving parents, my brother, and my sister for always believing in me, love, support and encouragement to follow my dreams. Finally, to Rishni Masimbula, my loving wife who has been by my side always, and without her, I could not be able to achieve success on this journey in the first place.

DECLARATION

I do hereby clear that the work reported in this project thesis was extensively carried out by me under the supervision of Associate Professor, Kazunori Nakashima. It describes the results of my own independent research except where due reference has been made in the text. No part of this project thesis has been submitted earlier or concurrently for the same or any other degree.

Date: 2021/08/23 Name: M. B. M. K. S. Godigamuwa

TABLE OF CONTENTS

LIST OF FIGURES

LIST OF TABLES

LIST OF ABBRIVIATIONS

B. circulans	*Bacillus circulans*
CBM	Carbohydrate-binding module
ChBD	Chitin-binding domain
EDS	Energy-dispersive X-ray spectroscopy
E. coli	*Escherichia coli*
HRP	Horseradish peroxidase
IPTG	Isopropyl β-D-1-thiogalactopyranoside
LB	Luria broth
NMWCO	Nominal molecular weight cut-off
PCR	Polymerase chain reaction
P. syringae	*Pseudomonas syringae*
SDS-PAGE	Sodium dodecyl sulfate-polyacrylamide gel electrophoresis
SEM	Scanning electron microscope
Sil	Silicatein
S. domuncula	*Suberites domuncula*
TBP	Titania-binding peptides
TEOS	Tetraethyl orthosilicate

CHAPTER 1

GENERAL INTRODUCTION

1.1. Background

Inorganic-organic hybrid materials are used as an excellent candidate for the development of functional and advanced materials in electronics, energy generation, water treatment and biomedical applications[1–3]. Various studies are being focused on the enhancement of properties of those hybrid materials. Among them, the incorporation of biomolecules such as live cells, drugs, and enzymes to produce smart and sophisticated materials is an attractive idea[4–6]. However, conventional methods used for synthesizing and coating inorganic polymers, such as silica, require harsh conditions such as high temperatures, extreme pH conditions, vacuum conditions, and caustic chemicals that are incompatible with biomolecules[7]. With those aspects, it becomes difficult to fabricate biomolecules entrapped inorganic-organic hybrid materials using conventional methods. Therefore, biomimetic approaches have been studied for synthesizing of inorganic polymers[8, 9].

Silica is used as an inorganic matrix in hybrid materials due to its chemical and physical stability, biocompatibility, and nontoxicity[10]. As a biological route to fabricate silica, different types of enzymes and peptides that can catalyze silica polymerization have been studied. Silicatein is an enzyme found in sponges that can catalyze silica polymerization under physiological conditions[11]. However, silicateins show aggregation properties in aqueous media which makes them difficult to handle in applications. This aggregation property could be solved by fusing a soluble protein tag.

To form silica on an organic matrix, silicatein should be immobilized on the organic matrix. In some studies, silicatein has been immobilized on materials by doing surface

modifications such as applying chemicals on solid surfaces[12]. However, the silica polymerizing activity of silicatein was significantly lost upon contact with the solid surface[13]. Simpler and milder alternative methods to immobilize silicatein without direct surface contact are important to preserve the silica polymerization activity of silicatein. Solid binding proteins are such smart tools found from the studies related to degradation enzymes. Enzyme fused with solid binding proteins can selectively bind on a target material. The same strategy can be used to immobilize silicatein on a target material by fusing silicatein with a solid binding protein.

In this study, the fabrication of silica-based biohybrid materials in physiological conditions using novel interfacial catalysts composed of silicatein, soluble proteins, and solid-binding proteins has been studied. Using the developed novel interfacial catalyst, a model enzyme has been successfully immobilized in the inorganic-organic hybrid material while protecting its activity.

1.2. Literature review

1.2.1. Inorganic-organic hybrid materials

Scientists are paying attention to inorganic-organic hybrid materials due to their predominant properties such as physical, optical, mechanical, biological, and chemical properties. Before man-made hybrid materials are made, nature has already created remarkable inorganic-organic hybrid materials with sophisticated properties million years ago[1, 14]. Such a high level of naturally available examples are hydroxyapatite ($Ca_{10}(PO_4)_6(OH)_2$) in bones and teeth of mammals[15], calcium carbonate ($CaCO_3$) in molluscan shells[16], amorphous silica (SiO_2) in diatoms[17] and marine sponges[18], and magnetite (Fe_3O_4) in chiton teeth[19].

Depending upon the interaction between organic and inorganic materials, inorganic-organic hybrid materials are classified into two categories: Class I and Class II. In Class I, the interaction between organic and inorganic materials is only physical interaction such as hydrogen bonding, and π-π interaction (aromatic interaction). Specific functional groups in materials involve forming physical interactions between the two materials[20–22]. In contrast, in Class II, chemical bonding occurs between two different phases[23–28].

Inorganic-organic hybrid materials are applied in various applications due to their enhanced properties. Some of the main applications have been summarized in Figure 1-1[29–41].

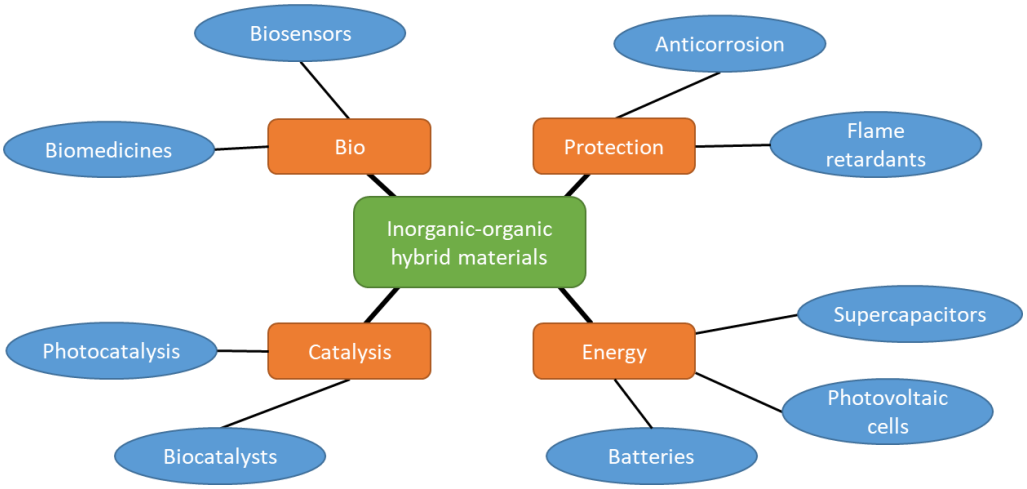

Figure 1- 1: Main applications areas of inorganic-organic materials.

Scientists are developing novel inorganic-organic hybrid materials that can immobilize live cells and biomolecules such as enzymes. However, conventional methods used for the synthesis of inorganic polymers, and coating of materials by inorganic polymers, require high temperatures, extreme pH conditions, vacuum conditions, and caustic chemicals that are incompatible with biomolecules[7]. Therefore, biomimetic approaches to synthesize inorganic polymers and coating of materials with inorganic polymers have been studying for the past few years[8, 9].

1.2.2. Silica and silicatein

Silica is known as the most abundant mineral in the Earth's crust and is a highly biocompatible material[4]. Since conventional methods used for synthesizing and coating with silica, involve high temperatures, extreme pH conditions, vacuum conditions, and caustic chemicals, immobilization of biomolecules is difficult[7]. Therefore, scientists had a keen interest to find biological routes to synthesize silica under mild conditions for the immobilization of biomolecules in the silica matrix to fabricate novel materials.

Silica has been found in many eukaryotes, including protists, diatoms, sponges, mollusks, and higher plants. The size of biologically produced silica structures such as shells of diatoms and the skeletons of sponges ranges from nano-scale to microscale. It has been reported that these biosilica contain small amounts of organic substances[17, 18, 42–44] that facilitate the formation of structures while synthesizing of biosilica under mild conditions[17, 45].

The skeletons of demosponges compose silica in the most common needle-shaped structures called spicules[46]. A marine demosponge's (*Tethya aurantia*) skeleton contains needle-shaped clear spicules[18]. Generally, it is about 75% of the dry weight of the organism. That afforded to isolate the protein from axial filaments found in each spicule, to discover the biosilicification mechanism in these animals[18, 47]. From the axial filaments of spicules, three similar protein subunits, named silicatein α (29 kDa), β (28 kDa), and γ (27 kDa) have been identified in a particular ratio (α:β:γ = 12:6:1) as repeating units[18].

Through analyzing the sequences of silicateins, it was found that they are highly homologous to cathepsins L, a family of cysteine proteases[48] including the position of three internal disulfide bridges and the three-dimensional structures. The amino acid sequences of mature silicatein α, β, and human cathepsin L has been shown in Figure 1-2. Cysteine, histidine, and asparagine are the active sites of most cysteine proteases while serine, histidine, and asparagine are the catalytic triad in silicateins.

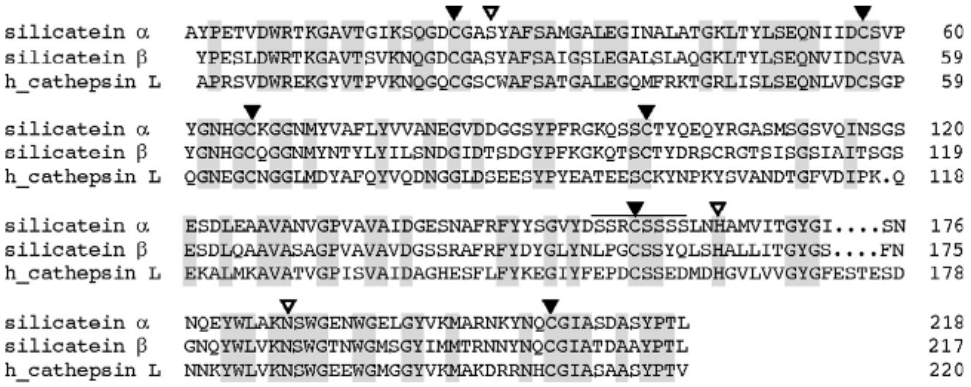

Figure 1- 2: Amino acid sequences of mature silicatein *α*, *β*, and human cathepsin L. Identical amino acids are highlighted. Filled and opened arrows show cysteine involved in disulfide bonds in cathepsin L and catalytic triad, respectively. The image was obtained from chapter fourteen in methods in enzymology written by Shimizu, K. and Morse, D. E.[49].

It has been found that silicateins isolated from axial filaments, and recombinant silicatein *α* expressed in bacteria can catalyze the silica polymerization using silicon alkoxides such as tetraethyl orthosilicate (TEOS) in vitro at neutral pH and room temperature[50]. To get a deep understanding of silicatein, recombinant silicatein was used. Analyzing the activities of recombinant silicateins, the mechanism of catalysis was revealed[11, 51–53]. According to that the silicon alkoxide precursor is hydrolyzed by the serine–histidine catalytic pair, homologous cysteine–histidine pair in the cysteine proteases, and the related serine–histidine pair in the serine proteases (Figure 1-3) [49, 50].

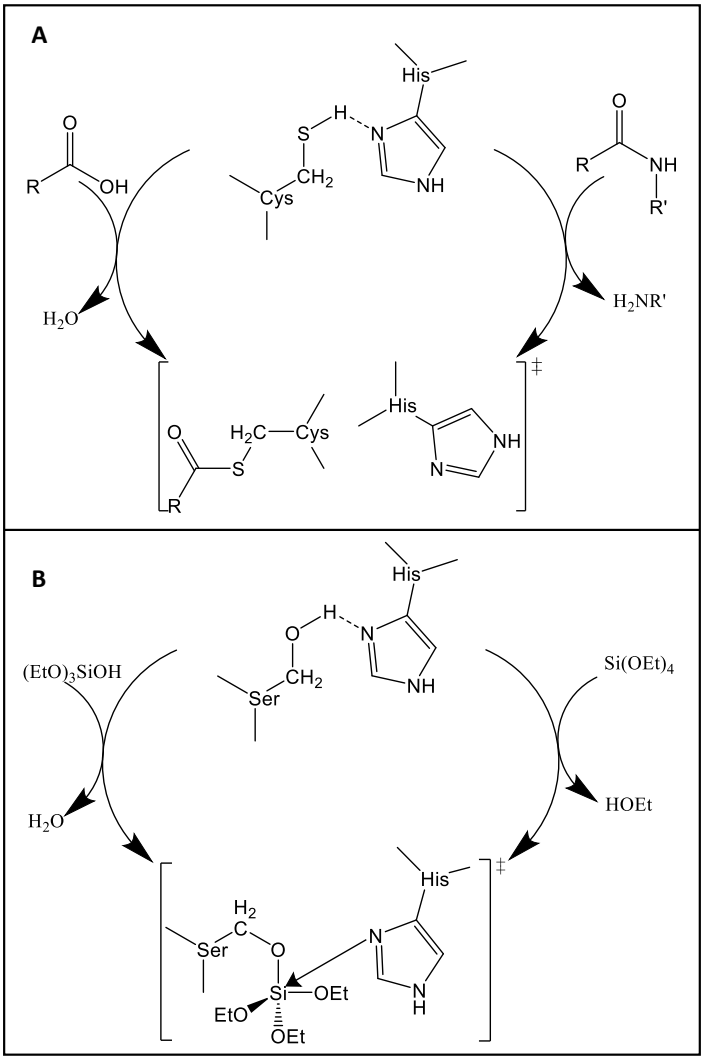

Figure 1- 3: Reaction mechanism of silicatein catalysis. (A) Cysteine protease-mediated cleavage of a peptide bond. (B) Silicatein-mediated hydrolysis of alkoxide TEOS. The image was regenerated using Brutchey R.L. and Morse D.E. (2008)[54] and chapter fourteen in methods in enzymology written by Shimizu, K. and Morse, D. E.[49].

Silicatein can not only catalyze the formation of silica under mild conditions but also many industrially important materials including polysilsesquioxanes (silicones) such as polyphenylsilsesquioxane (from phenyltriethoxysilane) and polymethylsilsesquioxane (from methyltriethoxysilane), and a large number of metal oxides including the TiO_2 (from the water-stable and -soluble precursor, titanium

bis(ammonium lactato) dihydroxide)[8], Ga_2O_3 from $Ga(NO_3)_3$[52], zirconia (ZrO_2) and the orthorhombic perovskite-like $BaTiOF_4$ from $BaTiF_6$[49, 55]. As shown in Figure 1-4, silicatein can catalyze the hydrolysis of TEOS into silicic acid followed by polycondensation of silicic acid into silica[50].

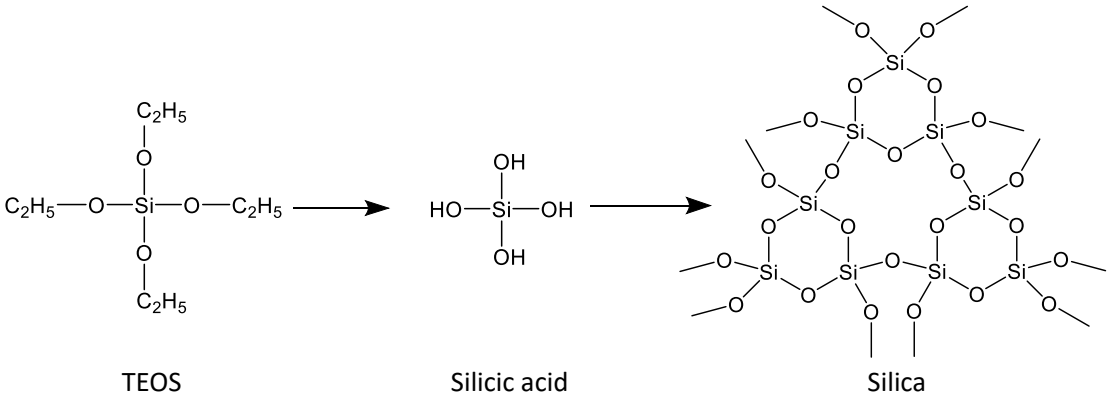

Figure 1- 4: The hydrolysis of TEOS into silicic acid followed by polycondensation of silicic acid into silica by silicatein.

Silicatein is expressed in sponges with a propeptide sequence at the N-terminus[56]. Silicatein with propeptide is inactive and does not show a self-assemble property. Hydrophobic patches, located on the surface of the silicatein molecules have been identified as the driving force for its aggregation. The hydrophobic patches in the mature silicatein molecule are known to be localized between aa135-150, close to the N-terminus of the protein, and this hydrophobic segment is covered by the propeptide[57]. After cleavage of the propeptide sequence, the resulting mature silicatein shows catalytic activity and the self-assemble property due to the exposure of the hydrophobic region[56]. The hydrophobic region that is responsible for the aggregation of silicatein in aqueous solutions is shown in Figure 1-5.

A

111 LQDYPEAVDW RTKGAVTAVK DQGD**CGASYA FSAFGALEGA**
151 NALAKGNAVS LSEQNIIDCS IPYGNHGCHG GNFYDAFLYV
191 IANEGVDQDS AYPFVGKQSS CNYNSKYKGT SFSGFVSIKS
141 GSESDLQAAV SNVGPVSVAI DGANSAFRFY YSGVYDSSRC
171 SSSSLNHAFV VTGYGSYNGK KYWLAKNSWG TNWGNSGYVF
320 FARNKYNQCG IATDASYPTL

B

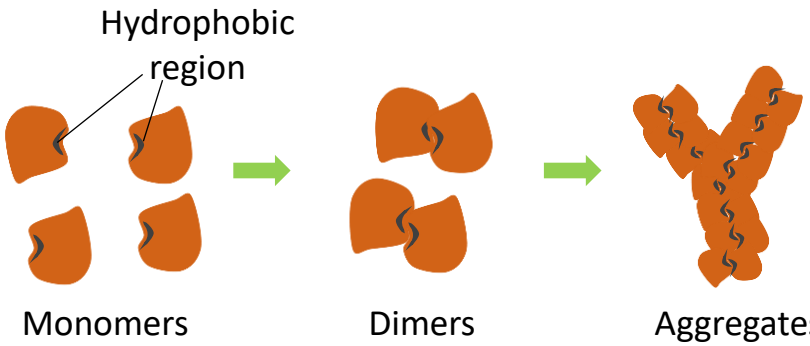

Figure 1- 5: Hydrophobic region of mature silicatein responsible for the aggregation. (A) Amino acid sequence of mature silicatein (aa115-330) composes the hydrophobic region (Bold, aa135-150), (B) Aggregation of silicatein.

1.2.3. Recombinant protein

Proteins are plying a critical role in biological systems facilitating many biological processes in a cell, including gene expression, cell growth, proliferation, nutrient uptake, intercellular communication, and apoptosis[58]. The information of the protein has stored in DNA. During the protein synthesis, DNA is first transcribed into RNA, then RNA is translated into protein[59]. For the studying of health and disease and the development of biomimetic processes related to enzymes, it was needed to get express the target proteins through cost-effective, simple, speedy processes with an adequate

yield[59]. Using recombinant DNA technology, DNA of different species can be introduced into other species to express the foreign proteins in the host species[60]. Further, by combining the DNA of different proteins, two or more proteins can be combined to express as one protein[59]. Those combined proteins are known as fusion proteins or chimeric proteins.

Recombinant proteins are proteins encoded by recombinant DNA that has been cloned in an expression vector to express the target protein in a host cell such as *Escherichia coli*, or yeast[61]. Proteins in other species can be expressed in those host cells after optimizing the gene sequence of the particular protein for the host species[62]. Apart from the direct expression, protein is expressed as a fusion protein[13, 63]. Fusion proteins consist of the protein of interest combined with other proteins or protein tags fused in either the N- or C-terminus of the interest. Fusion of other proteins or protein tags to the interest protein could help for purification[63], detection[64, 65], or enhancement of its activity[66].

1.2.4. Solid binding proteins

When studying the mechanism of degradation enzymes, it was found that some degradation enzymes have a noncatalytic solid binding domain and a catalytic domain[67]. The solid binding domain helps the enzyme to bind with the target material allowing the catalytic domain to degrade the material efficiently as illustrated in Figure 1-6. Among them, cellulase, an enzyme that acts on cellulosic material, and chitinase, an enzyme that works on chitin material, have been extensively studied.

The binding domains in cellulase enzymes are known as a carbohydrate-binding module (CBM)[68]. CBMs were previously classified as cellulose-binding domains since their affinity on cellulose was discovered initially[69, 70]. However, it was found

that CBMs can bind carbohydrates other than cellulose[68]. More than 300 putative sequences of CBMs in different species have been identified[71]. They have been classified into around 50 different families based on amino acid sequence, binding specificity, and structure[71].

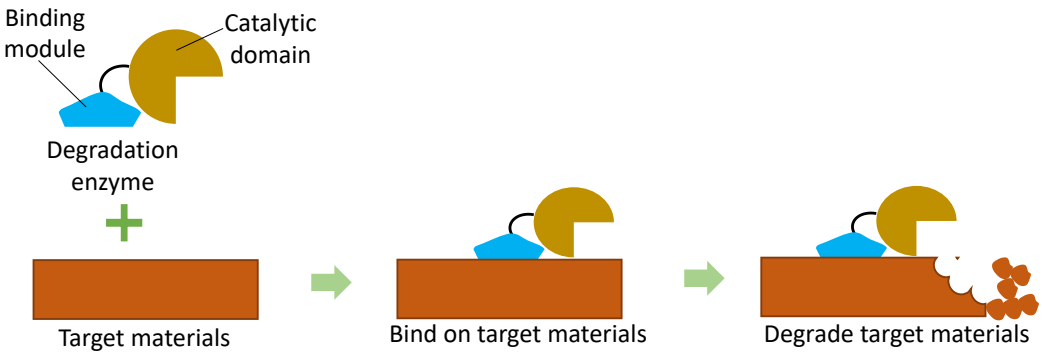

Figure 1- 6: Simple illustration of the action of degradation enzyme with a solid binding domain and a catalytic domain.

The binding domain found in chitinase enzymes is known as a chitin-binding domain (ChBD)[72]. ChBD has been used in many applications such as for immobilization of live cells on chitin material by surface displaying of ChBD[73], for protein purification[74], and metal ion recovery by immobilizing of metal-binding fusion proteins on chitin material[75]. With this proven binding ability, this could be the best binding tag for the adsorption of fusion proteins on chitin.

1.3. Scope of the thesis

The scope of this thesis is designing novel interfacial catalysts compose of silicatein, soluble tag, and solid binding domain to catalyze the silica formation on organic matrixes under mild conditions and to immobilize a model enzyme in the hybrid material while protecting its enzymatic activity. This thesis consists of five sections as illustrated in Figure 1-9.

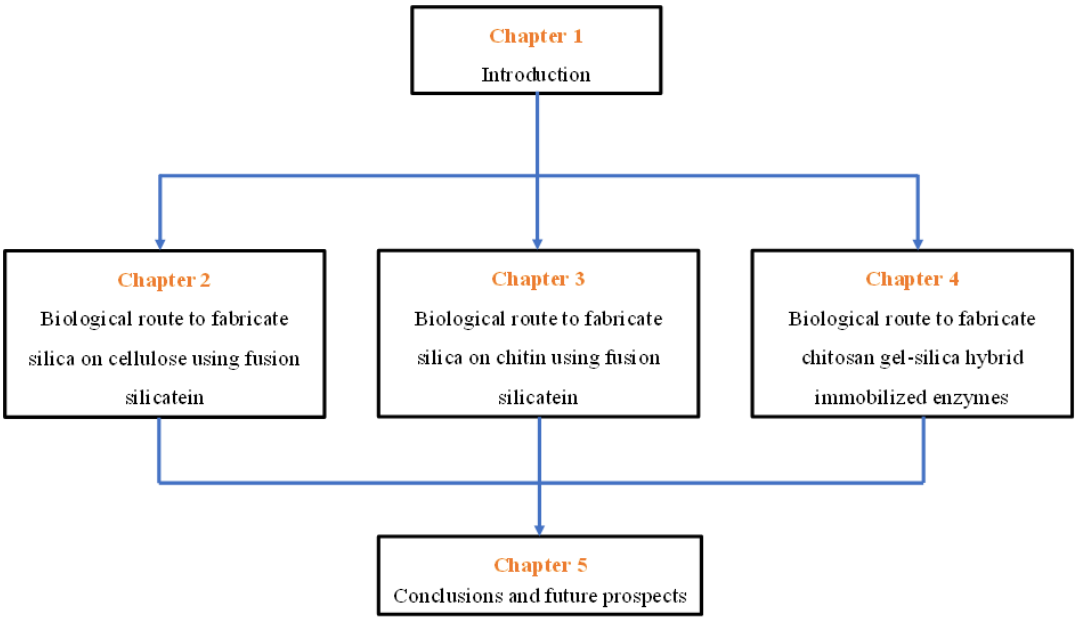

Figure 1- 7: Scope of the thesis.

1.4. Originality and the usefulness of the study

In this thesis, novel interfacial catalysts composed silicatein, soluble proteins, and soil-binding domains have been designed to fabricate hybrid materials containing silica under mild conditions. Soluble tags were used to avoid the aggregation of silicatein in aqueous media that cause it difficult to handle in applications. Binding modules were used to immobilize silicatein of the target materials. As cellulose, chitin and chitosan gel were used as target materials, CBM for the cellulose and ChBD for chitin and chitosan gel were employed.

Using the created interfacial catalysts, silica-cellulose, silica-chitin and silica-chitosan gel hybrid material were fabricated under mild conditions. Further, a model enzyme was immobilized in the silica-chitosan gel hybrid material while protecting its activity. Therefore, these findings can be used to create novel inorganic-organic hybrid materials immobilized live cells and biomolecules such as enzymes.

CHAPTER 2

BIOLOGICAL ROUTE TO FABRICATE SILICA ON CELLULOSE USING FUSION SILICATEIN

2.1 Introduction

Silicatein catalyzes silica polymerization under room temperature, neutral pH, and low pressure[10]. Using that incredible property, scientists have been developed biosilica formed by silicatein to immobilize live cells and biomolecules such as enzymes[11,12]. However, the low solubility of silicatein due to its aggregation property brings some problems when handling it in applications. Therefore, the solubility of silicatein in aqueous media should be improved for future applications of making hybrid materials using silicatein. It has been reported that the fusion of a soluble tag is the best approach to enhance the solubility of low soluble proteins[76]. Therefore, in this study, a soluble protein tag, ProS2 that has been previously studied to improve the solubility of silicatein by our research group while protecting its enzymatic activity, was used. ProS2 is a tandem repeat of the N-terminus domain of Protein S from *Myxocuccus xanthus,* and it has been previously studied for its ability to enhance the solubility of human proteins in *E. coli*[77]. Additionally, Nakashima et al. found that after silicatein was fused with ProS2, resulted in ProS2-Sil showed good solubility in aqueous media.

Cellulose has been used as an organic material to fabricate hybrid materials. It is the most abundant polysaccharide on the earth and is used in many applications, including cosmetics, pharmaceuticals, drug delivery systems, analytical devices, and tissue engineering[68, 78, 79]. Biological route for the fabrication of silica-coated cellulose hybrid materials with biocompatibility is a novel tool that can use in

biomedical applications such as control drug release, tissue engineering, bone regeneration, and biosensors[80–84].

For the immobilization of silicatein on cellulose to form a silica-cellulose hybrid material, CBM was employed in this study. CBM is a non-catalytic domain in the cellulase enzyme. It anchors carbohydrates such as cellulose, allowing the catalytic domain to degrade cellulose effectively and efficiently[71]. Figure 2-1 shows a schematic diagram to show the degradation of cellulose using cellulase enzyme.

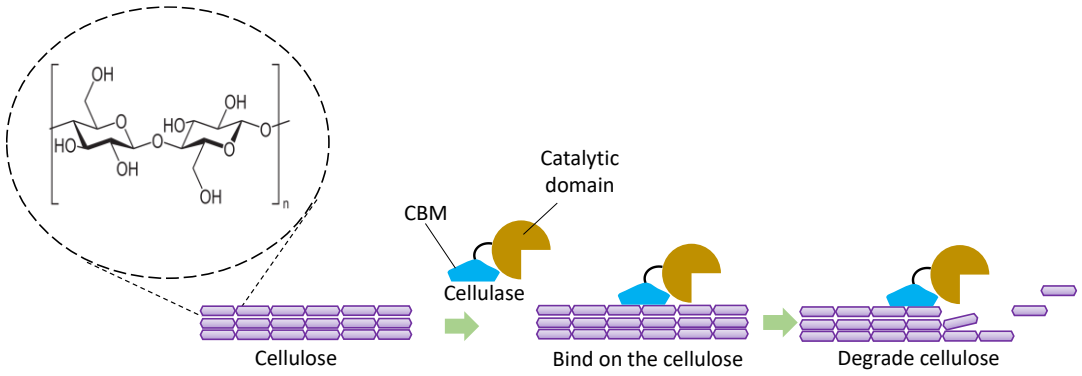

Figure 2- 1: The structure of cellulose and schematic diagram to show the degradation of cellulose using cellulase enzyme.

In this study, to fabricate silica-cellulose hybrid materials, an interfacial catalyst that is soluble and can bind on cellulose was studied. Silicatein (Sil) was fused with CBM to get Sil-CBM, and the solubility of Sil-CBM was observed. Even though Sil-CBM could get expressed successfully, it was difficult to obtain due to its lack of solubility. Therefore, it was necessary to improve the solubility of Sil-CBM. To improve the solubility, ProS2 tag was fused with Sil-CBM. Together, ProS2-Sil-CBM could be soluble and can be immobilized on cellulose to act as an interfacial catalyst to form silica on cellulose as shown in Figure 2-2. This catalyst could be used to fabricate

a silica layer on the cellulose material in mild conditions. These findings will contribute to the fabrication of inorganic-organic biohybrid materials to immobilize biomolecules in order to create novel hybrid materials, which can be applied in many technological and biomedical applications.

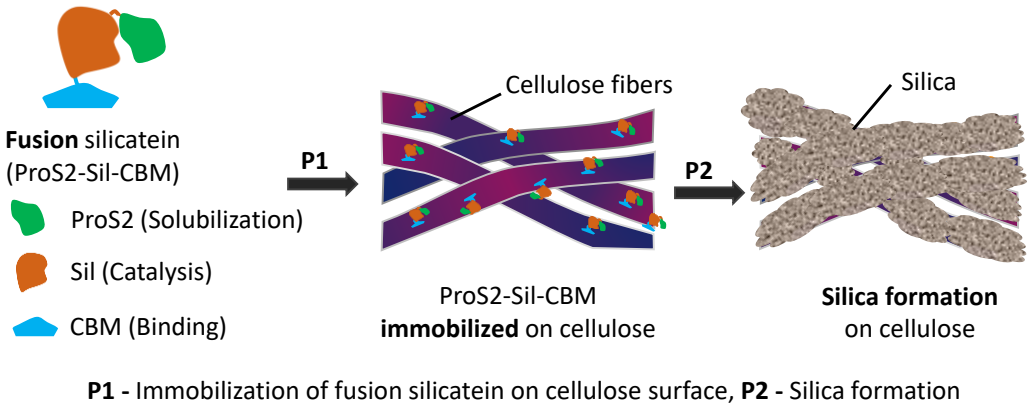

Figure 2- 2: Conceptual diagram to show silica formation on cellulose through the ProS2-Sil-CBM.

2.2 Objective

The objective of this study was to fabricate silica-cellulose hybrid materials under mild conditions by using an interfacial catalyst compose silicatein with improved solubility and binding property on cellulose by fusing with a soluble tag, ProS2 and CBM.

2.3 Materials and methods

2.2.1. Construction of the fusion genes and vectors

Silicatein α cDNA from *Suberites domuncula* (accession number CAI46305), which encodes the mature enzyme (aa115-330), and CBM3 cDNA from *Clostridium thermocellum* (accession number Q06851) were synthesized by Eurofins Genomics with optimization for expression in *E. coli*. As illustrated below, gene and vector construction were performed to express ProS2-Sil, Sil-CBM and ProS2-Sil-CBM. Among them, ProS2-Sil is a soluble fusion silicatein that has been studied previously in our laboratory. Therefore, ProS2-Sil was used as a control to check the solubility and enzymatic activity. The nucleotide sequence of primers used in this work and PCR conditions are shown in Table 2-1 and Table 2-2, respectively.

Table 2- 1: Nucleotide sequence of primers used in this study.

Primer	Nucleotide sequence
F1	CGAAGGTAGGCATATGGACTATCCGGAAGCAGTG
F2	CATCATCATCATATGGACTATCCGGAAGCAGTG
F3	TCGAAGGTAGGCATATGGACTATCCGGAAGCAGTG
F4	TCTTATCCAACCCTGACACCGACCAAGGGAGCA
R1	ATTCGGATCCCTCGAGCAGGGTTGGATAAGAGGC
R2	TCCCTTGGTCGGTGTCAGGGTTGGATAAGAGGC
R3	ATTCGGATCCCTCGAG GCCACCGGGTTCTTTACC

Table 2- 2: PCR conditions for gene amplification and overlap PCR

Stage	PCR for cloning gene		Overlap PCR		Cycles
	Temperature (°C)	Time	Temperature (°C)	Time	
Pre denaturation	98.0	30 s	98.0	30 s	-
Denaturation	98.0	10 s	98.0	10 s	35
Annealing	55.0	15 s	56.7	5 s	
Extension	72.0	5 s	72.0	5 s	
Final extension	72.0	1 min	72.0	1 min	-

ProS2-Sil: The gene encoded silicatein was amplified using F1 and R1 primers. The amplified gene was subcloned into pCold ProS2 expression vector at *Nde*I and *Xho*I restriction enzyme sites using In-Fusion (Takara Bio Inc., Japan) to express the protein named ProS2-Sil.

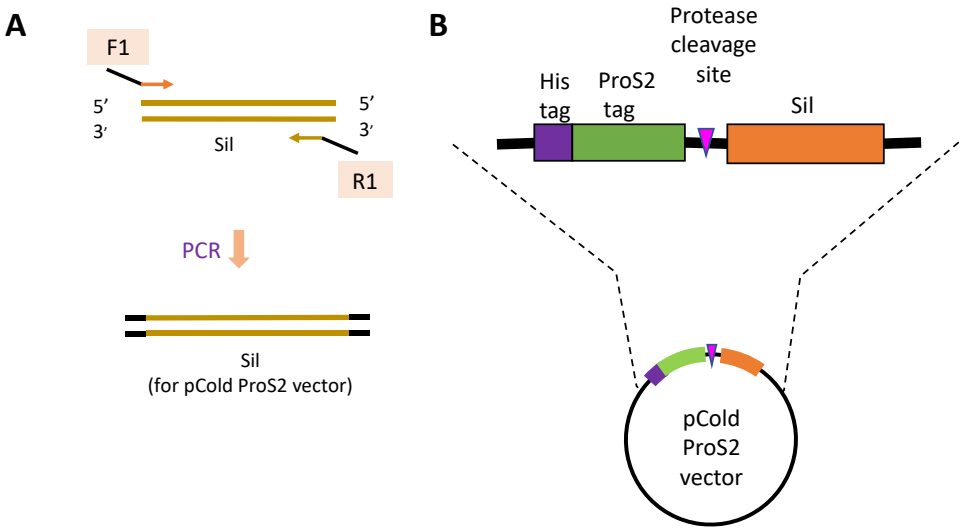

Figure 2- 3: Gene and vector construction to express ProS2-Sil. (A) Gene construction through PCR. (B) The gene order of ProS2-Sil.

Sil-CBM: The gene encoded silicatein amplified with F2 and R2 primers, and CBM3 gene amplified with F4 and R3 were combined using overlap PCR. The amplified gene was inserted into pCold II expression vector at *Nde*I and *Xho*I restriction enzyme sites to express the protein named Sil-CBM.

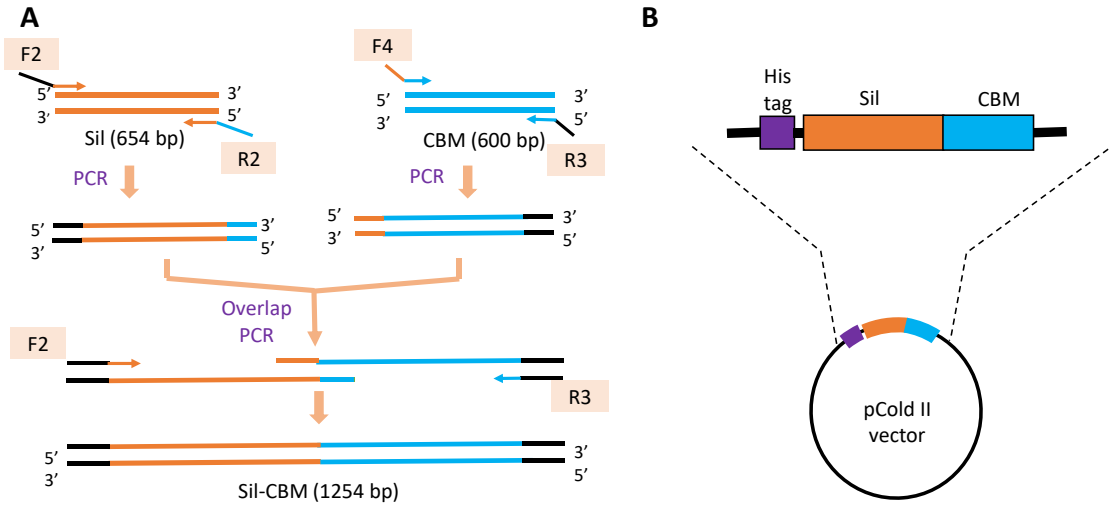

Figure 2- 4: Gene and vector construction to express Sil-CBM. (A) Gene construction through PCR. (B) The gene order of Sil-CBM.

ProS2-Sil-CBM: At the same time, the gene encoded silicatein amplified with F3 and R2 primers, and CBM3 gene amplified with F4 and R3 were combined using overlap PCR. The amplified gene was inserted into pCold ProS2 expression vector at *Nde*I and *Xho*I restriction enzyme sites to express the protein named ProS2-Sil-CBM.

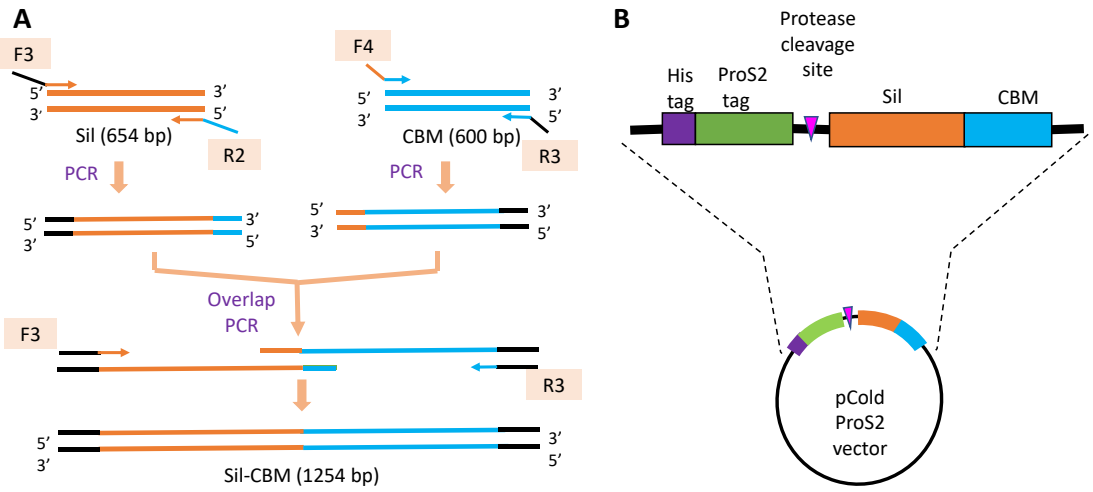

Figure 2- 5: Gene and vector construction to express ProS2-Sil-CBM. (A) Gene construction through PCR. (B) The gene order of ProS2-Sil-CBM.

Here, pCold II and pCold ProS2 were used as expression vectors. The vector maps of these expression vectors are shown in Figure S8 (Appendix II). These vectors are known as cold shock expression vectors. They can induce the expression of the target protein resulting in highly pure proteins while suppressing the growth of *E. coli*. In addition, since these vectors have His-tag sequences, Ni-NTA column purification using the His-tag is possible after protein expression.

Finally, to check the correctness of the constructed vectors after multiplication in *E. coli* DH5α, DNA sequencing was conducted.

2.2.2. Expression of the recombinant proteins

The transformed *E. coli* with the respective vectors to express ProS2-Sil, Sil-CBM and ProS2-Sil-CBM were precultured separately at 37 °C while shaking at 160 rpm for 16 h in Luria broth (LB) medium supplemented with 100 µg/mL ampicillin. Then, aliquots of cultures were added into freshly prepared LB-Amp medium and incubated at 37 °C while shaking at 160 rpm. When the OD_{600} = 0.5, the cultures were cooled

down to 15 °C and left for 30 min. Protein expression was induced with 1.0 mM isopropyl β-D-1-thiogalactopyranoside (IPTG) and was grown for an additional 24 h at 15 °C while shaking at 160 rpm. Bacterial cells were harvested by centrifugation (4000 × g, 20 min, 4 °C). Resultant pellets were resuspended in sonication buffer (20 mM Tris/HCl, pH 8.0, 1 mM EDTA, 0.5 M NaCl) and cells were disrupted by using an ultrasound disintegrator (VCX-130, Sonic & Materials Inc., USA). Then the samples were centrifuged (25, 000 × g, 20 min, 4 °C). The precipitated fractions were washed twice with lysis buffer containing a surfactant (20 mM Tris/HCl, pH 8.0, 1 mM EDTA, 0.5 M NaCl, 4% TritonX-100) and washed twice with ultra-pure water to remove membrane proteins. Resulted inclusion bodies were used for the purification of target proteins.

2.2.3. Purification of recombinant proteins

After washing the inclusion bodies (insoluble faction) containing the target fusion proteins, 300 mg of the inclusion bodies were added into 5 mL of denaturation buffer containing urea (50 mM Tris/HCl, pH 8.0, 8 M urea, 10 mM DTT), and the mixture was shaken at 160 rpm for 2 to 3 h until the solution gets clear. Then the mixture was centrifuged (25, 000 × g, 20 min, 4 °C) for the removal of insoluble impurities. Next, the denatured target proteins in the supernatant were purified by immobilized metal ion affinity chromatography on a 5 mL Ni-NTA column as previously reported[57]. The content of the buffers and the procedure followed during the Ni-NTA column purification have been mentioned in Table 2-3 and Table 2-4, respectively. The denaturation buffer and the buffers used in the Ni-NTA column purification can be stored at -20 °C for one week. Before using those, they should be brought to room temperature. When passing the buffers and the denatured target proteins through the Ni-NTA column using a syringe, a syringe filter (Hawach Scientific, nylon membrane,

0.22 µm pore size) was used to prevent damages could occur by entering foreign particles into the Ni-NTA column. The proteins purified using the Ni-NTA column were still in the denatured condition. Therefore, they should be subjected to refolding to obtain the active proteins.

Table 2- 3: Content of the buffers used for Ni-NTA column purification.

Solution	Ingredients				
	Urea	**NaCl**	**Phosphoric acid**	**Imidazole**	**DTT**
Wash buffer 1	8 M	300 mM	50 mM	5 mM	10 mM
Wash buffer 2	8 M	300 mM	50 mM	25 mM	10 mM
Elution buffer	8 M	300 mM	50 mM	500 mM	10 mM

Table 2- 4: Procedure followed during the Ni-NTA column purification.

Solution	Volume	Rate	Role
Distilled water	2 CV	10 mL/min	Washing
Wash buffer 1	5 CV	10 mL/min	Equilibration
Loading buffer containing the target protein	1 CV	5 mL/min	Loading the protein
Wash buffer 1	6 CV	5 mL/min	Washing
Wash buffer 2	6 CV	10 mL/min	Washing
Elution buffer	5 CV	10 mL/min	Eluting the target protein

2.2.4. Refolding and ultrafiltration of purified proteins

For the refolding of proteins, the urea used as denaturant should be removed from the solution. For that, a dialysis method was used for each protein. The dialysis membrane (Thermo Fisher Scientific, 6000-8000 nominal molecular weight cut-off (NMWCO)), was placed in a beaker containing distilled water and washed while stirring with a magnetic stir bar. The dialysis membrane was opened, and the inside of the dialysis membrane was washed. The end of the dialysis membrane was bound with a clip, and the protein solution recovered by the Ni-NTA column purification was filled followed by the clipping the other end without trapping air bubbles. Then the dialysis membrane containing the protein was submerged in the refolding buffer (50 mM tris/HCl, pH 8.5, 0.5 M L-Arginine, 9 mM red/glutathione, 1 mM ox/glutathione, 0.3 M NaCl, 1 mM KCl) (purified protein volume filled into dialysis membrane: refolding buffer volume, 1:20). Dialysis was performed at 4 °C for 36 hours while stirring the buffer solution with a magnetic stir bar[85, 86]. The refolding buffer was exchanged twice during the dialysis. After 36 h hours, the protein solution in the dialysis membrane was transferred to a centrifuge tube and centrifuged at 4 °C, 15, 000 × g for 15 min to confirm that precipitation could not be performed. The refolding buffer of the target proteins was then replaced with 50 mM Tris/HCl buffer (pH 9.0, 8 mM NaCl) by ultrafiltration (Amicon® Ultra-15 centrifuge filters, 10000 NMWCO). Finally, the concentrations of refolded proteins were calculated using the Bradford assay (Bradford Protein Assay Kit, Takara Bio Inc., Japan)[87].

2.2.5. The solubility of recombinant proteins

The purified recombinant proteins were assayed for their aggregation property. ProS2-Sil and ProS2-Sil-CBM were added separately into 50 mM Tris/HCl buffer (pH 7.4, 150 mM NaCl) to obtain final concentration of 10 μM each. The solutions were

incubated at 25 ℃ for 24 h. During the incubation period, samples were monitored to see whether the solutions become turbid or not.

2.2.6. Cleavage of ProS2 tag

ProS2-Sil-CBM was subjected to ProS2 tag removal test by site-specific protease which can cleave the peptide sequence between ProS2 and Sil. ProS2-Sil-CBM (10 μM) in Tris/HCl buffer was treated with HRV 3C Protease (10 U/mL, Takara Bio Inc., Japan) at 25 ℃ for 1 h. During the incubation period, the sample mixture was observed to check turbidity caused by protein aggregation.

2.2.7. Determination of enzymatic activity

The enzymatic activities of fusion silicateins were determined as previously described[7]. ProS2-Sil or ProS2-Sil-CBM (1.66 μM each) and 100 mM TEOS as the substrate for the enzymes were incubated in Tris/HCl buffer at 25 °C while shaking at 185 rpm for 24 h[9]. As a control, silica polymerization activity was determined in the absence of proteins with the same conditions. The formed biosilica was recovered by centrifugation (13000 rpm, 10 min, 4 °C) and washed three times with ethanol and three times with ultra-pure water, followed by freeze-drying. Freeze-dried biosilica samples were hydrolyzed to silicic acid by 1 M NaOH for 30 min at 90 °C and neutralized with HCl. The concentration of silicic acid (hydrolyzed silica) was then determined by the molybdenum blue colorimetric method[18]. The absorbance values were determined at 810 nm to calculate absolute amounts of silicic acid based on the calibration curve using a silicon standard solution (1000 ppm, Wako Pure Chemical Industries Ltd., Japan).

2.2.8. Adsorption of fusion silicateins on cellulose and silica formation

To check the adsorption of fusion proteins on cellulose, a piece of cellulose filter paper (1.0 × 0.5 cm, Whatman No. 1 filter paper) was added into 50 mM Tris/HCl

buffer solutions containing 4.25 µM of ProS2-Sil or ProS2-Sil-CBM, and the solutions were shaken for 1.5 h at 25 °C. During shaking, 20 µL of aliquots of the solution were periodically taken to analyze the remaining concentration of protein by Bradford assay. After 1.5 h, the piece of cellulose was recovered and washed twice with 50 mM Tris/HCl buffer. The cellulose filter paper with ProS2-Sil-CBM was subjected to silica formation using 100 mM TEOS as the precursor in the 50 mM Tris/HCl buffer at 25 °C while shaking at 185 rpm for 24 h[9]. The treated cellulose paper was recovered and washed three times with ethanol and three times with ultra-pure water, followed by freeze-drying for 2 days. A similar experiment was conducted for a control without adding ProS2-Sil-CBM.

2.2.9. Scanning electron microscope analysis

After freeze-drying, formed biosilica on cellulose materials was examined using a scanning electron microscope (SEM) (Acceleration voltage: 5 kV, JEOL JSM-IT200 InTouchScope™, German) without coating. Elements present on the cellulose surfaces subjected to silica formation were analyzed by using energy-dispersive X-ray spectroscopy (EDS) (Without coating, acceleration voltage: 10 kV for point EDX, JEOL JSM-IT200 InTouchScope™, German).

2.3. Results and discussion

In the present study, a functional soluble silicatein that can bind to cellulose to form silica on cellulose was designed. That can act as an interfacial catalyst to fabricate a cellulose-silica hybrid material under ambient conditions. The specificity of this method is there is no need to do any surface modifications or chemical treatments. As the silica matrix is formed on cellulose under physiological conditions, it will allow to immobilize live cells, biomolecules, and enzymes to create new functional materials.

2.4.1. Expression of fusion proteins

After the construction of vectors to express each protein, the correctness of the vectors was confirmed by DNA sequencing. Then they were transformed into *E. coli* for the protein expression. Amino acid sequences of fusion silicateins expressed in this study are shown in Figure S1-3 (Appendix I).

ProS2-Sil: Figure 2-6 shows the transformed *E. coli* to express ProS2-Sil. After successful transformation, protein expression was performed.

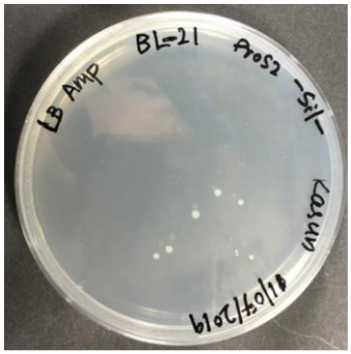

Figure 2- 6: Transformed *E. coli* to express ProS2-Sil.

The molecular weight of the ProS2-Sil was 46 kDa. Figure 2-7 shows the sodium dodecyl sulfate-polyacrylamide gel electrophoresis (SDS-PAGE) analysis of ProS2-

Sil. As shown in Figure 2-7A ProS2-Sil has expressed as an insoluble protein called inclusion bodies. Overexpression of recombinant proteins in *E. coli* often results in protein production as inclusion bodies[88]. Those inclusion bodies are insoluble, inactive, and relatively pure, intact proteins. The protein should be refolded into its active form through dialysis or dilution[89]. Therefore, after the denaturation of ProS2-Sil, ProS2-Sil could be purified by using Ni-NTA column purification followed by refolding and ultrafiltration. Figure 2-7B shows the SDS-PAGE analysis after Ni-NTA column purification and refolding of purified protein.

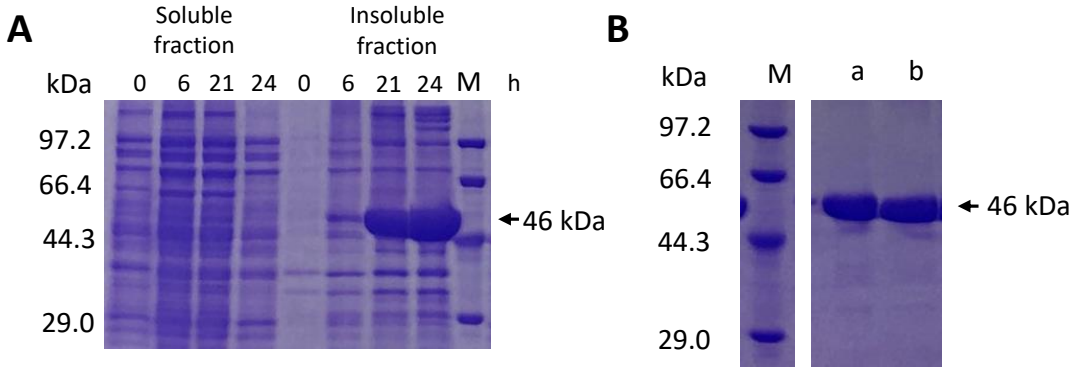

Figure 2- 7: SDS-PAGE analysis for ProS2-Sil. (A) SDS-PAGE analysis for expression. (B) (a) after Ni-NTA column purification, (b) after refolding of purified protein. M: Molecular weight maker.

Sil-CBM: The constructed vector to express Sil-CBM was transformed into *E. coli*. The transformed *E. coli* to express Sil-CBM and the colony polymerase chain reaction (PCR) done to check the successfulness of the transformation are shown in Figure 2-8.

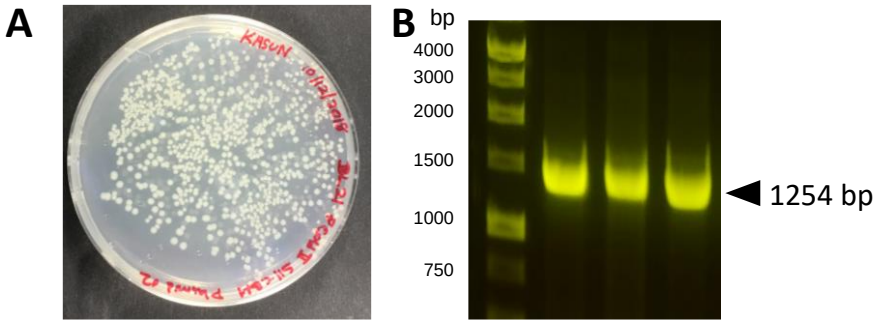

Figure 2- 8: Transformation of *E. coli* to express Sil-CBM. (A) Transformed *E. coli* to express Sil-CBM. (B) Colony PCR.

The molecular weight of the Sil-CBM was 44 kDa. Figure 2-9 shows the SDS-PAGE analysis of Sil-CBM. As shown in Figure 2-9A Sil-CBM also has expressed as an insoluble protein. Therefore, after denaturation of Sil-CBM, Sil-CBM was purified by using Ni-NTA column purification followed by refolding and ultrafiltration. SDS-PAGE analysis in Figure 2-9B shows Sil-CBM after Ni-NTA column purification and after refolding.

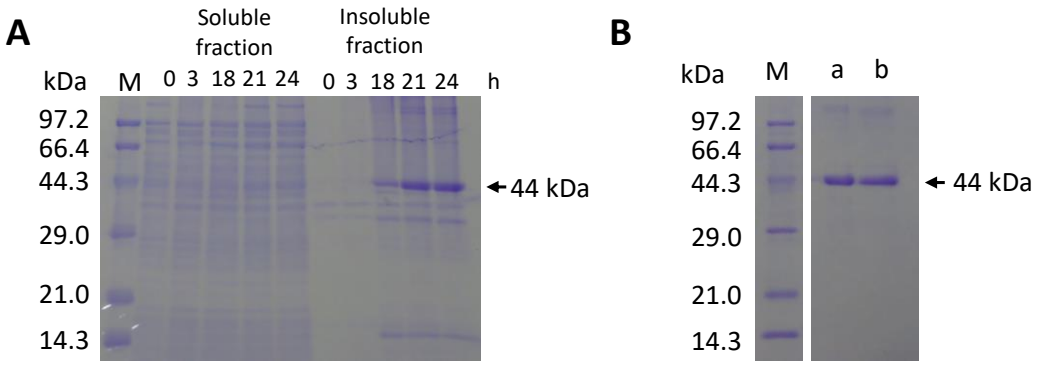

Figure 2- 9: SDS-PAGE analysis for Sil-CBM. (A) SDS-PAGE analysis for expression. (B) (a) after Ni-NTA column purification, (b) after refolding of purified protein. M: Molecular weight maker.

ProS2-Sil-CBM: The constructed vector to express ProS2-Sil-CBM was transformed into *E. coli* (Figure 2-10A). The transformation was confirmed by colony PCR as shown in Figure 2-10B.

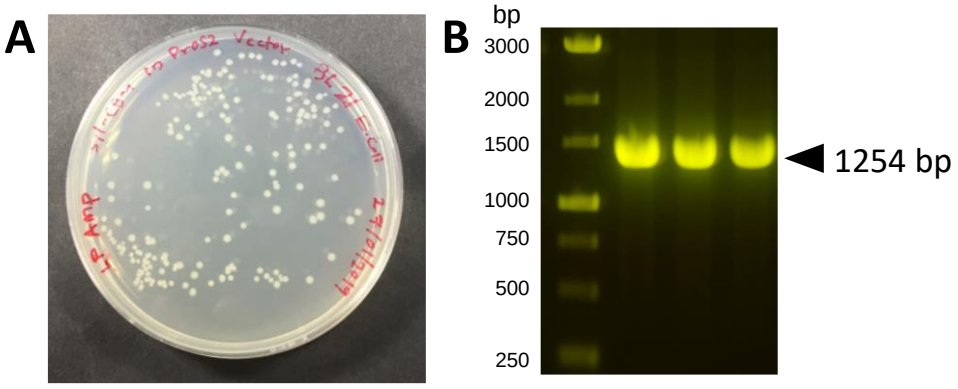

Figure 2- 10: Transformation of *E. coli* to express ProS2-Sil-CBM. (A) Transformed *E. coli* to express ProS2-Sil-CBM. (B) Colony PCR.

Figure 2-11 shows the SDS-PAGE analysis for expression, after Ni-NTA column purification and after refolding of ProS2-Sil-CBM. According to the SDS-PAGE analysis shown in Figure 2-11A, ProS2-Sil-CBM was mainly expressed as insoluble inclusion bodies. These fusion proteins were subjected to refolding. Figure 2-11B shows the SDS-PAGE analysis before and after the refolding of ProS2-Sil-CBM. This observation confirmed that the target proteins were refolded successfully. L-Arginine, a protein stabilizer found in the refolding buffer, was replaced with Tris/HCl buffer using ultrafiltration because it has been reported that amines like L-arginine catalyze silicic acid polymerization[90].

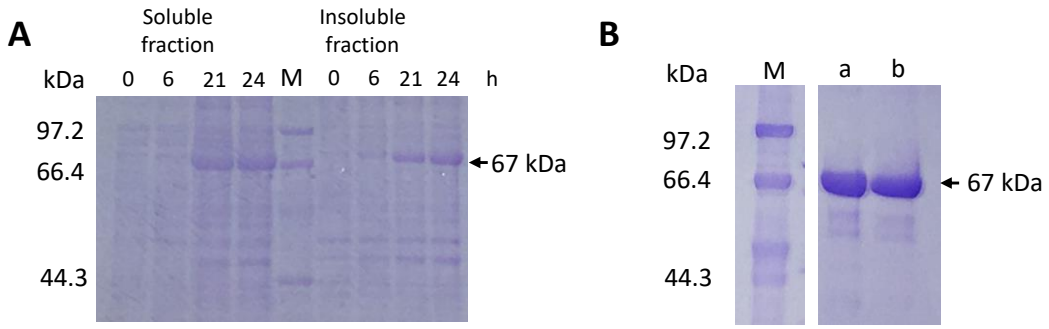

Figure 2- 11: SDS-PAGE analysis for ProS2-Sil-CBM. (A) SDS-PAGE analysis for expression. (B) (a) after Ni-NTA column purification, (b) after refolding of purified protein. M: Molecular weight maker.

Before the Ni-NTA column purification, the inclusion bodies were washed with Triton X-100, a nonionic detergent. Washing with a nonionic detergent such as Triton X-100 and Tween 20 removes membrane proteins, most of which are proteases. The presence of those proteases would degrade the refolded target proteins. Since the inclusion bodies are insoluble, before the Ni-NTA column purification they should be denatured to make them soluble. Figure 2-12 shows a simplified illustration to understand the process during the denaturation, purification and refolding of protein. First, the inclusion bodies containing the target proteins were denatured using urea as the denaturant (Figure 2-12A). Then the insoluble proteins became soluble but those were inactive. Since the proteins were in a soluble form, the target protein was purified using the Ni-NTA column purification. Finally, by removing the denaturant (urea) by dialysis, active protein in soluble form was obtained. In the dialysis method, the dialysis membrane allows passing the urea to the refolding buffer as shown in Figure 2-12B. Removal of the denaturant from the target protein resulted in the active target proteins by folding them into their active structure[88].

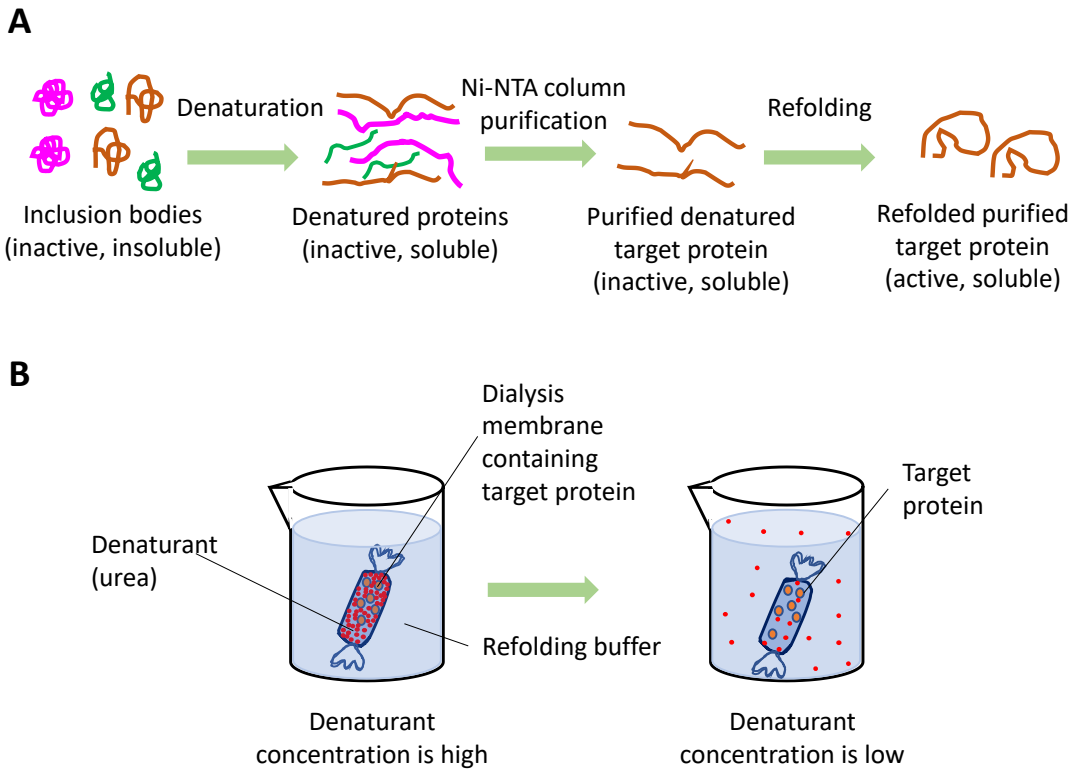

Figure 2- 12: Denaturation, purification and refolding of proteins. (A) The process of obtaining purified active soluble protein (the target protein has been shown in brown colour). (B) Removal of denaturant using dialysis.

2.4.2. The solubility of fusion proteins

Self-assembly of proteins is an interesting property that is integral in the formation of highly ordered protein architectures. Previous researches examined the self-assembly of silicateins that leads to structure-guiding property when mixing specified ratios of silicateins such as silicatein α and silicatein β to form nanosilica structures and filaments[91, 92]. Those studies suggested that self-assembled silicatein can also catalyze silica polymerization. However, the recombinant silicateins show aggregation property, which results in the formation of randomly arranged aggregates to form precipitates. To make material fabrication for future applications, silicatein, as a

catalyst should be kept in a soluble form without aggregation until it is adsorbed on cellulose to get uniform adsorption on the material. Among the proteins expressed, ProS2-Sil and ProS2-Sil-CBM were obtained in a soluble form after the refolding while Sil-CBM became turbid by forming aggregates just after the refolding. This observation suggested that ProS2-Sil and ProS2-Sil-CBM have improved solubility in aqueous media. This solubility improvement could be due to the fusion of ProS2 tag.

Therefore, the solubility of ProS2-Sil and ProS2-Sil-CBM was further studied. Figure 2-13 shows the solubility of ProS2-Sil and ProS2-Sil-CBM without and with the cleavage of soluble ProS2 tag by site-specific protease.

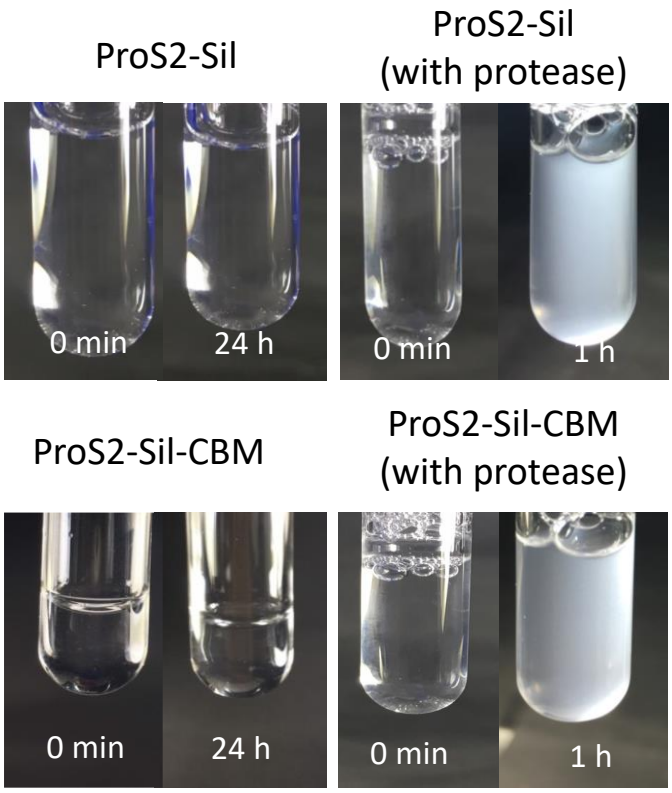

Figure 2- 13: Solubility of proS2-Sil and ProS2-Sil-CBM without and with cleavage of ProS2 tag.

The solutions containing ProS2-Sil and ProS2-Sil-CBM remained clear for 24 h while the solutions containing ProS2-Sil and ProS2-Sil-CBM treated with the protease formed a cloudy solution within 1 h. ProS2-Sil-CBM showed good solubility in aqueous media for 24 h confirming that the fusion of ProS2 tag had greatly improved the solubility of ProS2-Sil-CBM by inhibiting the aggregation of silicatein. SDS-PAGE analysis revealed that the protease did not cause an unspecific cleavage of ProS2-Sil-CBM (Figure 2-14). However, after cleavage, Sil-CBM showed a relatively lower intensity band. That may be due to the precipitation of Sil-CBM after removal of ProS2 tag. The hydrophobic region reported at the N-terminus of silicatein could be responsible for the aggregation of silicatein[57, 93]. The fusion of ProS2 tag could cover the hydrophobic region, resulting in the enhancement of silicatein solubility.

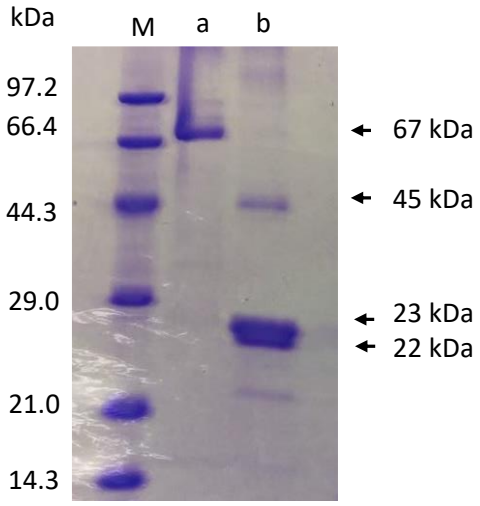

Figure 2- 14: ProS2-Sil-CBM with and without cleavage of ProS2 tag using protease. (a) Control: without cleavage of ProS2-Sil-CBM (67 kDa) (b) Reaction solution after cleavage with HRV 3C protease: include Sil-CBM (44 kDa), ProS2 (23 kDa) and HRV 3C protease (22 kDa). M: Molecular weight marker.

Recombinant silicatein is expressed as inclusion bodies that are inactive and insoluble. Recently a soluble expression of silicatein has been reported by fusing silicatein with a trigger factor, a ribosome-associated molecular chaperone[94]. However, that approach should be further studied to investigate the possibility of soluble expression of silicatein fused with different fusion tags.

2.4.3. Silica forming activity in an aqueous solution

After confirming the solubility of fusion silicateins, it is important to consider their silica forming activities since it is necessary to keep a high silica forming activity of the fusion silicatein. Silicatein catalyzes the hydrolysis of TEOS into silicic acid and the polycondensation of silicic acid into silica[50] (Figure 1-6). For the quantification of silica polymerization activity, silica formed during the incubation period in each sample was recovered by centrifugation, and washing with ethanol and distilled water. Washing with ethanol helps to remove unreacted TEOS from the silica particles. Then the recovered silica was hydrolyzed into silicic acid separately. The silicic acid concentration was measured using the molybdenum blue colorimetry method, and silica polymerization activities were expressed as the concentration of silicic acid. Figure 2-15 shows the silica polymerization activity of ProS2-Sil and ProS2-Sil-CBM. According to the results, the silica polymerizing activity of ProS2-Sil and ProS2-Sil-CBM was 13.3 mM and 12.0 mM, respectively. However, the fusion tags could negatively affect the enzymatic activity of silicatein. Previous work showed that pro-silicatein, which contains propeptide sequence at the N-terminus of silicatein, inhibits the enzymatic activity of silicatein[56]. In this study, the fusion of ProS2 at the N-terminus and CBM at the C-terminus of silicatein did not inhibit the silica forming activity of silicatein.

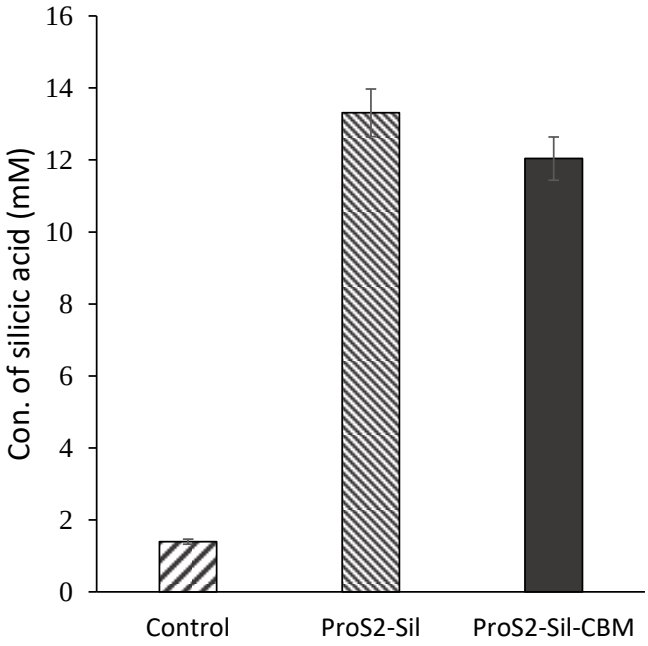

Figure 2- 15: Enzymatic activity of fusion silicateins. In the control experiment, the activity was determined in the absence of proteins (Control). Experiments were conducted in triplicate; data represent the average of three experiments with error bars indicating the standard deviation.

2.4.4. Adsorption on cellulose

CBM is a module of a cellulose-degrading enzyme that can bind to cellulosic materials[64, 71]. Many studies related to CBM reported that CBM is a promising binding domain that can use on cellulose[68]. CBMs have been grouped into distinct families based on amino acid sequence similarities. The CBM used for this study belongs to Family 3, which shows the affinity for non-crystalline cellulose and crystalline cellulose[64]. It has been reported that the same CBM fused with metal-binding proteins and peptides have been successfully immobilized on cellulose material

in recent studies[95, 96]. To investigate the adsorption of ProS2-Sil-CBM on cellulose, cellulose was treated with ProS2-Sil-CBM.

Figure 2-16 shows the time course of adsorption of fusion silicateins on cellulose. ProS2-Sil-CBM showed a 98% adsorption on cellulose within 1.5 h, confirming that it can rapidly bind to cellulose. These results indicate that the binding ability of CBM was not affected although the fusion silicatein was fused at the N-terminus of silicatein. Based on the results, 1.5 h time point was selected as the optimum equilibrium adsorption time. On the other hand, ProS2-Sil did not show adsorption on cellulose even after 1.5 h (Figure 2-16), suggesting that the CBM tag was necessary for the adsorption of fusion silicatein on cellulose. According to the studies related to the mechanism of CBM, it has been reported that CBM was bound to cellulose through hydrophobic interaction[71].

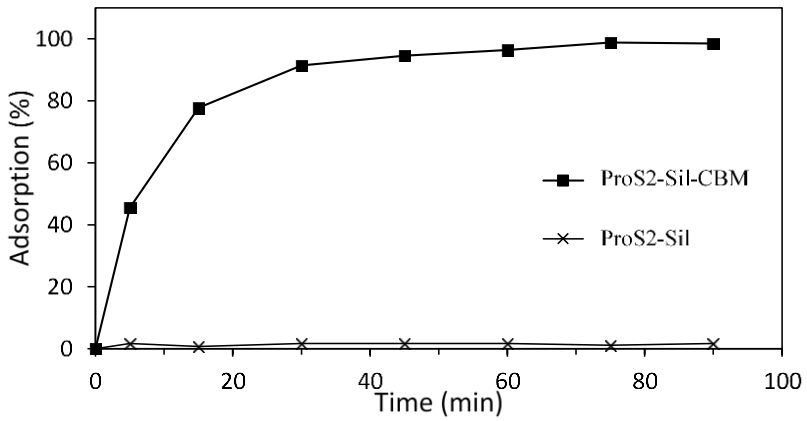

Figure 2- 16: Adsorption studies of fusion silicateins on cellulose**.**

2.4.5. Silica formation on cellulose

Previous studies have reported the structure-guiding properties of silicatein in forming characteristic silica structures such as silica filaments, indicating that silicatein indeed possesses silica forming activity[91, 97]. Therefore, immobilized silicatein could be

used to form a silica layer on the silicatein-immobilized material. In the present study, fusion silicatein, ProS2-Sil-CBM was immobilized on cellulose, and the polymerizing activity of silicatein to form silica on cellulose material was studied. Figure 2-17 represents the SEM images of cellulose fibers of filter papers subjected to silica formation with or without adsorption of ProS2-Sil-CBM. Figure 2-17A (with adsorption of ProS2-Sil-CBM) displays a clear deposition of silica on the cellulose fibers. In contrast, Figure 2-17B (without adsorption of ProS2-Sil-CBM) shows the clear appearance of cellulose fibers without any silica deposition.

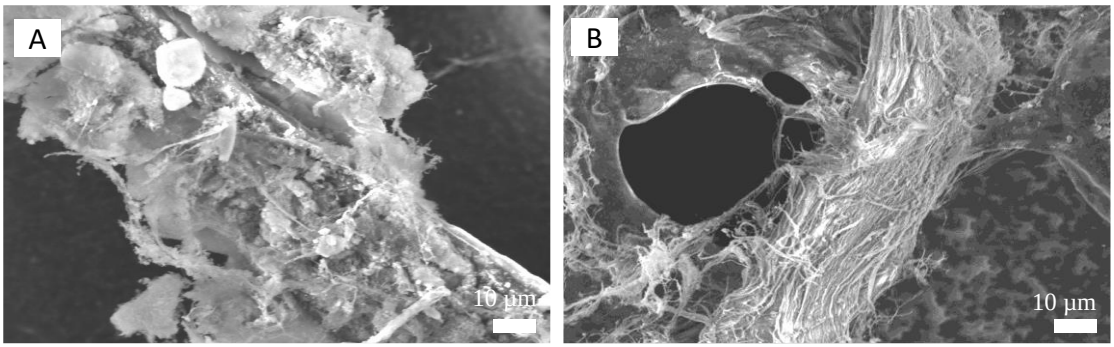

Figure 2- 17: SEM analysis of cellulose after silica formation. (A) with adsorption of ProS2-Sil-CBM, (B) without adsorption of ProS2-Sil-CBM.

Elemental analysis of the cellulose surface was done by using SEM-EDS to confirm the silica formation (Figure 2-18). Figure 2-18A shows the elemental analysis of the surface of cellulose fibers, which were overlaid on the previous SEM images. On the cellulose surface subjected to silica formation with adsorption of ProS2-Sil-CBM, the distribution of O and Si was mainly seen (Figure 2-18A left-side panel). In contrast, O and C were observed on cellulose subjected to silica formation without adsorption of ProS2-Sil-CBM (Figure 2-18A right-side panel). The presence of Si element on the cellulose fiber would suggest the formation of silica on the cellulose catalyzed by ProS2-Sil-CBM. Figure 2-18B shows the point EDS spectra of the same samples. Those

data also represent the presence of Si on the cellulose surface treated with ProS2-Sil-CBM whereas there was no such observation in the sample subjected to silica formation without immobilization of the fusion silicatein. These results suggest that immobilized fusion silicatein can catalyze the silica formation on a cellulose base material.

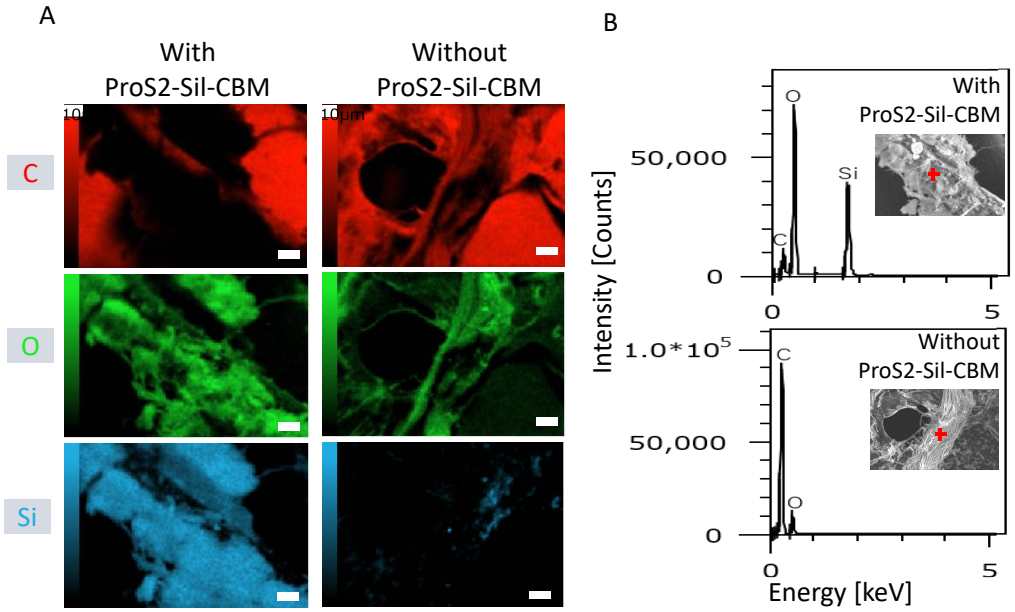

Figure 2- 18: Elemental and EDS analysis of cellulose subjected to silica formation. Cellulose was subjected to silica formation with or without adsorption of ProS2-Sil-CBM on cellulose. (A) Elemental analysis. Size bars indicate 10 μm. (B) EDS analysis.

Since ProS2-Sil did not adsorb on cellulose, silica polymerization was conducted in the presence of unbound ProS2-Sil (4.25 μM) in a solution as a control. However, SEM-EDS analysis of the treated cellulose showed a negligible amount of silica on cellulose in this system (Figure 2-19), which is a similar result as the cellulose treated without adsorption of ProS2-Sil-CBM (Figure 2-18). These results suggested that silicatein should be bound on the cellulose material to form silica on a target material.

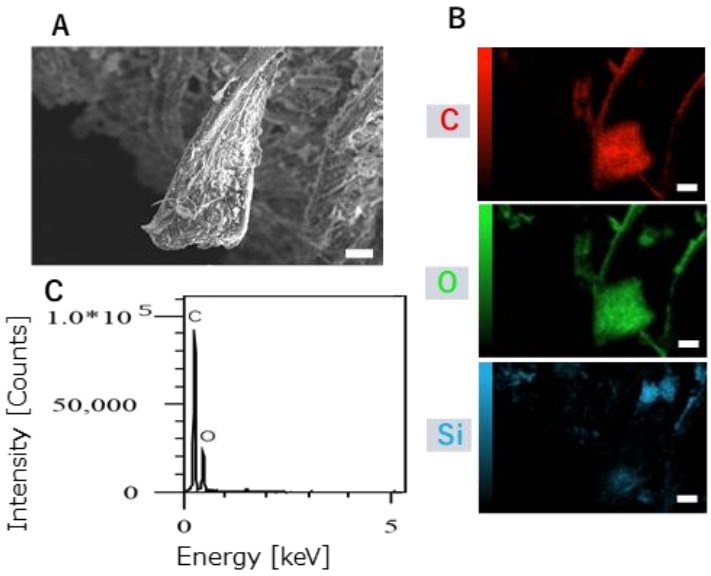

Figure 2- 19: SEM-EDS analysis of cellulose subjected to silica formation in the presence of ProS2-Sil (4.25 µM) in the solution. (A) SEM analysis (B) Elemental analysis. (C) EDS analysis. Size bars = 10 µm.

In many experiments, pre-hydrolyzed TEOS (silicic acid) has been used as a precursor. However, it has been reported that concentrations of silicic acid above 1 mM undergo autopolycondensation[88]. Autopolycondensation would occur in bulk solutions and may decrease the formation of silica on cellulose material. Therefore, direct use of TEOS would be an advantage to control autopolycondesation, allowing for the use of slightly higher concentrations such as 100 mM to increase the silica formation by the enzymatic reaction. In the previous studies, silicatein has been immobilized by directly applying chemicals on solid surfaces to form silica on materials[12]. However, the silica forming activity of silicatein was significantly lost upon contact with the solid surface[13]. Simpler and milder alternative methods to immobilize silicatein without direct surface contact are important to preserve the silica polymerization activity of silicatein. As demonstrated in this study, silicatein was immobilized on cellulose via CBM, avoiding direct contact of silicatein with cellulose

material. Therefore, this strategy can be efficiently employed to fabricate biohybrid material using silicatein.

However, in this study, the thickness of the silica formed on cellulose material was not studied. The thickness of silica on the cellulose could be changed by changing the time given for the silica polymerization. As another approach, after silica is formed on the cellulose material, silicatein fused with a silica binding tag could be immobilized on the silica. Using this method layer by layer silica disposition can be obtained on the material with controlled thickness.

2.5. Conclusions

Among expressed fusion silicateins, Sil-CBM was highly aggregated and difficult to obtain after refolding. ProS2-Sil and ProS2-Sil-CBM could be obtained as soluble forms. ProS2 soluble tag in ProS2-Sil-CBM maintained the solubility of the fusion protein in aqueous media for more than 24 h. Cleavage of the ProS2 tag led to the aggregation of Sil-CBM. ProS2-Sil and ProS2-Sil-CBM show similar silica polymerization activities. The fusion of ProS2 tag and CBM with silicatein did not inhibit the silica polymerization activity. ProS2-Sil-CBM showed 98% adsorption on cellulose at room temperature, and it acted as an interfacial catalyst to form silica on cellulose at room temperature and neutral pH. Overall, this technique could be used to design new proteins to form silica coatings on materials by changing the solid binding module.

CHAPTER 3

BIOLOGICAL ROUTE TO FABRICATE SILICA ON CHITIN USING FUSION SILICATEIN

3.1. Introduction

Many studies have reported the availability of inorganic-organic hybrid materials in nature from elementary to most complex organisms such as coccoliths, shells, diatom, and magnetotactic bacteria[98]. Those inorganic-organic hybrid materials compose biopolymers other than cellulose such as chitin, collagen, and proteins with inorganic compounds such as silica, calcium carbonate, calcium phosphates, calcium oxalates, and iron oxides[98]. In some studies, it has been reported silica-coated chitin hybrid materials which play an important role in the biomedicine field[99]. However, fabrication of silica on chitin in those studies has not been done using biological routes. Fabrication of silica-chitin hybrid materials under ambient conditions could enhance the applications allowing the immobilization of live cells and biomolecules.

Chitin is found in the exoskeleton of arthropods and the cell walls of fungi and yeast[100]. It is the second most abundant polysaccharide next to cellulose. Recent studies have found the availability of chitin within the biosilica in diatoms cell walls[101] and the skeletal structures of demosponges[102] as well as glass sponges[103–105]. Due to its biocompatibility, biodegradability, and non-toxic nature, chitin is used in agriculture, water and wastewater treatment, packaging materials, cosmetics, and biomedicine[106–108]. Due to the vast application of chitin, a study on the fabrication of silica on chitin using a biological route is imperative. To fabricate silica on chitin, silicatein should be immobilized on the target material[7].

As CBM is used for the cellulose base materials as the binding module, when changing the base material, the binding tag should be changed. There may be positive or negative impacts when fusing the silicatein with a binding domain. The impact could occur when changing the binding domain or changing the fusing position at either N-terminus or C-terminus. Therefore, it is imperative to study another fusion silicatein that is suitable for chitin. Other than CBMs that show affinity on cellulose, many different solid-binding modules have been studied. Those solid-binding modules show an affinity for different target materials such as chitin[72, 109], zeolite[110], and metals[111]. The use of a solid-binding module to immobilize silicatein helps to avoid direct contact between silicatein and the solid surface. They can also be used to purify proteins, immobilize proteins to enhance their stability, and bind materials together to form nanostructures[112–114].

Chitinases are a group of enzymes that can hydrolyze chitin and are found in organisms such as bacteria, insects, higher plants, and animals[109]. They belong to the glycoside hydrolase families 18 and 19[115, 116]. Chitinase consists of two domains: a catalytic domain and a chitin-binding domain (ChBD). Chitinase binds to chitin material with the help of the ChBD while allowing the catalytic domain to effectively degrade chitin[109]. The ChBD found in chitinase A1 in *Bacillus circulans* WL-1 is a low-molecular-weight protein that can selectively bind to chitin[72]. The tertiary structure of the chitin-binding domain of chitinase A1 is shown in Figure 3-1. Similar to the fusion protein ProS2-Sil-CBM which is explained in Chapter 2, a protein fused with the ChBD can also be selectively adsorbed onto chitin. In this study, silicatein was fused with the ChBD, for the immobilization of silicatein on chitin, and a novel soluble tag, for the enhancement of silicatein's solubility in an aqueous medium.

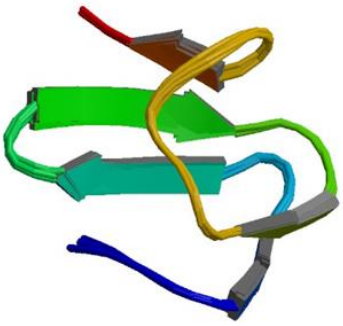

Figure 3- 1: The tertiary structure of the chitin-binding domain of chitinase A1 (PDB ID - 1ED7).

In the present study, silicatein (Sil) was fused with ChBD to get Sil-ChBD, and the solubility of Sil-ChBD was observed. Even though Sil-ChBD could get expressed successfully, it was difficult to obtain in a soluble form due to its lack of solubility. Therefore, it was necessary to improve the solubility of Sil-ChBD. To improve the solubility, ProS2 tag was fused to the N-terminus of Sil-ChBD. Together the interfacial catalyst, ProS2-Sil-ChBD was soluble. However, it showed a relatively low silica polymerization activity than the ProS2-Sil, a soluble fusion silicatein. Therefore, it was necessary to change the order of fusion proteins. Since the pCold ProS2 expression vector is a patented one, changing the ProS2 tag was difficult. Instead of ProS2 it may need another soluble tag that can handle without restriction.

A solubilizing tag is a short polypeptide chain that can enhance the solubility of a protein by fusing with a target protein using genetic recombination technology. Recent studies have shown that the fusion of a hydrophilic protein tag with a less water-soluble protein could enhance the solubility of the fusion protein in aqueous media[77, 117]. The ice nucleus protein InaK from *Pseudomonas syringae* consists of three main domains: InakN at the N-terminus, which binds to the membrane; the ice nucleus site,

which consists of repeating sequences; and InakC at the C-terminus, which extends to the cell surface (Figure 3-2). InakC is known to exhibit very high hydrophilicity[65]. Therefore, InakC is a soluble protein tag that can use to replace the ProS2.

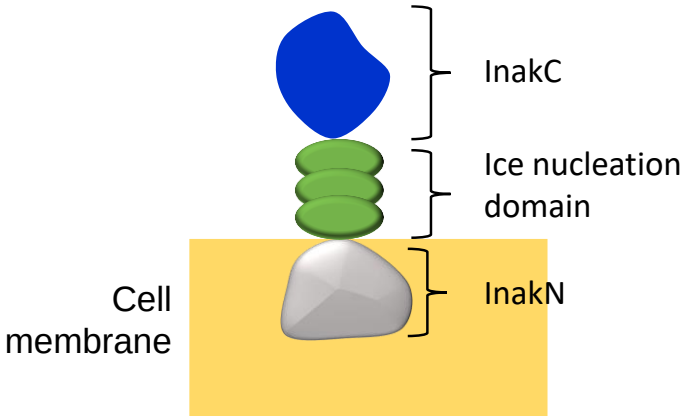

Figure 3- 2: Conceptual drawing of InaK.

Accordingly, to fabricate silica-chitin hybrid materials using a fusion silicatien containing both InakC and ChBD, was designed. Here the both InakC and ChBD were fused to the N-terminus of silicatein. Together, InakC-ChBD-Sil could be soluble and bound to chitin to act as an interfacial catalyst to form silica on chitin under mild conditions. The conceptual diagram of silica formation on chitin is shown in Figure 3-3. Since silica formation is carried out under mild conditions, this approach is a promising technique for the fabrication of inorganic-organic biohybrid materials to immobilize live cells and biomolecules such as proteins and drugs, in order to design next-generation materials while enhancing their application in technological and biomedical fields.

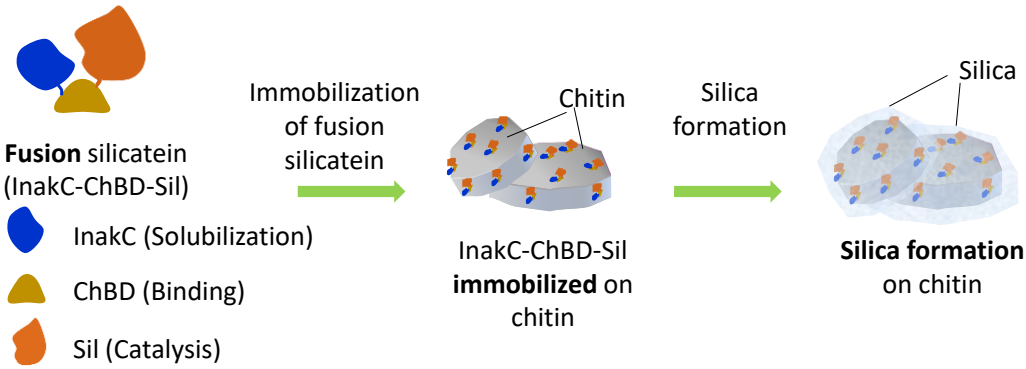

Figure 3- 3: The conceptual diagram to show silica formation on chitin through the fusion silicatein.

3.2. Objective

The objective of this study was to fabricate silica-chitin hybrid materials using the fusion silicatien that is soluble and can bind on chitin to act as an interfacial catalyst to form silica on chitin under mild conditions.

3.3. Materials and methods

3.3.1. Construction of the fusion genes

Silicatein *α* cDNA from *S. domuncula* (accession number CAI46305), which encodes the mature enzyme (aa115-330), the InakC gene from *P. syringae* (accession number AAB66891), and the ChBD gene from *B. circulans* WL-1 (accession number AAA81528, aa 655–697) were synthesized by Eurofins Genomics with optimization for expression in *E. coli*. As illustrated below the gene and vector construction were performed to express three fusion silicateins, Sil-ChBD, ProS2-Sil-ChBD and InakC-ChBD-Sil. The nucleotide sequence of primers and PCR conditions used in this work are shown in Table 3-1 and Table 3-2, respectively.

Table 3- 1: Nucleotide sequence of primers used in this study.

Primer	Nucleotide sequence
F1	CATCATCATCATATGGACTATCCGGAAGCAGTG
F2	TCTTATCCAACCCTGGCCTGGCAAGTCAACACT
F3	TCGAAGGTAGGCATATGGACTATCCGGAAGCAGTG
F4	ATCATCATCATCATATGTTTCGTCTGTGGGATGGC
F5	GGGCCCTCCGCGGGTGCCTGGCAAGTCAACACT
F6	TTGTGGCAGCTGCAGGACTATCCGGAAGCAGTG
R1	GTTGACTTGCCAGGCCAGGGTTGGATAAGAGGC
R2	ATTCGGATCCCTCGAGCTGCAGCTGCCACAACGC
R3	GTTGACTTGCCAGGCACCCGCGGAGGGCCCCTG
R4	TGCTTCCGGATAGTCCTGCAGCTGCCACAACGC
R5	ATTCGGATCCCTCGAGCAGGGTTGGATAAGAGGC

Table 3- 2: PCR conditions for gene amplification and overlap PCR.

Stage	PCR for cloning gene		Overlap PCR		Cycles
	Temperature (°C)	Time	Temperature (°C)	Time	
Pre denaturation	98.0	30 s	98.0	30 s	-
Denaturation	98.0	10 s	98.0	10 s	35
Annealing	55.0	15 s	56.7	5 s	
Extension	72.0	5 s	72.0	5 s	
Final extension	72.0	1 min	72.0	1 min	-

Sil-ChBD: As illustrated in Figure 3-4, The gene encodes silicatein amplified with F1 and R1 primers, and ChBD gene amplified with F2 and R2 were combined using overlap PCR. The amplified gene was inserted into pCold II expression vector (Takara Bio Inc., Japan) cut at *Nde*I and *Xho*I restriction enzyme sites using In-Fusion (Takara Bio Inc., Japan) to express the protein named Sil-ChBD.

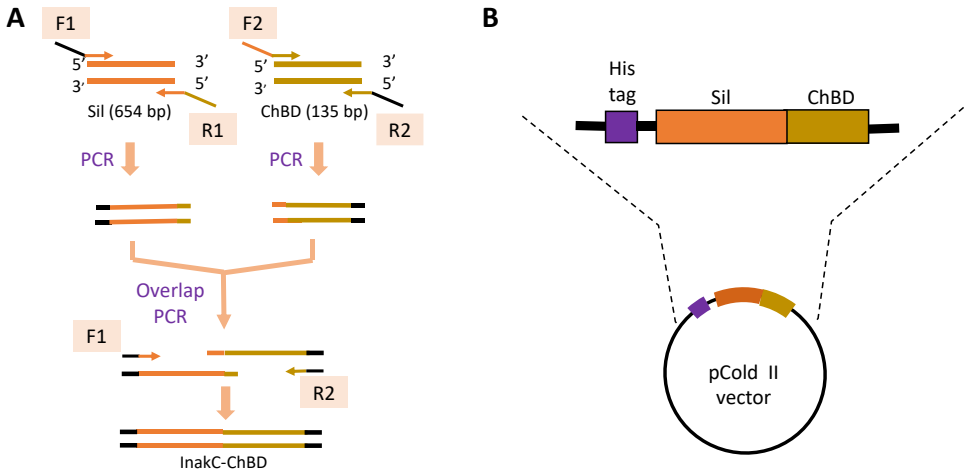

Figure 3- 4: Gene and vector construction to express Sil-ChBD. (A) Gene construction through PCR. (B) The gene order of Sil-ChBD.

ProS2-Sil-ChBD: Figure 3-5 illustrates the gene and vector construction for the expression of ProS2-Sil-ChBD. The gene Sil-ChBD in pCold II vector was amplified with F3 and R2 primers. The amplified gene was inserted into pCold ProS2 expression vector (Takara Bio Inc., Japan) cut at *Nde*I and *Xho*I restriction enzyme sites using In-Fusion to express the protein named ProS2-Sil-ChBD.

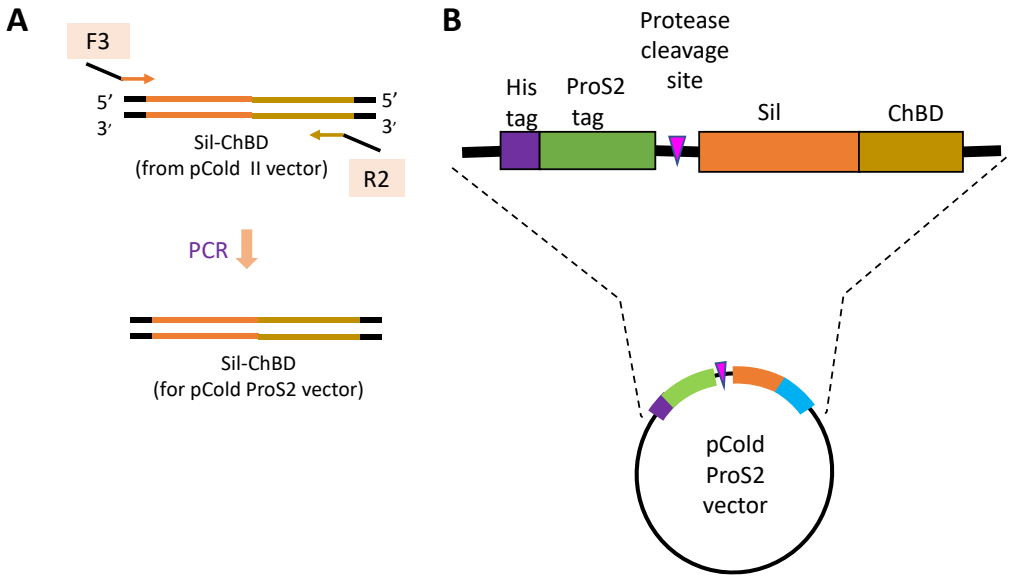

Figure 3- 5: Gene and vector construction to express ProS2-Sil-ChBD. (A) Gene construction through PCR. (B) The gene order of ProS2-Sil-ChBD.

InakC-ChBD-Sil: Figure 3-6 illustrates the gene and vector construction to express InakC-ChBD-Sil. InakC, ChBD, and silicatein genes were amplified using the set of F4-R3, F5-R4, and F6-R5 primers, respectively. The amplified InakC and ChBD genes were combined through overlap PCR to obtain the InakC-ChBD gene. Next, the InakC-ChBD-Sil gene was obtained by combining the InakC-ChBD gene with the amplified Sil gene using overlap PCR. The InakC-ChBD-Sil gene was subcloned into the pCold II expression vector cut at *Nde*I and *Xho*I restriction enzyme sites to construct the pCold_InakC-ChBD-Sil vector.

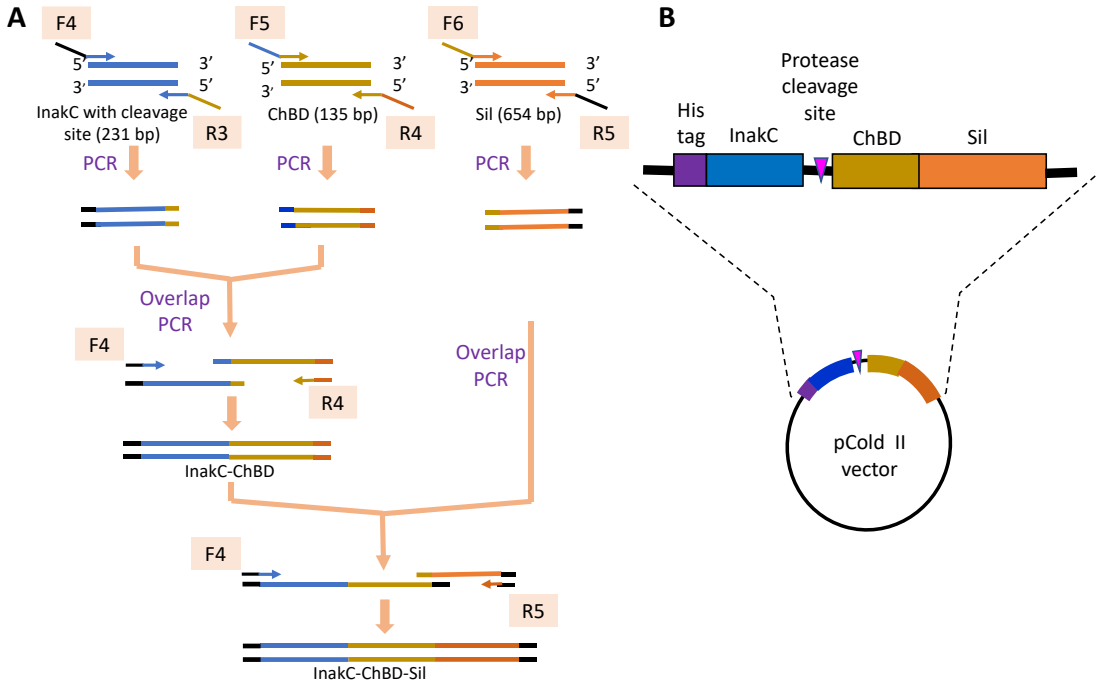

Figure 3- 6: Gene and vector construction to express InakC-ChBD-Sil. (A) Gene construction through PCR. (B) The gene order of InakC-ChBD-Sil.

Finally, the transformation of the constructed vectors into *E. coli* BL21(DE3) was performed, and the success of transformation was check using colony PCR.

3.3.2. Expression of recombinant proteins

E. coli BL21(DE3) cells transformed with the constructed vectors to express Sil-ChBD, ProS2-Sil-ChBD and InakC-ChBD-Sil were grown separately at 15 °C with shaking at 160 rpm for 24 h in LB by inducing protein expression using 1.0 mM IPTG, as previously reported[117]. The bacterial cells were harvested by centrifugation at 4000 × g and 4 °C for 20 min. The resultant pellets were resuspended in sonication buffer (20 mM Tris/HCl, pH 8.0; 1 mM EDTA; and 0.5 M NaCl), and the cells were disrupted using an ultrasound disintegrator (VCX-130, Sonic & Materials Inc., USA). The samples were then centrifuged at 25, 000 × g and 4 °C for 20 min. The precipitated

fractions were washed twice with lysis buffer containing a surfactant (20 mM Tris/HCl, pH 8.0; 1 mM EDTA; 0.5 M NaCl; and 4% TritonX-100) and washed twice with ultrapure water to remove membrane proteins. Resulted inclusion bodies were used for the purification of target proteins.

3.3.3. Purification of recombinant proteins

After washing the inclusion bodies (insoluble faction) containing the target fusion proteins, 300 mg of the inclusion bodies were added into 5 mL of denaturation buffer containing urea (50 mM Tris/HCl, pH 8.0, 8 M urea, 10 mM DTT), and the mixture was shaken at 160 rpm for 2 to 3 h until the solution gets clear. Then the mixture was centrifuged (25, 000 × g, 20 min, 4 °C) for the removal of insoluble impurities. Next, the denatured target proteins in the supernatant were purified by immobilized metal ion affinity chromatography on a 5 mL Ni-NTA column as previously reported[57]. The content of the buffers and the procedure followed during the Ni-NTA column purification were similar to Table 2-3 and Table 2-4 in Chapter 2, respectively. When passing the buffers and the denatured target proteins through the Ni-NTA column using a syringe, a syringe filter (Hawach Scientific, nylon membrane, 0.22 μm pore size) was used to prevent damages could occur by entering foreign particles into the Ni-NTA column. The proteins purified using the Ni-NTA column were still in the denatured condition. Therefore, they should be subjected to refolding to obtain the active proteins.

3.3.4. Refolding and ultrafiltration of purified proteins

For the refolding of proteins, the urea used as denaturant should be removed from the solution. For that, a dialysis method was used for each protein. The dialysis membrane (Thermo Fisher Scientific, 6000-8000 NMWCO), was placed in a beaker containing distilled water and washed while stirring with a magnetic stir bar. The

dialysis membrane was opened, and the inside of the dialysis membrane was washed. The end of the dialysis membrane was bound with a clip, and the protein solution recovered by the Ni-NTA column purification was filled followed by the clipping the other end without trapping air bubbles. Then the dialysis membrane containing the protein was submerged in the refolding buffer (50 mM tris/HCl, pH 8.5, 0.5 M L-Arginine, 9 mM red/glutathione, 1 mM ox/glutathione, 0.3 M NaCl, 1 mM KCl) (purified protein volume filled into dialysis membrane: refolding buffer volume, 1:20). Dialysis was performed at 4 °C for 36 hours while stirring the buffer solution with a magnetic stir bar[85, 86]. The refolding buffer was exchanged twice during the dialysis. After 36 h hours, the protein solution in the dialysis membrane was transferred to a centrifuge tube and centrifuged at 4 °C, 15, 000 × g for 15 min to confirm that precipitation could not be performed. The refolding buffer of the target proteins was then replaced with 50 mM Tris/HCl buffer (pH 9.0, 8 mM NaCl) by ultrafiltration (Amicon® Ultra-15 centrifuge filters, 10000 NMWCO). Finally, the concentrations of refolded proteins were calculated using the Bradford assay (Bradford Protein Assay Kit, Takara Bio Inc., Japan)[87].

3.3.5. Assay for solubility of recombinant proteins and cleavage of InakC tag

The purified recombinant proteins were assayed for their self-assembly without and with cleavage of the ProS2 and InakC tags. ProS2-Sil-ChBD and InakC-ChBD-Sil were dissolved in 50 mM Tris/HCl buffer (pH 7.4, 150 mM NaCl) separately to obtain a final concentration of 10 μM each. The solutions were incubated at 25 °C for 24 h. During the incubation period, the solutions were monitored for turbidity.

3.3.6. Cleavage of ProS2 or InakC tag

ProS2-Sil-ChBD was subjected to removal of the ProS2 tag using a site-specific protease that can cleave the peptide sequence between ProS2 and Sil. Similarly, InakC-ChBD-Sil also was subjected to removal of the InakC tag using a site-specific protease that can cleave the peptide sequence between InakC and ChBD. ProS2-Sil-ChBD and InakC-ChBD-Sil (10 μM of each) in Tris/HCl buffer was separately treated with HRV 3C Protease (10 U, Takara Bio Inc., Japan) at 25 ℃ for 1 h. During the incubation period, the sample mixtures were observed for turbidity caused by the self-aggregation.

3.3.7. Determination of enzymatic activity

The enzymatic activity of the fusion silicateins was determined as previously described[7]. InakC-ChBD-Sil (1.66 μM) and 100 mM TEOS as the substrate for the enzymes were incubated in Tris/HCl buffer at 25 ℃ with shaking at 185 rpm for 24 h[9]. As a control, silica polymerization activity was determined in the absence of proteins under the same conditions. The formed biosilica was recovered using centrifugation at 16, 000 × g and 4 ℃ for 10 min and washed three times each with ethanol and ultrapure water, followed by freeze-drying. The freeze-dried biosilica samples were hydrolyzed to silicic acid by treating with 1 M NaOH for 30 min at 90 ℃ and neutralizing with HCl. The concentration of the silicic acid (hydrolyzed silica) was then determined using the molybdenum blue colorimetric method[18]. The absorbance values were determined at 810 nm wavelength to calculate the absolute amounts of silicic acid based on the calibration curve using a silicon standard solution (1000 ppm; Wako Pure Chemical Industries Ltd., Japan). Using the same method, the silica polymerization activity of ProS2-Sil, a solubility-enhanced silicatein obtained by fusing

with the ProS2 tag, which has an activity similar to that of mature silicatein, was calculated for comparison with that of InakC-ChBD-Sil.

3.3.8. Analysis of protein adsorption on chitin and silica formation

Reagent-grade chitin (Wako Pure Chemical Industries Ltd.) was used for protein adsorption. The specific surface area was measured by N_2 gas adsorption (Autosorb 6AG, Yuasa Ionics) and found to be 4.55 m^2/g. To analyze the adsorption of InakC-ChBD-Sil on chitin, 0.01 g of chitin was added to 50 mM Tris/HCl buffer solutions containing 10 µM of InakC-ChBD-Sil, and the solutions were shaken for 1.5 h at 25 °C. During shaking, 20 µL of the solutions without chitin were periodically aliquoted to analyze the remaining concentration of the protein using Bradford assay. After 1.5 h, the chitin was recovered by centrifuging and washed twice with 50 mM Tris/HCl buffer. The chitin material that absorbed InakC-ChBD-Sil was subjected to silica formation using 100 mM TEOS as the precursor in 50 mM Tris/HCl buffer at 25 °C with shaking at 185 rpm for 24 h[9]. The treated chitin was recovered and washed three times each with ethanol and ultrapure water, followed by freeze-drying for 2 days.

3.3.9. Scanning electron microscope analysis

After freeze-drying, the biosilica formed on the chitin material was examined using SEM (Acceleration voltage: 5 kV, JEOL JSM-IT200 InTouchScope™, Germany) without coating. Elements present on the chitin surfaces subjected to silica formation were analyzed using EDS (without coating; acceleration voltage: 10 kV for point EDS; JEOL JSM-IT200 InTouchScope™, Germany).

3.4. Results and discussion

3.4.1. Expression of fusion proteins

After the construction of vectors to express each protein, the correctness of the vectors was got confirmed by DNA sequencing. Then they were transformed into *E. coli* for the protein expression. Amino acid sequences of fusion silicateins expressed in this study are shown in Figure S4-6 (Appendix I).

Sil-ChBD: The constructed vector to express Sil-ChBD was transformed into *E. coli*. The transformed *E. coli* to express Sil-ChBD and the colony PCR done to check the successfulness of the transformation are shown in Figure 3-7.

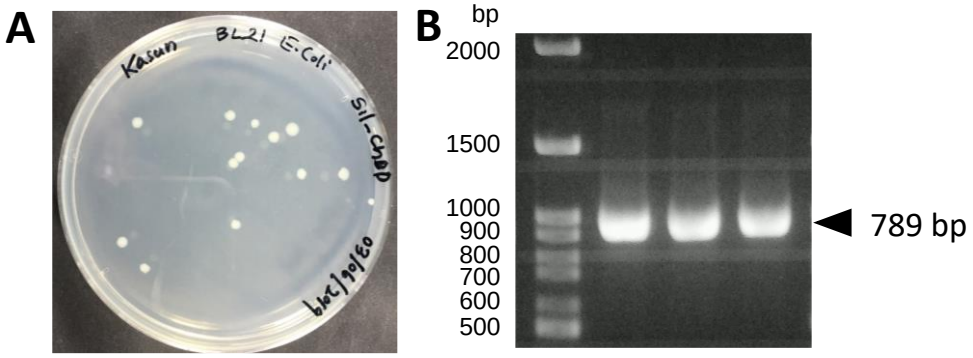

Figure 3- 7: Transformation of *E. coli* to express Sil-ChBD. (A) Transformed *E. coli* to express Sil-ChBD. (B) Colony PCR.

The molecular weight of the Sil-ChBD was 30 kDa. Figure 3-8 shows the SDS-PAGE analysis of Sil-ChBD. As shown in Figure 3-8A, Sil-ChBD has expressed as an insoluble protein. Protein overexpression may result in the formation of inclusion bodies, which are insoluble, inactive, and relatively pure, intact proteins. To obtain soluble and active proteins, purification under denaturation and refolding through

dialysis or dilution is typically performed[88, 89]. Here, urea (8 M) was used as the denaturant to dissolve the inclusion bodies before Ni-NTA column purification, and the purified target protein was refolded using dialysis. Therefore, after denaturation of Sil-ChBD using urea, Sil-ChBD was purified by using Ni-NTA column purification followed by refolding. SDS-PAGE analysis in Figure 3-8B shows Sil-ChBD after Ni-NTA column purification and refolding.

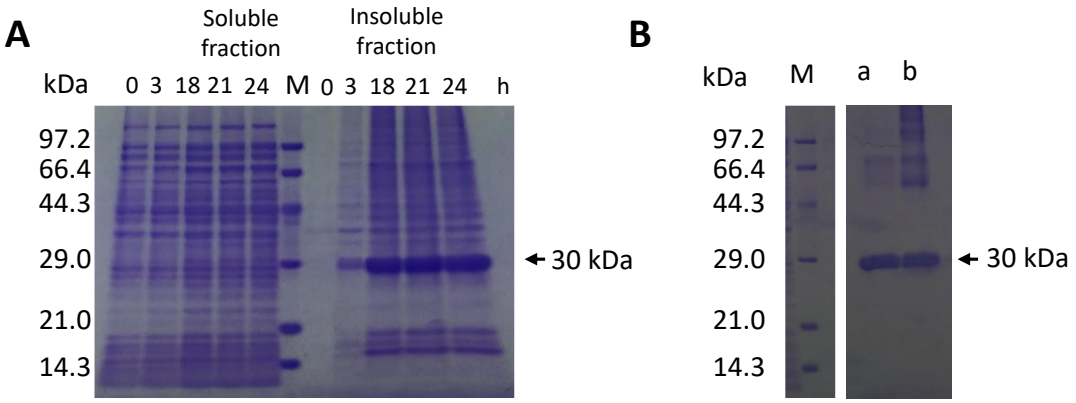

Figure 3- 8: SDS-PAGE analysis for Sil-ChBD. (A) SDS-PAGE analysis for expression of Sil-ChBD. (B) (a) after Ni-NTA column purification, (b) after refolding of purified protein. M: Molecular weight marker.

ProS2-Sil-ChBD: The constructed vector to express ProS2-Sil-ChBD was transformed into *E. coli* (Figure 3-9A). The transformation was confirmed by colony PCR as shown in Figure 3-9B.

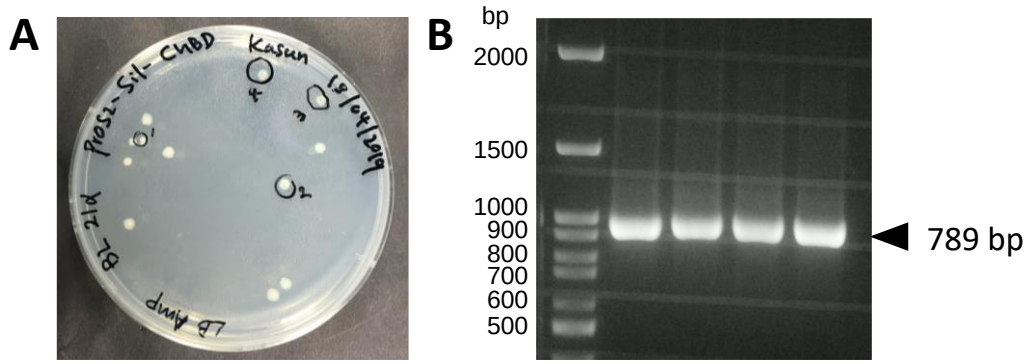

Figure 3- 9: Transformation of *E. coli* to express ProS2-Sil-ChBD. (A) Transformed *E. coli* to express ProS2-Sil-ChBD. (B) Colony PCR.

The molecular weight of the ProS2-Sil-ChBD was 53 kDa. Figure 3-10 shows the SDS-PAGE analysis of ProS2-Sil-ChBD. As shown in Figure 3-10A ProS2-Sil-ChBD also has expressed as an insoluble protein. Therefore, after denaturation of ProS2-Sil-ChBD, it was purified by using Ni-NTA column purification followed by refolding and ultrafiltration. SDS-PAGE analysis in Figure 3-10B shows ProS2-Sil-ChBD after Ni-NTA column purification and refolding.

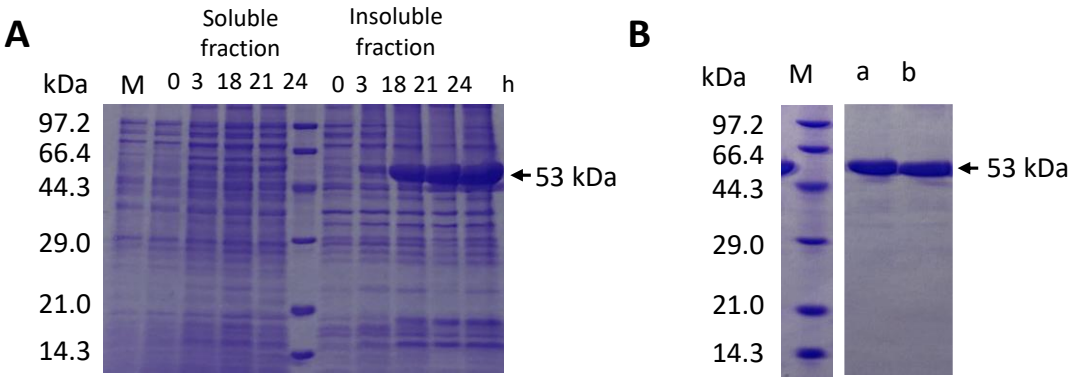

Figure 3- 10: SDS-PAGE analysis for ProS2-Sil-ChBD. (A) SDS-PAGE analysis for expression of ProS2-Sil-ChBD. (B) (a) after Ni-NTA column purification, (b) after refolding of purified protein. M: Molecular weight marker.

InakC-ChBD-Sil: The constructed vector to express InakC-ChBD-Sil was transformed into *E. coli*, and the success of the transformation was checked using colony PCR. Figure 3-11 shows the transformed *E. coli,* and the colony PCR results.

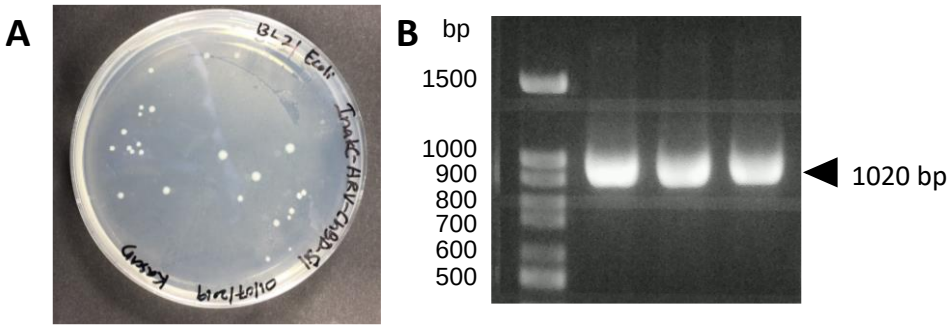

Figure 3- 11: Transformation of *E. coli* to express InakC-ChBD-Sil. (A) Transformed *E. coli* to express InakC-ChBD-Sil. (B) Colony PCR

Next, the protein expression and purification of the InakC-ChBD-Sil (38 kDa) were performed. Figure 3-12 shows the SDS-PAGE analysis for expression, after Ni-NTA column purification and refolding of InakC-ChBD-Sil. The SDS-PAGE results in Figure 3-12A shows the profiles of the soluble and insoluble proteins expressed in the transformed *E. coli* cells. Overexpression of the expected protein with molecular weight 38 kDa (between the 29.0 kDa and 44.3 kDa protein bands) in the insoluble fraction was observed. Figure 3-12B shows the SDS-PAGE results after Ni-NTA column purification and refolding of InakC-ChBD-Sil.

The refolding buffer was replaced with Tris/HCl buffer using ultrafiltration because it has been reported that amines such as L-arginine, a protein stabilizer used in the refolding buffer, catalyze silicic acid polymerization[90]. During this process, ProS2-Sil-ChBD and InakC-ChBD-Sil were successfully obtained just after ultrafiltration, while Sil-ChBD aggregated quickly in the ultrafiltration tube becoming turbid in the solution. Those observations suggested that ProS2-Sil-ChBD and InakC-ChBD-Sil

could be obtained in a soluble form while Sil-ChBD could not. Therefore, further solubility of ProS2-Sil-ChBD and InakC-ChBD-Sil were investigated.

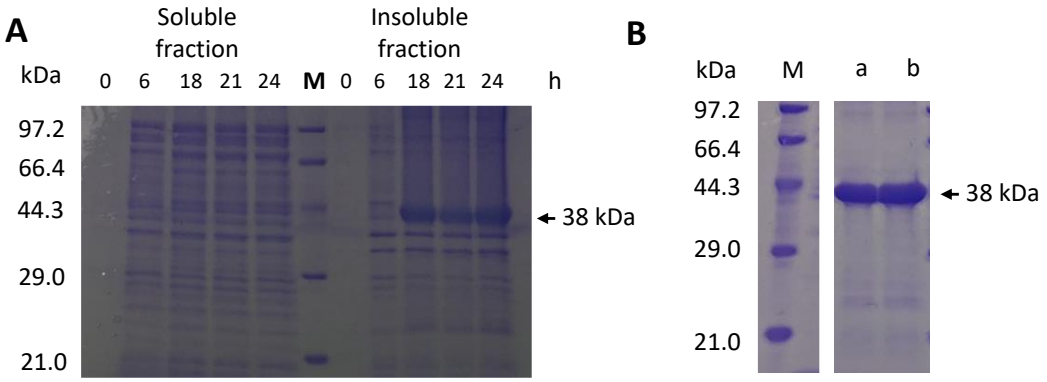

Figure 3- 12: SDS-PAGE analysis for InakC-ChBD-Sil. (A) SDS-PAGE analysis for expression of InakC-ChBD-Sil. (B) (a) after Ni-NTA column purification, (b) after refolding of purified protein. M: Molecular weight marker.

3.4.2. Solubility of fusion proteins

The solubility of ProS2-Sil-ChBD and InakC-ChBD-Sil in aqueous media were analyzed. It was found that InakC-ChBD-Sil maintained its solubility for more than 24 h without forming a cloud or precipitate in the aqueous solution. However, when the InakC tag was cleaved from InakC-ChBD-Sil using protease, ChBD-Sil self-aggregated to form a cloud and then precipitated within 1 h, as shown in Figure 3-13. Similar results were observed for the ProS2-Sil-ChBD (data are not shown). These results suggested that fusion of the InakC or ProS2 tag enhanced the solubility of the fusion silicatein. InakC is the truncated C-terminus of the InaK ice nucleation protein and is highly hydrophilic[118]. Studies have shown that the hydrophobic site located in the N-terminus of silicatein affects its self-aggregation in aqueous media[57, 93]. Similar to the results of Chapter 2, it was revealed that the fusion of InakC or ProS2 improved the solubility of the fusion silicateins in an aqueous media.

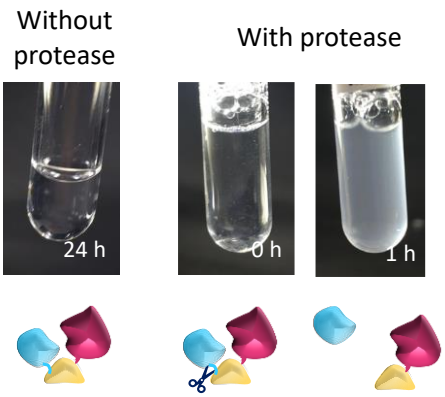

Figure 3- 13. Solubility of InakC-ChBD-Sil without and with cleavage of InakC tag.

3.4.3. Silica polymerization activity of soluble fusion silicatein

The silica polymerization activity of the soluble fusion silicateins in an aqueous solution was investigated using TEOS as a precursor. The silica formed during the silica polymerization reaction was isolated by centrifugation and washed with ethanol and ultra-pure water, followed by freeze-drying. Then, the silica was hydrolyzed by heating in 1M NaOH, and acidified with HCl to produce silicic acid. The silica polymerization activity was expressed as the concentration of silicic acid, which was measured by the molybdenum blue colorimetric method. The silica polymerization activity of ProS2-Sil-ChBD and InakC-ChBD-Sil were compared with another recently reported soluble silicatein called ProS2-Sil. Figure 3-14 shows the silica polymerization activity of ProS2-Sil, ProS2-Sil-ChBD and InakC-ChBD-Sil, which were 13.3 mM, 4.5 mM and 13.7 mM respectively. This suggests that InakC-ChBD-Sil showed the same activity as ProS2-Sil while ProS2-Sil-ChBD showed relatively low activity.

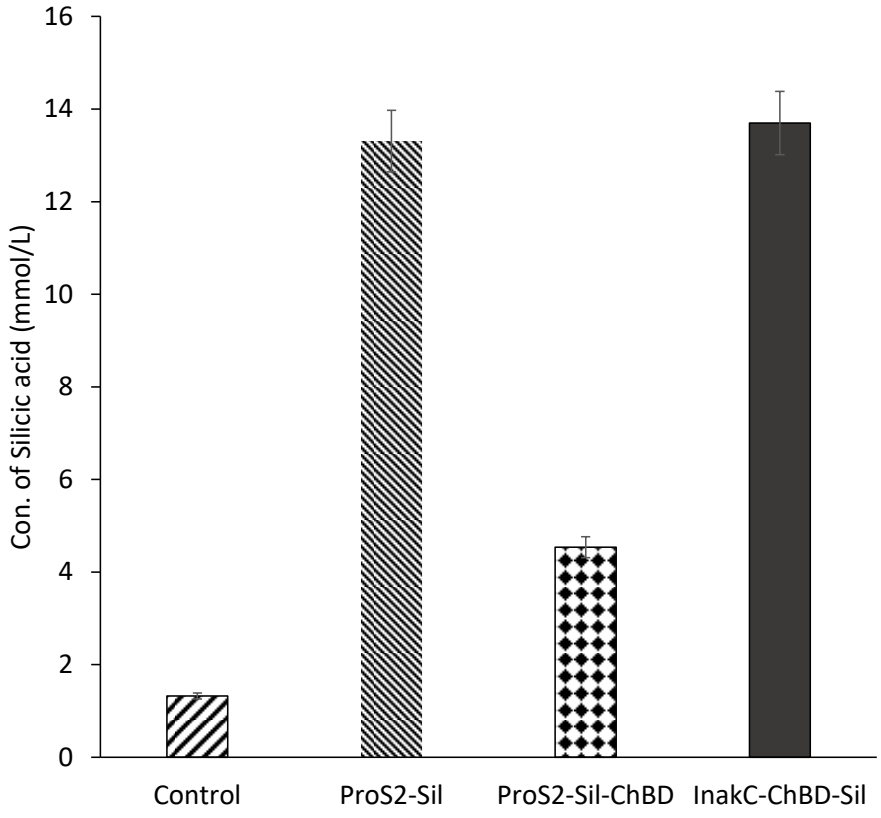

Figure 3- 14: Enzymatic activity of the fusion silicateins. In the control experiment, the activity was determined in the absence of proteins (Control). Experiments were conducted in triplicate; data represent the average of three experiments with error bars indicating the standard deviation.

Since a higher activity was shown by InakC-ChBD-Sil, it was studied for the adsorption on chitin and to use as an interfacial catalyst to fabricate silica on chitin.

3.4.4. Adsorption on chitin

These binding proteins show selective adsorption on a material. As chitin was used as the base material in this study, a ChBD was employed. The ChBD used in this study is a chitin-binding module of chitinase from *B. circulans* that has shown an affinity for chitin and chitosan[72]. Figure 3-15 shows the time course adsorption of the InakC-

ChBD-Sil on chitin. It showed almost 100% adsorption on chitin material within 1.5 h, indicating its rapid binding ability. The amount of InakC-ChBD-Sil adsorbed on chitin was 0.22 µmol/m^2. These results suggest that the fusion of both InakC and silicatein with ChBD did not inhibit its binding ability. According to the studies related to ChBD mechanism, ChBD was found to bind to chitin through hydrophobic interactions[72].

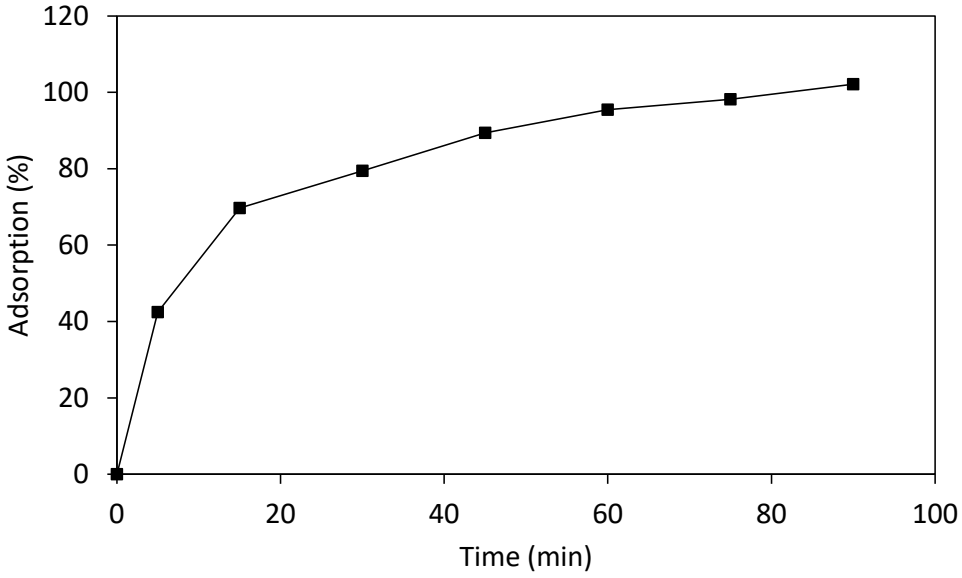

Figure 3- 15: Adsorption studies of InakC-ChBD-Sil on chitin

3.4.5. Silica formation on chitin

If silicatein is immobilized on a material, silica could be formed on the material. Therefore, InakC-ChBD-Sil was immobilized on chitin using ChBD, and it was subjected to silica formation. Figure 3-16 shows the SEM images of chitin subjected to silica formation with and without adsorption of InakC-ChBD-Sil. However, it was difficult to identify a clear difference between the SEM images with or without InakC-ChBD-Sil. Therefore, the elemental analysis of chitin was investigated using EDS.

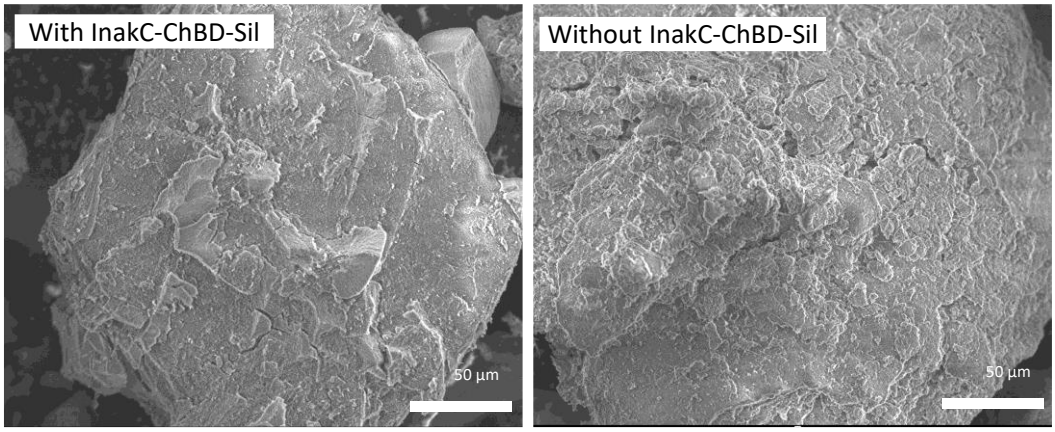

Figure 3- 16: SEM images of chitin after silica formation with and without adsorption of InakC-ChBD-Sil.

The elemental analysis and EDS spectrum resulted for chitin subjected to silica formation with and without adsorption of InakC-ChBD-Sil are shown in Figure 3-17. Chitin contains C, O, H, and N. Figure 3-17A shows the elements present on chitin samples that were subjected to silica formation with and without adsorption of InakC-ChBD-Sil. According to the results, it shows a higher amount of Si on the chitin with adsorption of InakC-ChBD-Sil than on that of without adsorption of InakC-ChBD-Sil. Nitrogen was not detected in the sample with InakC-ChBD-Sil. This could be due to the biosilica covering of chitin formed by the adsorbed fusion silicatein. EDS spectra in Figure 3-17B also suggested the same results.

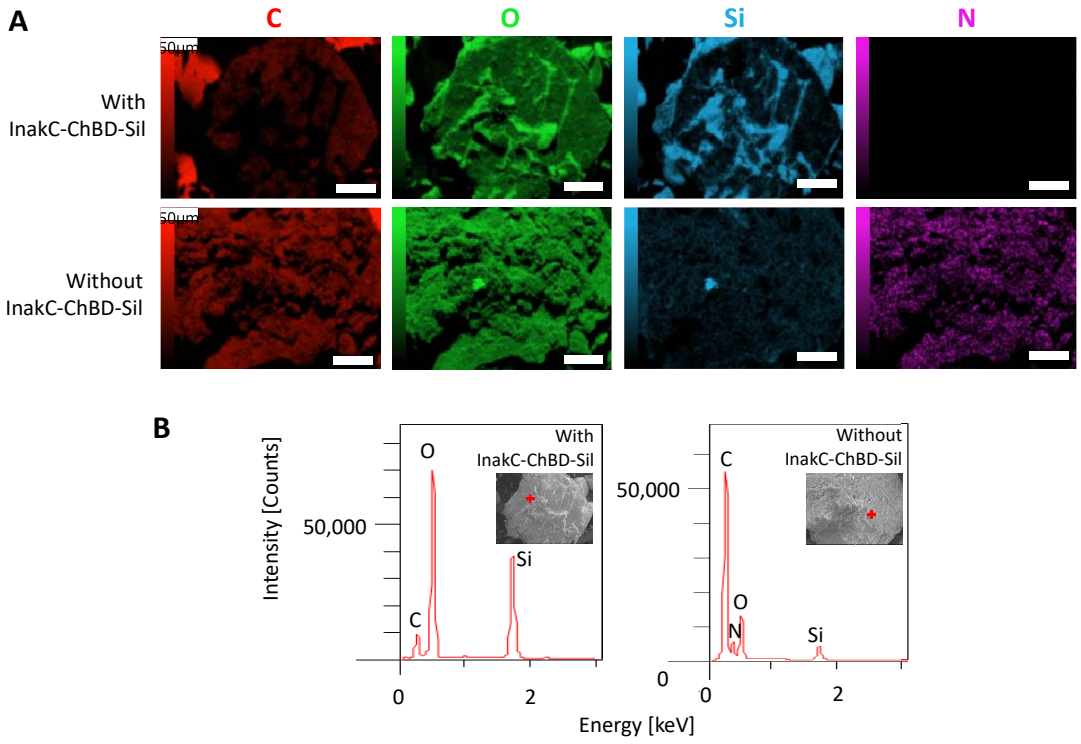

Figure 3- 17: Elemental analysis of chitin subjected to silica formation with and without adsorption of InakC-ChBD-Sil. (A) Elemental analysis. (B) EDS spectrum. Size bars indicate 50 µm.

In some studies, silicatein has been immobilized on solid surfaces by using chemical links or self-assembly property[7, 13]. In those methods, the orientation of silicatein was not uniform, and the direct contact of silicatein with the solid surface could reduce its enzymatic activity. The use of a solid binding module would provide moderate immobilization, thereby preserving the enzymatic activity of silicatien, and arranging the fusion silicatein in a uniform orientation[95, 96, 119]. The method demonstrated in this study could be a simpler alternative method to fabricate silica on a chitin material by immobilizing silicatein without direct surface contact to fabricate biohybrid materials using silicatein.

3.5. Conclusions

Among expressed fusion silicateins, Sil-ChBD was highly aggregated and difficult to obtain after refolding. ProS2-Sil-ChBD and InakC-ChBD-Sil could be obtained as soluble forms. ProS2 and InakC soluble tags in ProS2-Sil-ChBD and InakC-ChBD-Sil maintained the solubility of the fusion proteins in aqueous media for more than 24 h, respectively. ProS2-Sil-ChBD showed a lower silica polymerization activity than ProS2-Sil. InakC-ChBD-Sil showed almost similar silica polymerization activity of ProS2-Sil. Neither the fusion of InakC nor ChBD inhibited the silica polymerization activity of fusion silicatein. InakC-ChBD-Sil adsorbed on chitin within 1.5 h. InakC-ChBD-Sil adsorbed on chitin acts as an interfacial catalyst to form silica on chitin under ambient conditions. These findings will contribute to the design of new proteins to form inorganic coatings on materials by changing the solid binding module to fabricate next-generation materials.

CHAPTER 4

BIOLOGICAL ROUTE TO FABRICATE CHITOSAN GEL-SILICA HYBRID IMMOBILIZED ENZYMES

4.1. Introduction

In Chapters 2 and 3, silica-cellulose and silica-chitin hybrid materials were fabricated respectively. As an advancement, in this study, immobilization of an enzyme in a hybrid material was focused. Enzymes are used in various fields such as biomedicine, energy generation and chemical industry due to their inexpensiveness and environmentally friendliness[120, 121]. Among the significant studies focused on the improvement of enzymatic properties, the immobilization of enzymes on insoluble solid supports is a technique that is widely used[122]. This technique significantly improves the stability of the biomolecules such as enzymes under various reaction conditions and enhances the reusability of biomolecules[123]. Moreover, the enzymes can be removed from the system easily to get high purity products[124, 125].

With the increase of demand for biomaterials, various biocompatible materials have been developed focusing on properties, benefits, limitations, and the use of alternative resources for its preparations. Hydrogels are one of the biomaterials that have been studied due to their various properties such as mechanical properties, responsiveness, and biodegradability, biocompatibility[126].

Hydrogels are three-dimensional networks of hydrophilic polymers[127–131]. They are categorized into physical or chemical gels depending on the interaction formed with polymeric chains during the gelation. In physical gel, ionic crosslinks, hydrogen bonds, or hydrophobic interactions are formed. In contrast, in chemical gels, irreversible covalent bonds are formed[126]. The swelling ability of Hydrogels allows

them to act as natural tissues, and they can release drugs based on external factors such as pH, light, magnetic field, and temperature.

Attention to polysaccharide-based hydrogels has been paid in the last decade due to their biocompatibility, biodegradability, non-toxicity, and low cost. Polysaccharides such as starch, carboxymethylcellulose, alginate, carrageenan, and chitosan are some candidates studied for biomedical applications[126, 129, 132]. Among them, chitosan plays an important role in the area of biotechnology[130, 133, 134]. Chitosan is a derivative of chitin. It can be dissolved in a solution below pH 6.3 by converting amine groups to ammonium groups. The solubility property in low pH conditions can be used for the preparation of pH-responsive Hydrogels that can apply in controlled drug release, contact lenses, scaffolds, cell growth, agriculture, and regenerative medicine[126].

The formation of chitosan gel-silica hybrid materials by covering the chitosan gel with silica will enhance the applications[135], allowing protection for actives on the surface[136–141] and/or support for carrying biomolecules for chemical or biological functions[135, 142–147]. The chitosan gel covered by silica particles can induce pH changes in aqueous environments allowing an environment to immobilize sensitive enzymes in the chitosan gel matrix. To fabricate silica on chitosan gel matrix, the same fusion protein, InakC-ChBD-Sil could be used because chitosan gel is a derivative of chitin. Therefore, the fabrication of chitosan gel-silica hybrid materials under physiological conditions using the fusion silicatein, InakC-ChBD-Sil that showed adsorption on chitin, was studied. The same strategy was employed to fabricate chitosan gel-silica hybrid materials by encapsulating horseradish peroxidase (HRP), a model enzyme used in biotechnology[3, 13] as illustrated in Figure 4-1. In this process, HRP is immobilized in the chitosan gel matrix during the formation of chitosan gel beads.

Then InakC-ChBD-Sil is adsorbed on the HRP encapsulated chitosan gel beads. Next, they are subjected to silica formation to result in HRP encapsulated chitosan gel-silica hybrid material.

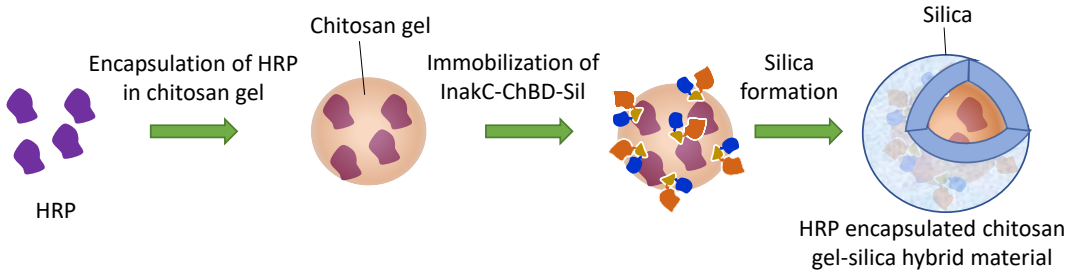

Figure 4- 1: The conceptual diagram to show the formation of HRP encapsulated chitosan gel-silica hybrid material.

HRP found in the roots of horseradish is a common enzyme used widely in the biochemistry field. It catalyzes the oxidation of various organic substrates such as 2,20-azino-di(3-ethylbenzothiazolin-6-sulfonate) (ABTS), 4-aminoantipyrine, phenol and benzidine, etc. by hydrogen peroxide[148–150]. For example, Figure 4-2 shows the reaction catalyzes by the HRP in the presence of organic substrates, 4-aminoantipyrine and phenol with hydrogen peroxide.

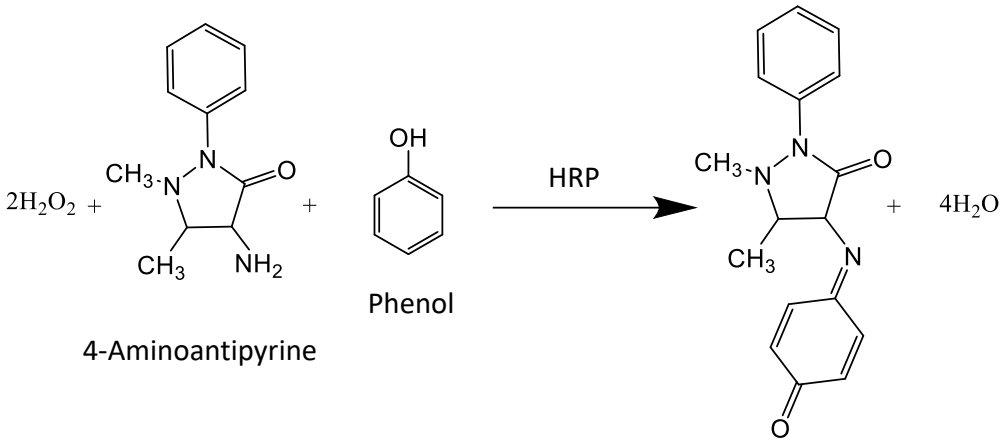

Figure 4- 2: Reaction catalysis by the HRP in the presence of 4-aminoantipyrine and phenol with hydrogen peroxide.

Another important factor that should be concerned is the detection of silica formed on chitosan gel. Even though SEM-EDS analysis can be used to detect gel samples, they should be freeze-dried to remove the water before the analysis. Since chitosan gel contains more than 90% of water, freeze-drying may affect the morphology. To overcome that problem, another method to detect the silica formed on chitosan was suggested using a fluorescent protein fused with a silica binding peptide. mCherry, a mutant fluorescent protein derived from the tetrameric *Discosoma* sp. red fluorescent protein, DsRed[151]. The excitation and emission maxima of mCherry are 587 nm and 610 nm, respectively. The silica binding peptide employed in this study was titania-binding peptide (TBP) (amino acid sequence: RKLPDAPGMHTW). It specifically binds to silica or titania. Together, TBP-mCherry can bind on silica, and emitted fluorescence from mCherry can be detected using a fluorescence microscope as illustrated in Figure 4-3.

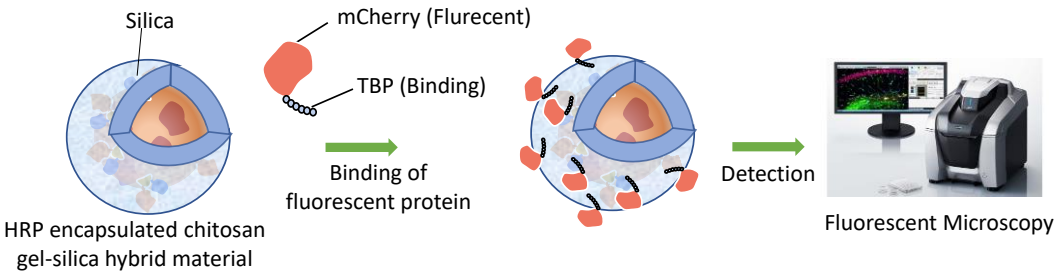

Figure 4- 3: The conceptual diagram to show detection of silica on the HRP encapsulated chitosan gel-silica hybrid.

4.2. Objective

The objective of this research was to fabricate a novel chitosan gel-silica hybrid material immobilized HRP by using the InakC-ChBD-Sil interfacial catalyst. This finding will expand the application of chitosan gel in biomedical applications. Further,

detection of silica formed on chitosan gel using a fluorescence microscope with the help of a fluorescent protein fused with a silica binding peptide was also focused.

4.3. Methodology

4.3.1. Optimization of chitosan percentage in gel beads

First, chitosan gel concentration was optimized to form gel beads. For that 1%, 2% and 3% (m/v) of chitosan solutions were prepared by dissolving chitosan in 2% (v/v) acetic acid. Then the chitosan solution was added into 1 M NaOH solution drop by drop using a syringe connected with a needle as shown in Figure 4-4. The formed gel beads in each case were collected and washed with 50 mM Tris/HCl buffer five times. Finally, the formed gel beads in each case were observed.

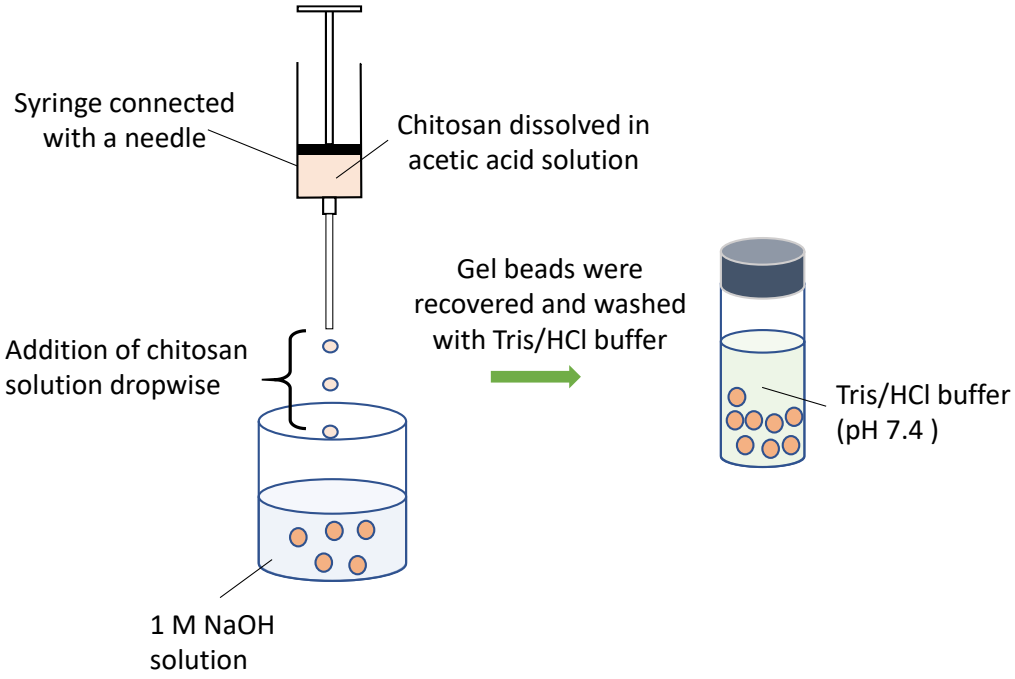

Figure 4- 4: Preparation of chitosan gel beads.

4.3.2. Immobilization of HRP in the chitosan gel matrix

HRP was added into 2% (v/v) acetic acid solution containing 3% (m/v) chitosan to be the final concentration of 0.01 mg/mL. Then the acetic acid solution containing chitosan gel and HRP was added into 1 M NaOH solution drop by drop using a syringe

connected with a needle. Immediately gel beads were recovered and washed with 50 mM Tris/HCl buffer five times.

4.3.2. Adsorption of InakC-ChBD-Sil on chitosan gel

To analyze the adsorption of the fusion proteins on chitin, chitosan gel beads (10 beads) were added to 50 mM Tris/HCl buffer solutions containing 10 μM of InakC-ChBD-Sil, and the solutions were shaken for 1.5 h at 25 °C. During the shaking, 20 μL of the solutions without chitosan gel were periodically aliquoted to analyze the remaining concentration of the protein using Bradford assay. After 2 h, the chitosan gel was recovered and washed twice with 50 mM Tris/HCl buffer.

4.3.3. Silica formation on the chitosan gel

Chitosan gel beads adsorbed InakC-ChBD-Sil were subjected to silica formation using 100 mM TEOS as the precursor in the 50 mM Tris/HCl buffer at 25 °C while shaking at 185 rpm for 24 h[9]. The treated chitosan gel beads were recovered and washed three times with ethanol and three times with ultra-pure water followed by freeze-drying for 2 days. Then the freeze-dried gel beads were observed using SEM-EDS. A similar experiment was conducted without adding InakC-ChBD-Sil as a control. For the detection of activity of HRP, chitosan gel beads subjected to silica formation with and without adsorption of InakC-ChBD-Sil were recovered by washing with Tris/HCl buffer.

4.3.4. Determination of the activity of HRP

For the preparation of 1.7 mM hydrogen peroxide, 1 mL of 30% hydrogen peroxide was added to 100 mL of ultra-pure water. Further, 1 mL of the solution was diluted to 50 mL with 200 mM potassium phosphate buffer (pH 7). For the preparation of phenol/aminoantipyrine (2.5 mM of 4-aminoantipyrine) solution, 810 mg of phenol and

25 mg of 4-aminoantipyrine were dissolved in 40 mL of ultra-pure water, and it was diluted to a final volume of 50 mL with ultra-pure water. Form freshly prepared above solutions, 467 µL of hydrogen peroxide (1.7 mM) and 500 µL of 2.5 mM phenol/aminoantipyrine were pipetted into a cuvette, and the solution was incubated in the spectrophotometer at 25 °C for 3-4 minutes to achieve temperature equilibration and establish a blank rate. Then, 33 µL of the HRP solution, or two chitosan gel beads with 33 µL of ultra-pure water was added to the cuvette, and an increase in absorbance value at 510 nm wavelength for 4-5 minutes was measured to calculate the activity of HRP. Equation 4-1 was used to calculate the activity of HRP where ΔA_{510} is the increase in absorbance value at 510 nm wavelength, and *6.58* is the absorption coefficient for 4-aminoantipyrine at 510 nm wavelength.

$$Activity\ \left(\frac{U}{mg}\right) = \frac{\frac{\Delta A_{510}}{minutes}}{6.58 \times \frac{enzyme\ amount\ (mg)}{volume\ of\ the\ reaction\ mixture\ (mL)}} \qquad (4-1)$$

The activity of HRP immobilized in chitosan gel beads that were subjected to silica formation with and without adsorption of InakC-ChBD-Sil was checked in 5 cycles by recovering them and adding them into cuvette containing freshly prepared hydrogen peroxide and phenol/aminoantipyrine solutions. Then the relative activity in each cycle was calculated using Equation 4-2.

$$Relative\ activity = \frac{Activity}{Initial\ activity} \times 100\% \qquad (4-2)$$

4.3.5. Expression of TBP-mCherry and mCherry

Gene encoding mCherry, optimized for expression in *E. coli*, was obtained from pmCherry vector (Clontech Laboratories, Inc., Takara Bio, vector number: PT3973-5).

It was amplified with F1, forward primer composes the sequence of TBP, and R1, revers primer as shown in Figure 4-5. The nucleotide sequence of primers and the PCR conditions used in the experiment has been mentioned in Table 4-1 and 4-2, respectively. The amplified gene was subcloned into pCold II expression vector at *Nde*I and *Xho*I restriction enzyme sites using In-Fusion (Takara Bio Inc., Japan) to express the protein named TBP-mCherry. To check the correctness of the constructed vector after multiplication in *E. coli* DH5α, DNA sequencing was conducted.

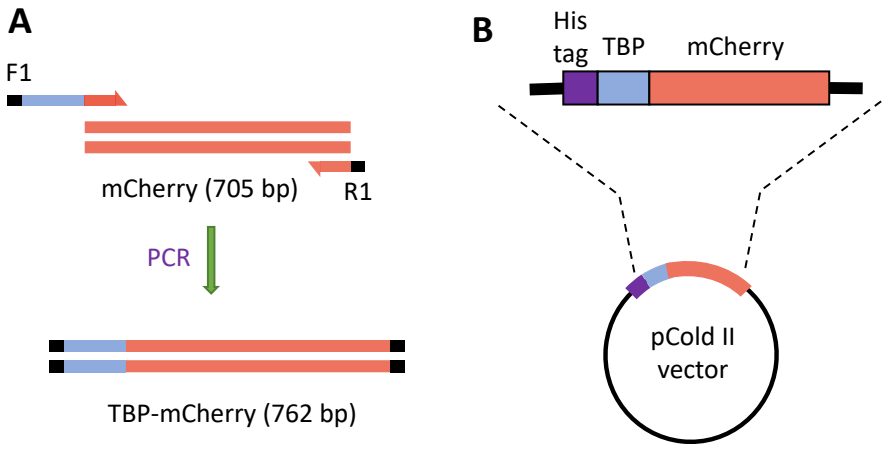

Figure 4- 5: Gene and vector construction to express TBP-mCherry. (A) Gene construction through PCR. (B) The gene order of TBP-mCherry.

Table 4- 1: Nucleotide sequence of primers used in this study.

Primer	Nucleotide sequence
F1	ATCATCATCATCATATGCGCAAACTGCCGGATGCGCCAG GCATGCATACCTGGGTGAGCAAGGGCGAGGAG
R1	ATTCGGATCCCTCGAGCAGGGTTGGATAAGAGGC

Table 4- 2: PCR conditions for gene amplification

Stage	PCR for cloning gene		Cycles
	Temperature (°C)	Time	
Pre denaturation	98.0	30 s	-
Denaturation	98.0	10 s	35
Annealing	55.0	15 s	
Extension	72.0	5 s	
Final extension	72.0	1 min	-

The transformed *E. coli* with the constructed vector was used to express TBP-mCherry at 15 °C by inducing the protein expression using 1.0 mM IPTG. After 24 h, bacterial cells were harvested by centrifugation (4000 × g, 20 min, 4 °C). Resultant pellets were resuspended in sonication buffer (20 mM Tris/HCl, pH 8.0, 1 mM EDTA, 0.5 M NaCl), and cells were disrupted by using an ultrasound disintegrator (VCX-130, Sonic & Materials Inc., USA). Then the samples were centrifuged (25, 000 × g, 20 min, 4 °C). The supernatant was collected, and TBP-mCherry was purified by immobilized metal ion affinity chromatography on a 5 mL Ni-NTA column. The content of the buffers and the procedure followed during the Ni-NTA column purification have been mentioned in Table 4-3 and 4-4, respectively. The elution buffer of the target protein was then replaced with 50 mM Tris/HCl buffer (pH 9.0, 8 mM NaCl) by ultrafiltration (Amicon® Ultra-15 centrifuge filters, 10, 000 NMWL). Finally, the concentrations of refolded proteins were calculated using the Bradford assay (Bradford Protein Assay Kit, Takara Bio Inc., Japan)[87].

Table 4- 3: Content of the buffers used for Ni-NTA column purification.

Solution	Ingredients			
	NaCl	**Phosphoric acid**	**Imidazole**	**DTT**
Wash buffer 1	300 mM	50 mM	5 mM	10 mM
Wash buffer 2	300 mM	50 mM	25 mM	10 mM
Elution buffer	300 mM	50 mM	500 mM	10 mM

Table 4- 4. Procedure followed during the Ni-NTA column purification.

Solution	Volume	Rate	Role
Distilled water	2 CV	10 mL/min	Washing
Wash buffer 1	5 CV	10 mL/min	Equilibration
Loading buffer containing the target protein	1 CV	5 mL/min	Loading the protein
Wash buffer 1	6 CV	5 mL/min	Washing
Wash buffer 2	6 CV	10 mL/min	Washing
Elution buffer	5 CV	10 mL/min	Eluting the target protein

4.3.6. Detection of silica on chitosan gel using TBP-mCherry

First, to investigate the adsorption of TBP-mCherry and mCherry on glass beads, glass beads were treated with 2.5 μM of TBP-mCherry or mCherry at 25 °C for 3 h. Recovered glass beads were washed with distilled water to remove the unbound proteins on the glass beads. Finally, the glass beads were observed using a fluorescence microscope (KEYENCE Fluorescence Microscope, BZ-X800).

For the detection of silica formed on chitosan gel beads, three beads of chitosan gel subjected to silica formation with and without adsorption of InakC-ChBD-Sil were treated with 2.5 μM of TBP-mCherry at 25 ℃ for 3 h. Then the beads were recovered and washed with distilled water to remove the unbound TBP-mCherry. Finally, the gel beads were observed using the fluorescence microscope.

4.5. Result and discussion

4.5.1. Optimization of chitosan percentage in gel beads

It was necessary to optimize the chitosan gel concentration to get nicely formed gel beads. Chitosan gel beads formed by changing the chitosan concentration are shown in Figure 4-6. According to the observation, 3% of chitosan gel beads showed a nice shape while lower concentrations (1% and 2%) of chitosan gel beads resulted in highly fragile particles. Therefore, 3% of chitosan was used for the formation of chitosan gel beads for further studies. The average weight of a gel bead was 6 mg.

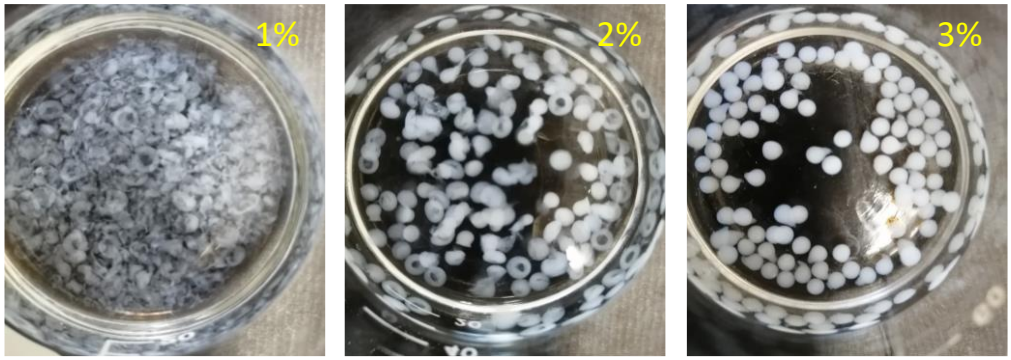

Figure 4- 6: Chitosan gel beads formed with different chitosan concentrations.

Chitosan gel can be formed in different shapes such as sheets[152] and spheres[153]. Since spherical gel beads are applied in many applications, in this study, spherical chitosan gel beads were formed.

4.5.2. Adsorption of InakC-ChBD-Sil on chitosan gel and silica formation

Figure 4-7 shows the adsorption of InakC-ChBD-Sil on chitosan gel. According to the data, InakC-ChBD-Sil showed significant adsorption on chitosan gel within 2 h. Therefore, chitosan gel adsorbed InakC-ChBD-Sil were subjected to silica formation using TEOS precursor. As a control, chitosan gel was subjected to silica formation without adsorption of InakC-ChBD-Sil.

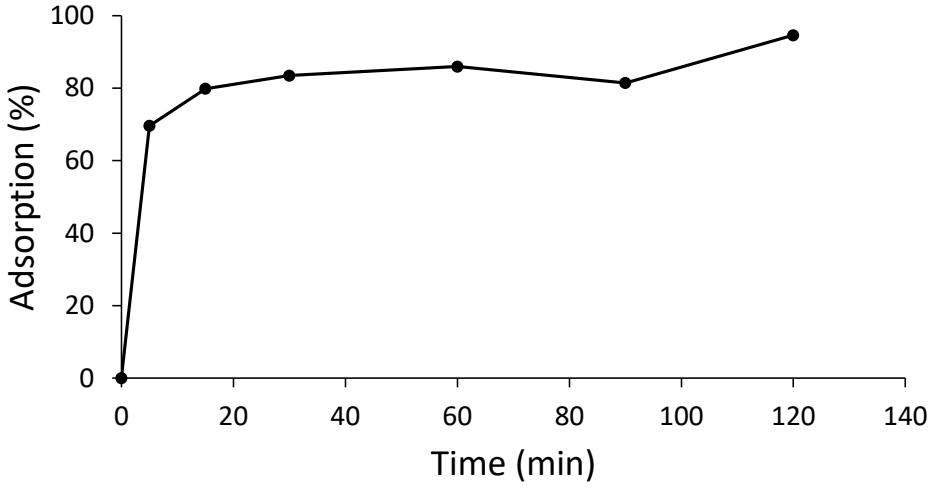

Figure 4- 7: Adsorption studies of InakC-ChBD-Sil on chitosan gel.

After freeze-drying, the elements present on the chitosan gel subjected to silica formation with and without adsorption of InakC-ChBD-Sil were observed using SEM-EDS (Figure 4-8). There was a deposition on chitosan gel with InakC-ChBD-Sil while a smooth surface was observed for the chitosan gel without InakC-ChBD-Sil as shown in Figure 4-8A. The elemental distribution shown in Figure 4-8B revealed a higher distribution of Si on chitosan gel with InakC-ChBD-Sil and a little on the chitosan gel without InakC-ChBD-Sil. EDS spectrum of the chitosan gel with InakC-ChBD-Sil in Figure 4-8C also revealed the presence of Si. These results suggested that InakC-ChBD-Sil has catalyzed the silica formation on the chitosan gel.

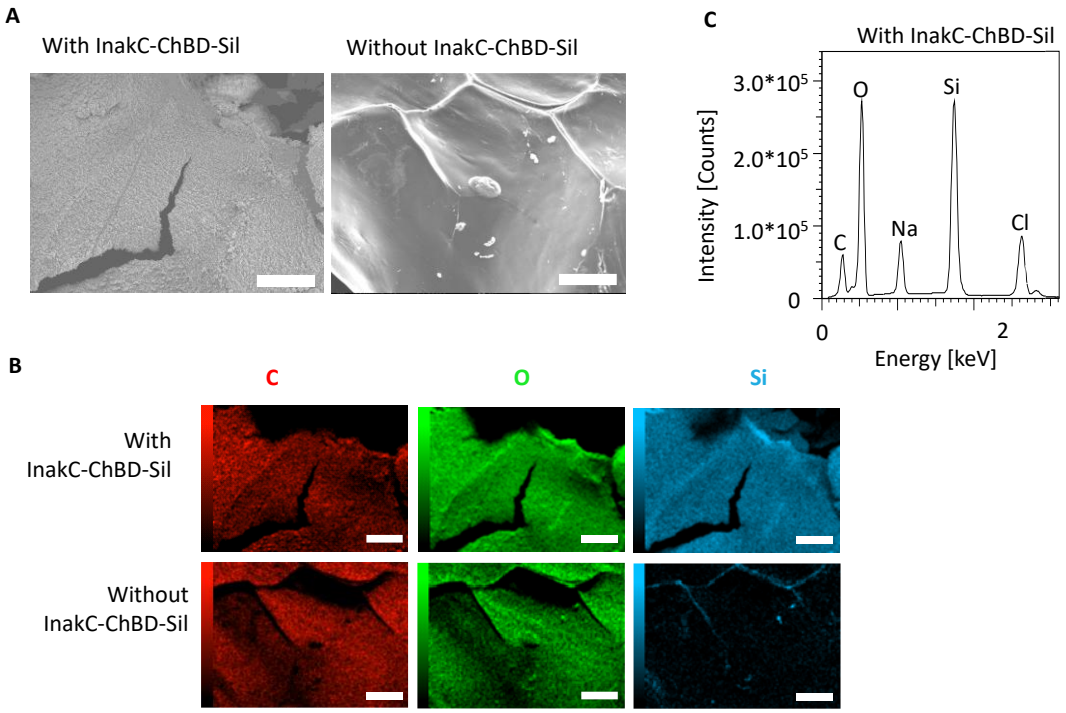

Figure 4- 8: SEM-EDS analysis of chitosan gel subjected to silica formation with and without adsorption of InakC-ChBD-Sil. (A) SEM images, (B) Elemental analysis, and (C) EDS spectrum. Size bars indicate 50 μm.

The chitosan gel-silica hybrid materials have been prepared using sol-gel processes for the application of heavy metal adsorption[154] and the development of biosensors[155]. In some studies, magnetic properties have been obtained by immobilization of Fe_3O_4 magnetic nanoparticles for the development of drug delivery systems[156]. Same way, magnetic nanoparticles also can be immobilized in the chitosan gel matrix along with biomolecules before the formation of silica on the chitosan gel bead. That allows fabricating biomolecules encapsulated chitosan gel-silica hybrid material with magnetic properties.

4.5.3. Enzymatic activity of HRP immobilized in the chitosan gel-silica matrix

Just after immobilization of HRP, the activity of HRP was examined. It was found a 40 U/mg activity. Then the HRP immobilized chitosan gel beads were subjected to

silica formation with and without adsorption of InakC-ChBD-Sil. Then the relative activity of HRP in chitosan gel was observed. Figure 4-9 shows the real and relative enzymatic activities of HRP subjected to silica formation with and without adsorption of InakC-ChBD-Sil. According to that, the relative activity of HRP in chitosan gel treated with InakC-ChBD-Sil was 85% after five cycles while the relative activity was 26% in the nontreated. That result suggested that the fabrication of silica layer on chitosan gel gave extra stability than without silica.

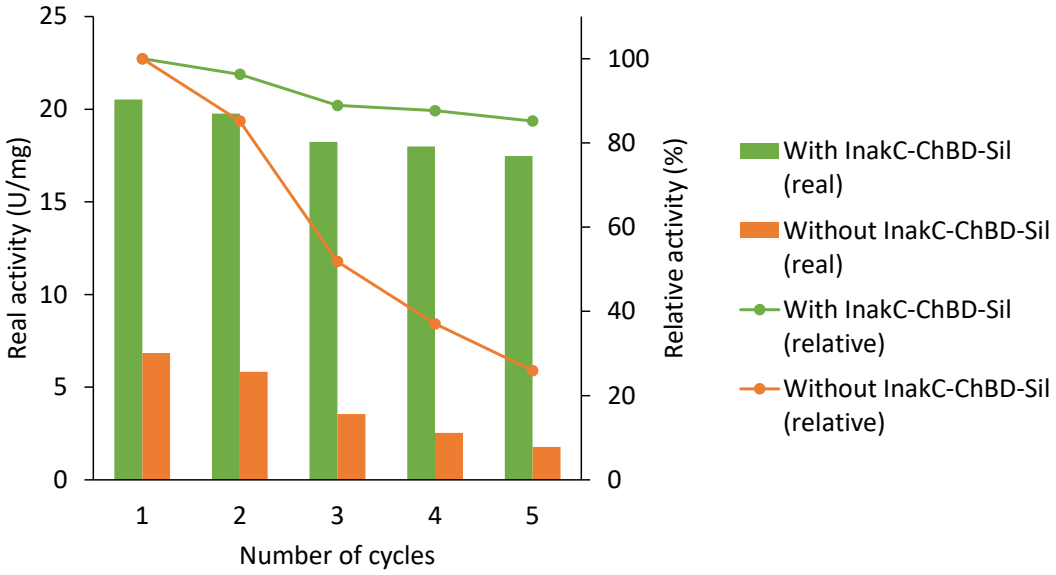

Figure 4- 9: Real and relative activities of HRP.

In previous studies, it has been shown that after immobilization of enzymes such as lipase[157], alcohol dehydrogenase[158], HRP[159], and trypsin[160] in chitosan gel matrix showed wide-working pH and temperature stability. The HRP immobilized in the novel chitosan gel-silica hybrid showed promising stability and reusability. Since silica is formed in mild conditions, enzymes could be immobilized in the silica matrix as well. Therefore, this will be a novel tool to apply biotechnological application.

The drastic drop in the relative activity of HRP immobilized in chitosan gel beads subjected to silica formation without adsorption of InakC-ChBD-Sil, could be due to the leaching of HRP due to the lack of surface coverage with silica. This phenomenon is shown in Figure 4-10. On the other hand, HRP immobilized in chitosan gel treated with InakC-ChBD-Sil formed a sufficient amount of surface coverage with silica to avoid the leaching of HRP from the hybrid material (Figure 4-10).

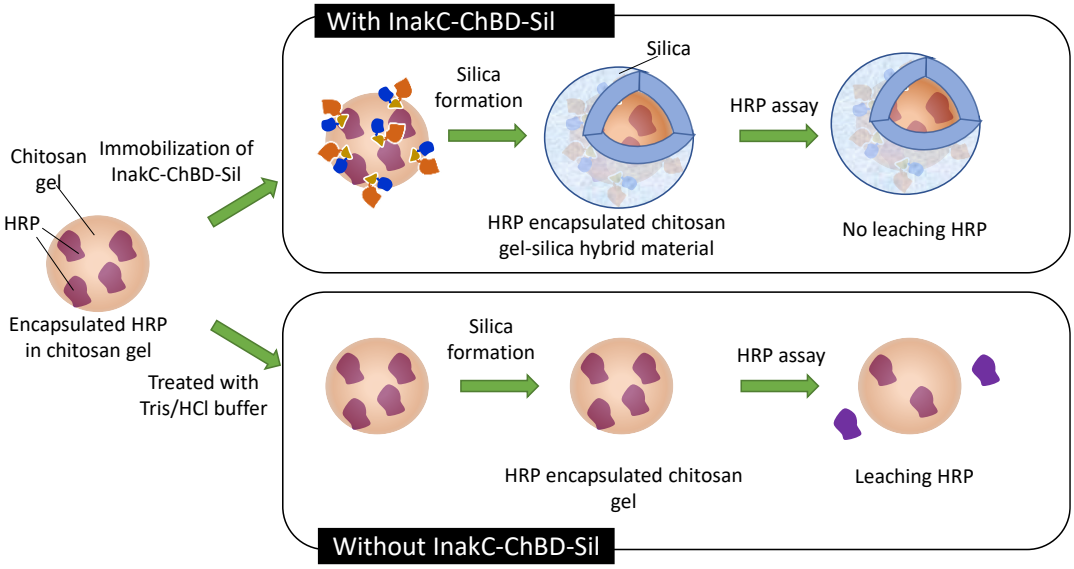

Figure 4- 10: Illustration of leaching of HRP during the enzymatic assay

4.5.4. Expression of TBP-mCherry

Fluorescent proteins are an important finding in biochemistry. Green fluorescent protein was first isolated from the jellyfish *Aequorea aequorea*[161]. Up to date, many fluorescent proteins have been identified in many species. They have expanded the ability to examine the behavior of proteins within living cells. Same way fluorescent proteins fused with different protein tags have been applied in many studies for the detection of materials [162]. Since the chitosan gel matrix was the organic matrix used in this study, detection of formed silica on the gel was difficult using SEM-EDS. Therefore, a fluorescence microscope method was used. To detect formed silica on

chitosan gel matrix, TBP-mCherry, a fusion protein with a silica binding tag and a fluorescence tag, was designed.

The constructed vector to express TBP-mCherry was transformed into *E. coli*. The transformed *E. coli* to express TBP-mCherry and the colony PCR done to check the successfulness of the transformation are shown in Figure 4-11.

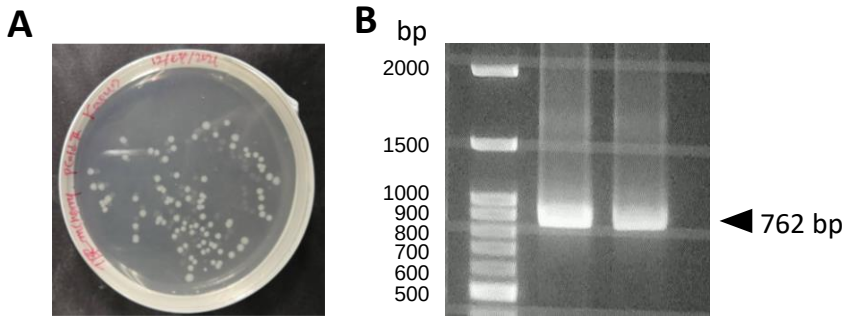

Figure 4- 11: Transformation of *E. coli* to express TBP-mCherry. (A) Transformed *E. coli* to express TBP-mCherry. (B) Colony PCR

The molecular weight of the TBP-mCherry was 29 kDa. The amino acid sequence of TBP-mCherry is shown in Figure S7 (Appendix I). Figure 4-12 shows the SDS-PAGE analysis of TBP-mCherry. As shown in Figure 4-11A, TBP-mCherry has expressed as a soluble protein. Therefore, it was purified directly using Ni-NTA column purification. SDS-PAGE analysis in Figure 4-12B shows TBP-mCherry after Ni-NTA column purification and refolding. Purified TBP-mCherry was used for the detection of silica on chitosan gel.

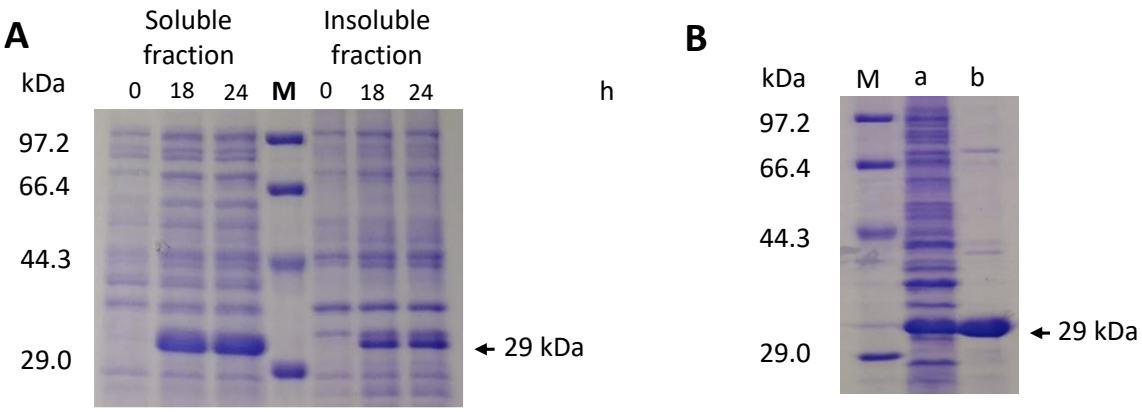

Figure 4- 12: SDS-PAGE analysis for TBP-mCherry. (A) SDS-PAGE analysis for expression of TBP-mCherry. (B) (a) cell lysate, (b) after Ni-NTA column purification. M: Molecular weight marker.

4.5.5. Detection of silica on chitosan gel using fluorescence microscope

To confirm the adsorption ability of TBP-mCherry on silica, at first, the adsorption of TBP-mCherry and mCherry on glass beads was evaluated. Figure 4-13 shows the microscope images of glass beads treated with TBP-mCherry or mCherry. According to the results, a bright fluorescence was observed in the glass beads treated with TBP-mCherry, and no fluorescence was detected in the glass bead treated with mCherry.

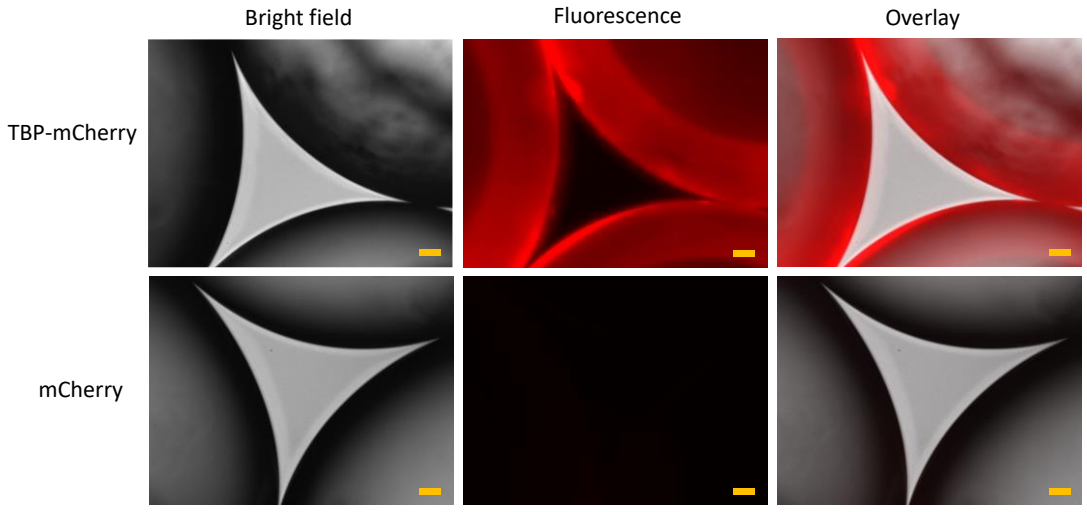

Figure 4- 13: Microscopic images of glass beads treated with TBP-mCherry and mCherry. Size bars indicate 100 μm.

Since TBP-mCherry has a silica binding tag, that had strongly bound on the glass surface. On the other hand, mCherry had not strongly bound on the glass surface since there was no silica binding tag. Figure 4-14 illustrates the phenomenon that happens when glass beads treated with TBP-mCherry and mCherry followed by washing with distilled water. Therefore, during the washing process, TBP-mCherry remained on the glass surface while mCherry washing off. Hence, those results suggested that TBP-mCherry can successfully bind on silica to detect the silica using the fluorescence microscope.

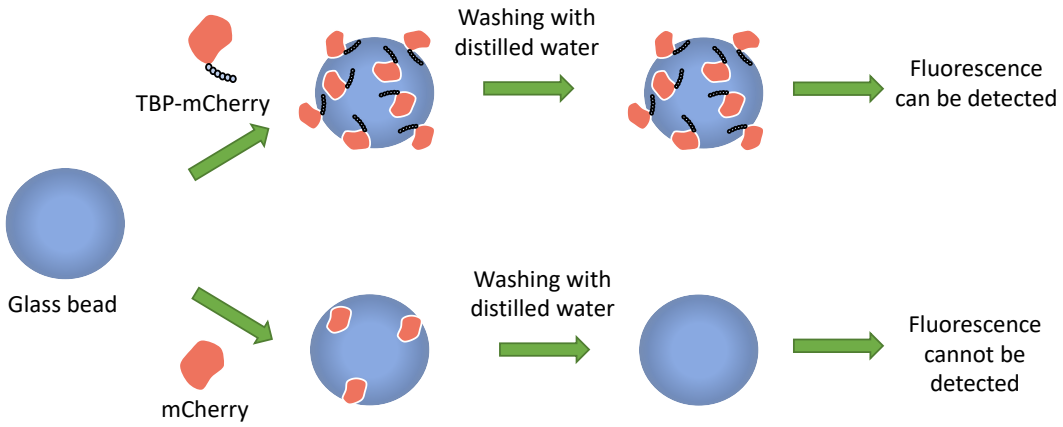

Figure 4- 14: Simple illustration to show the adsorption of fluorescent protein on glass beads through the silica binging peptide.

Next, to detect the silica formation on chitosan gel using TBP-mCherry, chitosan gel beads subjected to silica formation with and without adsorption of InakC-ChBD-Sil were used. Figure 4-15 shows the microscopic images after the TBP-mCherry treatment. Higher fluorescence was detected for the chitosan gel treated with InakC-ChBD-Sil than without InakC-ChBD-Sil.

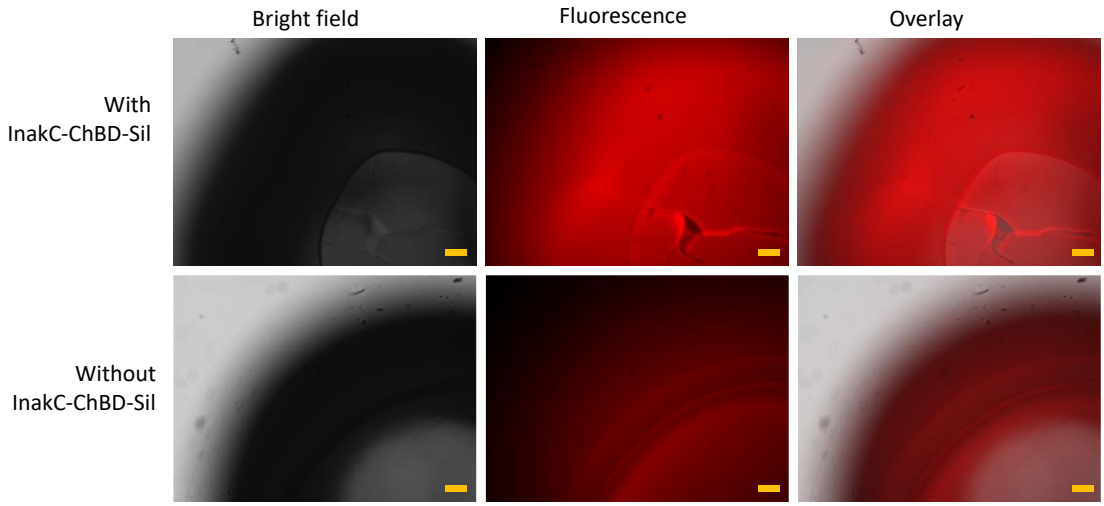

Figure 4- 15: Microscopic images of chitosan gel beads treated with TBP-mCherry. Size bars indicate 100 μm.

The detection of high fluorescence in chitosan gel treated with InakC-ChBD-Sil was ascribed to silica formed on the surface of the chitosan gel beads. However, a very lower fluorescent was observed for the chitosan gel beads without InakC-ChBD-Sil. This could be due to silica formed by the auto polycondensation of TEOS in the system. The detection of higher fluorescence in chitosan gel subjected to silica formation with adsorption of InakC-ChBD-Sil than without InakC-ChBD-Sil has been illustrated in Figure 4-16. On the other hand, a negligible amount of InakC-ChBD-Sil could be absorbed into the chitosan gel beads with no silica coating as the reverse process of leaching HRP from the chitosan gel (Figure 4-10). The theoretical isoelectric (PI) of the TBP mcherry was 6.3 and the pH of the solution used for the adsorption studies was 7.4. At that pH, the net charge of the TBP-mCherry was negative and the surface charge of chitosan gel beads were positive due to amine groups (pKa 9.7). Therefore, electrostatic interation also could take palce to adsorb small amount of TBP-mCherry on the chitosan gel beads. The overall results suggested that the chitosan gel beads

subjected to silica formation with adsorption of InakC-ChBD-Sil formed silica on the gel beads.

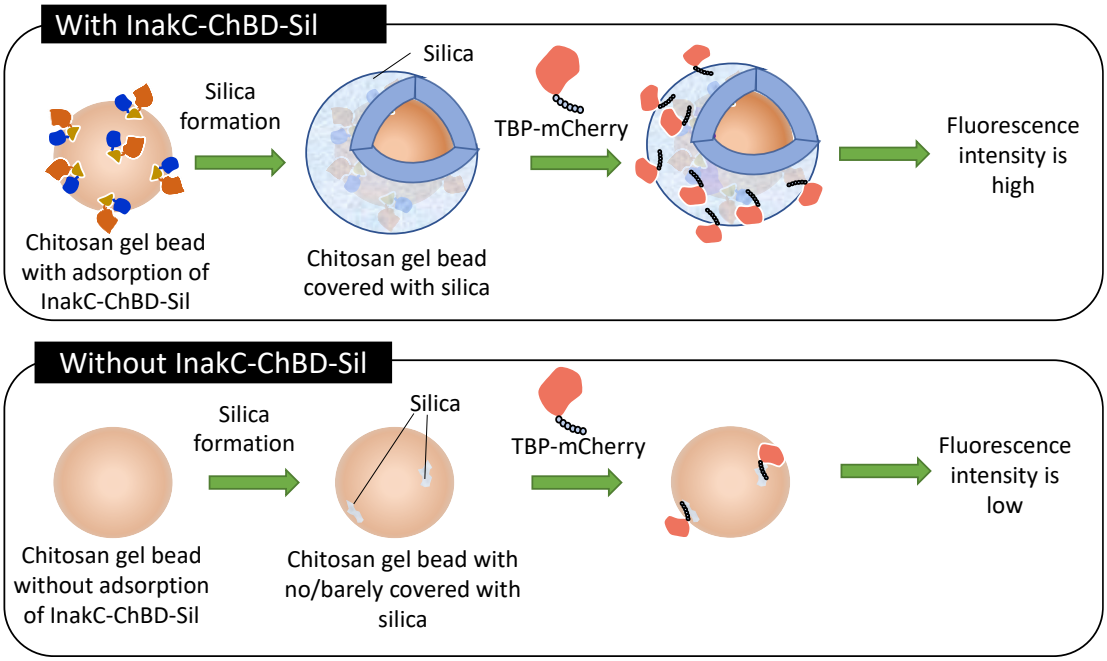

Figure 4- 16: Simple illustration to show the higher fluorescence intensity from chitosan gel beads with InakC-ChBD-Sil than without.

In some studies, fluorescent proteins fused with binding tags have been used in immunofluorescence assays for the detection of surface displaying of proteins on cell surfaces[163], and to investigate the binding ability of binding tags on target materials such as silica[164]. Therefore, the binding domain fused with fluorescent proteins allows detecting materials using a fluorescence microscope. Since silica is formed on the chitosan gel beads subjected to silica formation with adsorption of InakC-ChBD-Sil, TBP-mCherry successfully bound on the silica formed on the gel surface allowing the detection of silica using the fluorescence microscope. This approach can be used as a tool for the detection of materials.

4.6. Conclusion

InakC-ChBD-Sil adsorbed on chitosan gel and catalyzed the silica formation on chitosan gel beads successfully. HRP enzyme can be immobilized in the chitosan gel-silica hybrid materials successfully. Chitosan gel-silica hybrid materials facilitate stability for HRP. This strategy can be used to develop new materials to apply in biomedical applications. Further, TBP-mCherry can be used as a fluorescent tag to detect silica formed on chitosan gel using fluorescence microscope.

CHAPTER 5

CONCLUSIONS AND FUTURE PROSPECTS

In this thesis, biological routes to fabricate silica-cellulose, silica-chitin, silica-chitosan gel hybrid materials under mid conditions were studied. As interfacial catalysts, novel fusion silicateins were designed combining soluble tags for the solubility enhancement of silicatein and solid-binding modules for the immobilization of silicatein on target materials.

Since cellulose is the most abundant polysaccharide on the earth and is used in many applications, at first, cellulose was used as the organic matrix to fabricate silica. In this study, to increase the solubility of silicatein in aqueous media and to immobilize silicatein on cellulose, two tags were fused with silicatein. They were ProS2 and CBM, respectively. The fusion silicatein, ProS2-Sil-CBM was successfully expressed in *E. coli*. Based on the results, it showed that ProS2-Sil-CBM maintained its solubility in aqueous media for 24 h and showed almost the same activity as ProS2-Sil. ProS2-Sil-CBM adsorbed on cellulose within 1.5 h, and the adsorbed ProS2-Sil-CBM successfully catalyzed silica formation on cellulose.

Secondly, chitin was studied as another organic matrix to fabricate silica. In the present study, another novel fusion silicatein was designed by fusing silicatein with InakC and ChBD. The fusion silicatein, InakC-ChBD-Sil showed the almost same activity as ProS2-Sil. SEM-EDS results revealed that the adsorbed InakC-ChBD-Sil has successfully catalyzed the formation of silica on the chitin material.

As an advancement of the previous chapters, a spherical chitosan gel-silica hybrid material was fabricated, and HRP was successfully immobilized in the hybrid material as a model enzyme. Here, chitosan gel was the organic matrix used to form the silica-

based hybrid material. InakC-ChBD-Sil was investigated to form chitosan gel-silica hybrid material since chitosan is derived from chitin. According to the adsorption studies, InakC-ChBD-Sil showed significant adsorption on chitosan gel. InakC-ChBD-Sil adsorbed on chitosan gel and formed silica on chitosan gel successfully. During the preparation of chitosan gel beads, HRP was immobilized in the gel matrix, and they were subjected to silica formation by adsorbed InakC-ChBD-Sil. According to the enzymatic activity test, it was found that HPR can be successfully immobilized in the chitosan gel-silica hybrid material while exhibiting its activity. For the detection of silica formed on chitosan gel using fluorescence microscope, a fusion protein called TBP-mCherry was designed. Using TBP-mCherry successfully detected the silica formed on chitosan gel. These findings suggested that the chitosan gel-silica hybrid material can be used to encapsulate enzymes in biomedical and environmental applications.

As many enzymes and peptides can catalyze the inorganic polymers under mild conditions, novel interfacial catalysts can be designed to fabricate various hybrid materials by changing the binding tag according to the base material. Further, enzymes could be immobilized in the silica matrix while the silica is formed on the material.

In this study, HRP was successfully immobilized in the chitosan-gel silica hybrid materials while protecting its enzymatic activity. In the same way, it is possible to investigate the immobilization of live cells in the chitosan gel-silica hybrid material without cell viability (Figure 5-1A).

Using the same way used to encapsulate HRP, agrochemical degradation enzymes could be immobilized in the chitosan gel-silica hybrid materials while protecting their enzymatic activities to use as a sustainable method to improve the quality of soil

polluted with agrochemicals such as herbicides and pesticides (Figure 5-1B). Furthermore, the silica coating method can be used in mineral processing to separate minerals by changing their surface properties by coating them with silica.

Since silica can be used to coat different shaped materials such as fibers, spheres, and rods, hollow silica fibers, spheres, or rods can be obtained followed by the degradation of base material (Figure 5-1C).

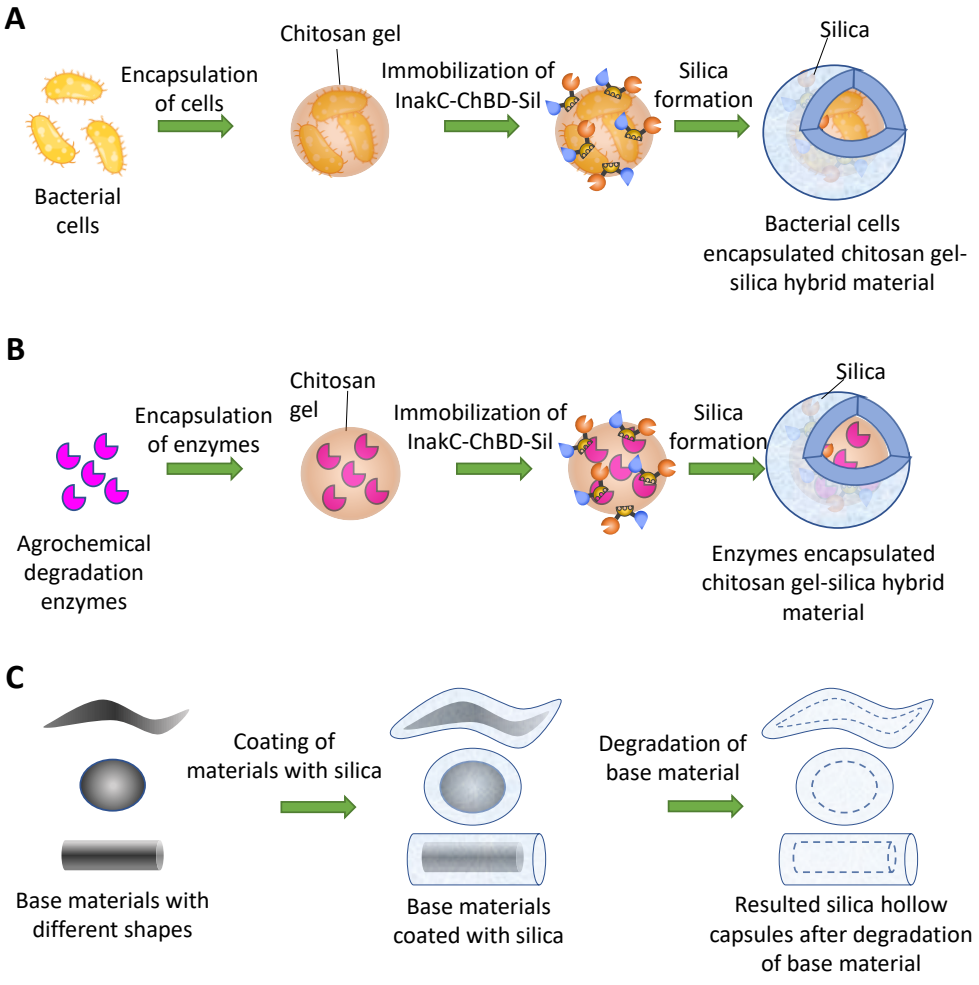

Figure 5- 1: Future prospects of the research. (A) Fabrication of live bacterial cells encapsulated chitosan gel-silica hybrid materials, (B) fabrication of agrochemical degradation enzymes encapsulated chitosan gel-silica hybrid materials, and (C) fabrication of silica hollow capsules.

REFERENCES

1. Sanchez C, Julián B, Belleville P, Popall M (2005) Applications of hybrid organic-inorganic nanocomposites. J Mater Chem 15:3559–3592. https://doi.org/10.1039/b509097k

2. Aversa R, Petrescu RV V., Apicella A, Petrescu FIT (2017) Nano-diamond hybrid materials for structural biomedical application. Am J Biochem Biotechnol 13:34–41. https://doi.org/10.3844/ajbbsp.2017.34.41

3. Cai WY, Xu Q, Zhao XN, et al (2006) Porous gold-nanoparticle-$CaCO_3$ hybrid material: Preparation, characterization, and application for horseradish peroxidase assembly and direct electrochemistry. Chem Mater 18:279–284. https://doi.org/10.1021/cm051442i

4. Müller WEG, Engel S, Wang X, et al (2008) Bioencapsulation of living bacteria (*Escherichia coli*) with poly(silicate) after transformation with silicatein-α gene. Biomaterials 29:771–779. https://doi.org/10.1016/j.biomaterials.2007.10.038

5. Luckarift HR, Spain JC, Naik RR, Stone MO (2004) Enzyme immobilization in a biomimetic silica support. Nat Biotechnol 22:211–213. https://doi.org/10.1038/nbt931

6. Trewyn BG, Giri S, Slowing II, Lin VSY (2007) Mesoporous silica nanoparticle based controlled release, drug delivery, and biosensor systems. Chem Commun 3236–3245. https://doi.org/10.1039/b701744h

7. Rai A, Perry CC (2010) Facile fabrication of uniform silica films with tunable physical properties using silicatein protein from sponges. Langmuir 26:4152–

4159. https://doi.org/10.1021/la903366a

8. Sumerel JL, Yang W, Kisailus D, et al (2003) Biocatalytically Templated Synthesis of Titanium Dioxide. Chem Mater 15:4804–4809. https://doi.org/10.1021/cm030254u

9. Müller WEG, Schröder HC, Burghard Z, et al (2013) Silicateins - A novel paradigm in bioinorganic chemistry: Enzymatic synthesis of inorganic polymeric silica. Chem - A Eur J 19:5790–5804. https://doi.org/10.1002/chem.201204412

10. Maher S, Kumeria T, Aw MS, Losic D (2018) Diatom Silica for Biomedical Applications: Recent Progress and Advances. Adv Healthc Mater 7:1–19. https://doi.org/10.1002/adhm.201800552

11. Roth KM, Zhou Y, Yang W, Morse DE (2005) Bifunctional small molecules are biomimetic catalysts for silica synthesis at neutral pH. J Am Chem Soc 127:325–330. https://doi.org/10.1021/ja045308v

12. Tahir MN, Schröder HC, Huth J, et al (2005) Formation of layered titania and zirconia catalysed by surface-bound silicatein. Chem Commun 5533–5535. https://doi.org/10.1039/b510113a

13. Ki MR, Yeo KB, Pack SP (2013) Surface immobilization of protein via biosilification catalyzed by silicatein fused to glutathione S-transferase (GST). Bioprocess Biosyst Eng 36:643–648. https://doi.org/10.1007/s00449-012-0818-x

14. Sanchez C, Arribart H, Guille MMG (2005) Biomimetism and bioinspiration as tools for the design of innovative materials and systems. Nat Mater 4:277–288.

https://doi.org/10.1038/nmat1339

15. Dorozhkin S V., Epple M (2002) Biological and medical significance of calcium phosphates. Angew Chemie - Int Ed 41:3130–3146. https://doi.org/10.1002/1521-3773(20020902)41:17<3130::AID-ANIE3130>3.0.CO;2-1

16. Weiner S, Addadi L (1997) Design strategies in mineralized biological materials. J Mater Chem 7:689–702. https://doi.org/10.1039/a604512j

17. Kröger N, Deutzmann R, Sumper M (1999) Polycationic peptides from diatom biosilica that direct silica nanosphere formation. Science (80-) 286:1129–1132. https://doi.org/10.1126/science.286.5442.1129

18. Shimizu K, Cha J, Stucky GD, Morse DE (1998) Silicatein α: Cathepsin L-like protein in sponge biosilica. Proc Natl Acad Sci U S A 95:6234–6238. https://doi.org/10.1073/pnas.95.11.6234

19. Lowenstram HA (1962) Goethite in Radular Teeth of Recent Marine Gastropods. Geol Soc Am Bull 73:279–280

20. Sarwar MI, Zulfiqar S, Ahmad Z (2009) Investigating the property profile of polyamide-alumina nanocomposite materials. Scr Mater 60:988–991. https://doi.org/10.1016/j.scriptamat.2009.02.034

21. Zhang P, Weng Z, Guo J, Wang C (2011) Solution-dispersible, colloidal, conjugated porous polymer networks with entrapped palladium nanocrystals for heterogeneous catalysis of the Suzuki-Miyaura coupling reaction. Chem Mater 23:5243–5249. https://doi.org/10.1021/cm202283z

22. Lionti K, Toury B, Boissière C, et al (2013) Hybrid silica coatings on

polycarbonate: Enhanced properties. J Sol-Gel Sci Technol 65:52–60. https://doi.org/10.1007/s10971-012-2715-9

23. Huang S, Fan D, Lei Y, Huang H (2004) Alkoxysilane-functionalized acrylic copolymer latexes. I. Particle size, morphology, and film-forming properties. J Appl Polym Sci 94:954–960. https://doi.org/10.1002/app.20972

24. Sardon H, Irusta L, Fernández-Berridi MJ, et al (2010) Synthesis of room temperature self-curable waterborne hybrid polyurethanes functionalized with (3-aminopropyl)triethoxysilane (APTES). Polymer (Guildf) 51:5051–5057. https://doi.org/10.1016/j.polymer.2010.08.035

25. McDowell JJ, Zacharia NS, Puzzo D, et al (2010) Electroactuation of alkoxysilane-functionalized polyferrocenylsilane microfibers. J Am Chem Soc 132:3236–3237. https://doi.org/10.1021/ja9089236

26. Julián B, Gervais C, Rager M-N, et al (2017) Solid-State 17O NMR Characterization of PDMS-MxOy (M) Ge(IV), Ti(IV), Zr(IV), Nb(V), and Ta(V)) Organic-Inorganic Nanocomposites. Chem Mater 521–529

27. Uilk JM, Mera AE, Fox RB, Wynne KJ (2003) Hydrosilation-cured poly(dimethylsiloxane) networks: Intrinsic contact angles via dynamic contact angle analysis. Macromolecules 36:3689–3694. https://doi.org/10.1021/ma021154x

28. Chujo Y, Ihara E, Kure S, Saegusa T (1993) Synthesis of triethoxysilyl-terminated polyoxazolines and their cohydrolysis polymerization with tetraethoxysilane. Macromolecules 26:5681–5586

29. Montemor MF (2014) Functional and smart coatings for corrosion protection:

A review of recent advances. Surf Coatings Technol 258:17–37. https://doi.org/10.1016/j.surfcoat.2014.06.031

30. Tran TH, Vimalanandan A, Genchev G, et al (2015) Regenerative Nano-Hybrid Coating Tailored for Autonomous Corrosion Protection. Adv Mater 27:3825–3830. https://doi.org/10.1002/adma.201501044

31. Strong LE, West JL (2015) Hydrogel-Coated Near Infrared Absorbing Nanoshells as Light-Responsive Drug Delivery Vehicles. ACS Biomater Sci Eng 1:685–692. https://doi.org/10.1021/acsbiomaterials.5b00111

32. Yan H, Teh C, Sreejith S, et al (2012) Functional mesoporous silica nanoparticles for photothermal-controlled drug delivery in vivo. Angew Chemie - Int Ed 51:8373–8377. https://doi.org/10.1002/anie.201203993

33. Amjadi M, Pichitpajongkit A, Lee S, et al (2014) Highly stretchable and sensitive strain sensor based on silver nanowire-elastomer nanocomposite. ACS Nano 8:5154–5163. https://doi.org/10.1021/nn501204t

34. Zheng T, Hu Y, Zhang Y, Pan F (2017) Formation of a hydrophobic and corrosion resistant coating on magnesium alloy via a one-step hydrothermal method. J Colloid Interface Sci 505:87–95. https://doi.org/10.1016/j.jcis.2017.05.092

35. Xu L, Wang W, Yu D (2017) Durable flame retardant finishing of cotton fabrics with halogen-free organophosphonate by UV photoinitiated thiol-ene click chemistry. Carbohydr Polym 172:275–283. https://doi.org/10.1016/j.carbpol.2017.05.054

36. Patra D, Vangal P, Cain AA, et al (2014) Inorganic nanoparticle thin film that

suppresses flammability of polyurethane with only a single electrostatically-assembled bilayer. ACS Appl Mater Interfaces 6:16903–16908. https://doi.org/10.1021/am504455k

37. Das D, Lee JF, Cheng S (2001) Sulfonic acid functionalized mesoporous MCM-41 silica as a convenient catalyst for Bisphenol-A synthesis. Chem Commun 21:2178–2179. https://doi.org/10.1039/b107155f

38. Das D, Lee JF, Cheng S (2004) Selective synthesis of Bisphenol-A over mesoporous MCM silica catalysts functionalized with sulfonic acid groups. J Catal 223:152–160. https://doi.org/10.1016/j.jcat.2004.01.025

39. Zeidan RK, Hwang SJ, Davis ME (2006) Multifunctional heterogeneous catalysts: SBA-15-containing primary amines and sulfonic acids. Angew Chemie - Int Ed 45:6332–6335. https://doi.org/10.1002/anie.200602243

40. Xia S, Li F, Li X, et al (2018) An inorganic-organic hybrid supramolecular framework as a high-performance anode for lithium-ion batteries. Dalt Trans 47:5166–5170. https://doi.org/10.1039/c8dt00335a

41. Largeot C, Portet C, Chmiola J, et al (2008) Relation between the ion size and pore size for an electric double-layer capacitor. J Am Chem Soc 130:2730–2731. https://doi.org/10.1021/ja7106178

42. Ehrlich H, Deutzmann R, Brunner E, et al (2010) Mineralization of the metre-long biosilica structures of glass sponges is templated on hydroxylated collagen. Nat Chem 2:1084–1088. https://doi.org/10.1038/nchem.899

43. Matsunaga S, Sakai R, Jimbo M, Kamiya H (2007) Long-Chain Polyamines (LCPAs) from marine sponge: Possible implication in spicule formation.

ChemBioChem 8:1729–1735. https://doi.org/10.1002/cbic.200700305

44. Poulsen N, Kröger N (2004) Silica morphogenesis by alternative processing of silaffins in the diatom *Thalassiosira pseudonana*. J Biol Chem 279:42993–42999. https://doi.org/10.1074/jbc.M407734200

45. Morse DE (1999) Silicon biotechnology: Harnessing biological silica production to construct new materials. Trends Biotechnol 17:230–232. https://doi.org/10.1016/S0167-7799(99)01309-8

46. Hooper JNA, Van Soest RWM (2002) Class *Demospongiae sollas*, 1885. In: Systema Porifera. Springer US, Boston, MA, pp 15–51

47. Weaver JC, Morse DE (2003) Molecular biology of demosponge axial filaments and their roles in biosilicification. Microsc Res Tech 62:356–367. https://doi.org/10.1002/jemt.10401

48. Povarova N V., Barinov NA, Baranov MS, et al (2018) Efficient silica synthesis from tetra(glycerol)orthosilicate with cathepsin- and silicatein-like proteins. Sci Rep 8:16759. https://doi.org/10.1038/s41598-018-34965-9

49. Shimizu K, Morse DE (2018) Silicatein: A Unique Silica-Synthesizing Catalytic Triad Hydrolase From Marine Sponge Skeletons and Its Multiple Applications, 1st ed. Elsevier Inc.

50. Cha JN, Shimizu K, Zhou Y, et al (1999) Silicatein filaments and subunits from a marine sponge direct the polymerization of silica and silicones in vitro. Proc Natl Acad Sci U S A 96:361–365. https://doi.org/10.1073/pnas.96.2.361

51. Cha JN, Stucky GD, Morse DE, Deming TJ (2000) Biomimetic synthesis of ordered silica structures mediated by block copolypeptides. Nature 403:289–

292. https://doi.org/10.1038/35002038

52. Kisailus D, Choi JH, Weaver JC, et al (2005) Enzymatic Synthesis and Nanostructural Control of Gallium Oxide at Low Temperature. Adv Mater 17:314–318. https://doi.org/10.1002/adma.200400815

53. Kisailus D, Truong Q, Amemiya Y, et al (2006) Self-assembled bifunctional surface mimics an enzymatic and templating protein for the synthesis of a metal oxide semiconductor. Proc Natl Acad Sci U S A 103:5652–5657. https://doi.org/10.1073/pnas.0508488103

54. Brutchey RL, Morse DE (2008) Silicattein and the translation of its molecular mechanism of biosilicification into low temperature nanomaterial synthesis. Chem Rev 108:4915–4934. https://doi.org/10.1021/cr078256b

55. Brutchey RL, Yoo ES, Morse DE (2006) Biocatalytic synthesis of a nanostructured and crystalline bimetallic perovskite-like barium oxofluorotitanate at low temperature. J Am Chem Soc 128:10288–10294. https://doi.org/10.1021/ja063107g

56. Müller WEG, Schröder HC, Muth S, et al (2013) The silicatein propeptide acts as inhibitor/modulator of self-organization during spicule axial filament formation. FEBS J 280:1693–1708. https://doi.org/10.1111/febs.12183

57. Schröder HC, Wang X, Manfrin A, et al (2012) Acquisition of structure-guiding and structure-forming properties during maturation from the pro-silicatein to the silicatein form. J Biol Chem 287:22196–22205. https://doi.org/10.1074/jbc.M112.351486

58. Siddhartha Roy HF (2020) Protein–Protein Interaction Regulators. Royal

Society of Chemistry, Cambridge

59. Young CL, Britton ZT, Robinson AS (2012) Recombinant protein expression and purification: A comprehensive review of affinity tags and microbial applications. Biotechnol J 7:620–634. https://doi.org/10.1002/biot.201100155

60. Andersen DC, Krummen L (2002) Recombinant protein expression for therapeutic applications. Curr Opin Biotechnol 13:117–123. https://doi.org/10.1016/S0958-1669(02)00300-2

61. Rosano GL, Ceccarelli EA (2014) Recombinant protein expression in *Escherichia coli*: advances and challenges. Front Microbiol 5:. https://doi.org/10.3389/fmicb.2014.00172

62. Trösemeier J-H, Rudorf S, Loessner H, et al (2019) Optimizing the dynamics of protein expression. Sci Rep 9:7511. https://doi.org/10.1038/s41598-019-43857-5

63. Coyle BL, Baneyx F (2014) A cleavable silica-binding affinity tag for rapid and inexpensive protein purification. Biotechnol Bioeng 111:2019–2026. https://doi.org/10.1002/bit.25257

64. Hong J, Ye X, Zhang YHP (2007) Quantitative determination of cellulose accessibility to cellulase based on adsorption of a nonhydrolytic fusion protein containing CBM and GFP with its applications. Langmuir 23:12535–12540. https://doi.org/10.1021/la7025686

65. Xu Y, Liu Q, Zhou L, et al (2008) Surface display of GFP by *Pseudomonas syringae* truncated ice nucleation protein in attenuated *Vibrio anguillarum* strain. Mar Biotechnol 10:701–708. https://doi.org/10.1007/s10126-008-9108-7

66. Lu P, Feng M-G (2008) Bifunctional enhancement of a β-glucanase-xylanase fusion enzyme by optimization of peptide linkers. Appl Microbiol Biotechnol 79:579–587. https://doi.org/10.1007/s00253-008-1468-4

67. Hall J, Black GW, Ferreira LMA, et al (1995) The non-catalytic cellulose-binding domain of a novel cellulase from *Pseudomonas fluorescens* subsp. cellulosa is important for the efficient hydrolysis of Avicel. Biochem J 309:749–756. https://doi.org/10.1042/bj3090749

68. Oliveira C, Carvalho V, Domingues L, Gama FM (2015) Recombinant CBM-fusion technology - Applications overview. Biotechnol Adv 33:358–369. https://doi.org/10.1016/j.biotechadv.2015.02.006

69. Tomme P, Van Tilbeurgh H, Pettersson G, et al (1988) Studies of the cellulolytic system of *Trichoderma reesei* QM 9414. Analysis of domain function in two cellobiohydrolases by limited proteolysis. Eur J Biochem 170:575–81. https://doi.org/10.1111/j.1432-1033.1988.tb13736.x

70. Gilkes NR, Warren RA, Miller RC, Kilburn DG (1988) Precise excision of the cellulose binding domains from two Cellulomonas fimi cellulases by a homologous protease and the effect on catalysis. J Biol Chem 263:10401–7

71. Shoseyov O, Shani Z, Levy I (2006) Carbohydrate Binding Modules: Biochemical Properties and Novel Applications. Microbiol Mol Biol Rev 70:283–295. https://doi.org/10.1128/mmbr.00028-05

72. Hashimoto M, Ikegami T, Seino S, et al (2000) Expression and characterization of the chitin-binding domain of chitinase A1 from *Bacillus circulans* WL-12. J Bacteriol 182:3045–3054. https://doi.org/10.1128/JB.182.11.3045-3054.2000

73. Wang J-Y, Chao Y-P (2006) Immobilization of cells with surface-displayed chitin-binding domain. Appl Environ Microbiol 72:927–31. https://doi.org/10.1128/AEM.72.1.927-931.2006

74. Zhou J, Chen J, Zhuang N, et al (2020) Immobilization and Purification of Enzymes With the Novel Affinity Tag ChBD-AB From *Chitinolyticbacter meiyuanensis* SYBC-H1. Front Bioeng Biotechnol 8:579. https://doi.org/10.3389/fbioe.2020.00579

75. Urbina J, Patil A, Fujishima K, et al (2019) A new approach to biomining: Bioengineering surfaces for metal recovery from aqueous solutions. Sci Rep 9:1–11. https://doi.org/10.1038/s41598-019-52778-2

76. Esposito D, Chatterjee DK (2006) Enhancement of soluble protein expression through the use of fusion tags. Curr Opin Biotechnol 17:353–358. https://doi.org/10.1016/j.copbio.2006.06.003

77. Kobayashi H, Yoshida T, Inouye M (2009) Significant enhanced expression and solubility of human proteins in *Escherichia coli* by fusion with protein S from *Myxococcus xanthus*. Appl Environ Microbiol 75:5356–5362. https://doi.org/10.1128/AEM.00691-09

78. Aïssa K, Karaaslan MA, Renneckar S, Saddler JN (2019) Functionalizing Cellulose Nanocrystals with Click Modifiable Carbohydrate-Binding Modules. Biomacromolecules 20:3087–3093. https://doi.org/10.1021/acs.biomac.9b00646

79. Kaneko K, Hara M, Nishino T, Maruyama T (2020) One-Step Biotinylation of Cellulose Paper by Polymer Coating to Prepare a Paper-Based Analytical Device. Anal Chem 92:1978–1987.

https://doi.org/10.1021/acs.analchem.9b04373

80. Wang SF, Wang XH, Gan L, et al (2011) Biosilica-glass formation using enzymes from sponges [silicatein]: Basic aspects and application in biomedicine [bone reconstitution material and osteoporosis]. Front Mater Sci 5:266–281. https://doi.org/10.1007/s11706-011-0145-1

81. Rezwan K, Chen QZ, Blaker JJ, Boccaccini AR (2006) Biodegradable and bioactive porous polymer/inorganic composite scaffolds for bone tissue engineering. Biomaterials 27:3413–3431. https://doi.org/10.1016/j.biomaterials.2006.01.039

82. Boccaccini AR, Erol M, Stark WJ, et al (2010) Polymer/bioactive glass nanocomposites for biomedical applications: A review. Compos Sci Technol 70:1764–1776. https://doi.org/10.1016/j.compscitech.2010.06.002

83. Tan L, Yu X, Wan P, Yang K (2013) Biodegradable Materials for Bone Repairs: A Review. J Mater Sci Technol 29:503–513. https://doi.org/10.1016/j.jmst.2013.03.002

84. Wiens M, Elkhooly TA, Schröder HC, et al (2014) Characterization and osteogenic activity of a silicatein/biosilica-coated chitosan-graft-polycaprolactone. Acta Biomater 10:4456–4464. https://doi.org/10.1016/j.actbio.2014.06.036

85. Jungbauer A, Kaar W (2007) Current status of technical protein refolding. J Biotechnol 128:587–596. https://doi.org/10.1016/j.jbiotec.2006.12.004

86. Schloßmacher U, Wiens M, Schröder HC, et al (2011) Silintaphin-1 – interaction with silicatein during structure-guiding bio-silica formation. FEBS J

Authors J Compil 278:1145–1155. https://doi.org/10.1111/j.1742-4658.2011.08040.x

87. Compton SJ, Jones CG (1985) Mechanism of dye response and interference in the Bradford protein assay. Anal Biochem 151:369–374. https://doi.org/10.1016/0003-2697(85)90190-3

88. Yamaguchi H, Miyazaki M (2014) Refolding techniques for recovering biologically active recombinant proteins from inclusion bodies. Biomolecules 4:235–251. https://doi.org/10.3390/biom4010235

89. Kanarjov P, Reedo V, Acik IO, et al (2008) Luminescent materials based on thin metal oxide films doped with rare earth ions. Phys Solid State 50:1727–1730. https://doi.org/10.1134/S1063783408090278

90. Mizutani T, Nagase H, Ogoshi H (1998) Silicic acid polymerization catalyzed by amines and polyamines. Chem. Lett. 133–134

91. Murr MM, Morse DE (2005) Fractal intermediates in the self-assembly of silicatein filaments. Proc Natl Acad Sci U S A 102:11657–11662. https://doi.org/10.1073/pnas.0503968102

92. Gardères J, Elkhooly TA, Link T, et al (2016) Self-assembly and photocatalytic activity of branched silicatein / silintaphin filaments decorated with silicatein-synthesized TiO_2 nanoparticles. Bioprocess Biosyst Eng 39:1477–1486. https://doi.org/10.1007/s00449-016-1619-4

93. Wang X, Schloßmacher U, Wiens M, et al (2012) Silicateins, silicatein interactors and cellular interplay in sponge skeletogenesis: Formation of glass fiber-like spicules. FEBS J 279:1721–1736. https://doi.org/10.1111/j.1742-

4658.2012.08533.x

94. Sparkes EI, Kettles RA, Egedeuzu CS, et al (2020) Improved Production and Biophysical Analysis of Recombinant Silicatein-α. Biomolecules 10:1209. https://doi.org/10.3390/biom10091209

95. Mwandira W, Nakashima K, Togo Y, et al (2020) Cellulose-metallothionein biosorbent for removal of Pb(II) and Zn(II) from polluted water. Chemosphere 246:125733. https://doi.org/10.1016/j.chemosphere.2019.125733

96. Togo Y, Nakashima K, Mwandira W, Kawasaki S (2020) A novel metal adsorbent composed of a hexa-histidine tag and a carbohydrate-binding module on cellulose. Anal Sci 36:459–464. https://doi.org/10.2116/ANALSCI.19P356

97. Schröder HC, Grebenjuk VA, Wang X, Müller WEG (2016) Hierarchical architecture of sponge spicules: Biocatalytic and structure-directing activity of silicatein proteins as model for bioinspired applications. Bioinspiration and Biomimetics 11:041002. https://doi.org/10.1088/1748-3190/11/4/041002

98. Faustini M, Nicole L, Ruiz-Hitzky E, Sanchez C (2018) History of Organic–Inorganic Hybrid Materials: Prehistory, Art, Science, and Advanced Applications. Adv Funct Mater 28:1704158. https://doi.org/10.1002/adfm.201704158

99. Ehrlich H, Janussen D, Simon P, et al (2008) Nanostructural organization of naturally occurring composites-Part II: Silica-chitin-based biocomposites. J Nanomater 2008:1–8. https://doi.org/10.1155/2008/670235

100. Elieh-Ali-Komi D, Hamblin MR (2016) Chitin and Chitosan: Production and Application of Versatile Biomedical Nanomaterials. Int J Adv Res 4:411–427

101. Brunner E, Richthammer P, Ehrlich H, et al (2009) Chitin-based organic networks: An integral part of cell wall biosilica in the diatom *Thalassiosira pseudonana*. Angew Chemie - Int Ed 48:9724–9727. https://doi.org/10.1002/anie.200905028

102. Ehrlich H, Simon P, Carrillo-Cabrera W, et al (2010) Insights into chemistry of biological materials: Newly discovered silica-aragonite-chitin biocomposites in demosponges. Chem Mater 22:1462–1471. https://doi.org/10.1021/cm9026607

103. Ehrlich H, Krautter M, Hanke T, et al (2007) First evidence of the presence of chitin in skeletons of marine sponges. Part II. Glass sponges (Hexactinellida: Porifera). J Exp Zool Part B Mol Dev Evol 308B:473–483. https://doi.org/10.1002/jez.b.21174

104. Ehrlich H, Maldonado M, Parker AR, et al (2016) Supercontinuum Generation in Naturally Occurring Glass Sponges Spicules. Adv Opt Mater 4:1608–1613. https://doi.org/10.1002/adom.201600454

105. Ehrlich H (2010) Chitin and collagen as universal and alternative templates in biomineralization. Int Geol Rev 52:661–699. https://doi.org/10.1080/00206811003679521

106. Jayakumar R, Menon D, Manzoor K, et al (2010) Biomedical applications of chitin and chitosan based nanomaterials - A short review. Carbohydr Polym 82:227–232. https://doi.org/10.1016/j.carbpol.2010.04.074

107. Madhumathi K, Binulal NS, Nagahama H, et al (2009) Preparation and characterization of novel β-chitin-hydroxyapatite composite membranes for tissue engineering applications. Int J Biol Macromol 44:1–5. https://doi.org/10.1016/j.ijbiomac.2008.09.013

108. Borchard G (2001) Chitosans for gene delivery. Adv Drug Deliv Rev 52:145–150. https://doi.org/10.1016/S0169-409X(01)00198-3

109. Itoh Y, Kawase T, Nikaidou N, et al (2002) Functional analysis of the chitin-binding domain of a family 19 chitinase from *Streptomyces griseus* hut6037: Substrate-binding affinity and cis-dominant increase of antifungal function. Biosci Biotechnol Biochem 66:1084–1092. https://doi.org/10.1271/bbb.66.1084

110. Nygaard S, Wendelbo R, Brown S (2002) Surface-Specific Zeolite-Binding Proteins. Adv Mater 14:1853–1856

111. Yang M, Choi BG, Park TJ, et al (2011) Site-specific immobilization of gold binding polypeptide on gold nanoparticle-coated graphene sheet for biosensor application. Nanoscale 3:2950–2956. https://doi.org/10.1039/c1nr10197h

112. Care A, Bergquist PL, Sunna A (2015) Solid-binding peptides: Smart tools for nanobiotechnology. Trends Biotechnol 33:259–268. https://doi.org/10.1016/j.tibtech.2015.02.005

113. Costa S, Almeida A, Castro A, Domingues L (2014) Fusion tags for protein solubility, purification, and immunogenicity in *Escherichia coli*: The novel Fh8 system. Front Microbiol 5:1–20. https://doi.org/10.3389/fmicb.2014.00063

114. Kimple ME, Brill AL, Pasker RL (2013) Overview of affinity tags for protein purification. Curr Protoc Protein Sci 73:608–616. https://doi.org/10.1002/0471140864.ps0909s73

115. Vogt S, Kelkenberg M, Nöll T, et al (2018) Rapid determination of binding parameters of chitin binding domains using chitin-coated quartz crystal

microbalance sensor chips. Analyst 143:5255–5263. https://doi.org/10.1039/C8AN01453A

116. Neeraja C, Anil K, Purushotham P, et al (2010) Biotechnological approaches to develop bacterial chitinases as a bioshield against fungal diseases of plants. Crit Rev Biotechnol 30:231–241. https://doi.org/10.3109/07388551.2010.487258

117. Godigamuwa K, Nakashima K, Okamoto J, Kawasaki S (2020) Biological Route to Fabricate Silica on Cellulose Using Immobilized Silicatein Fused with a Carbohydrate-Binding Module. Biomacromolecules 21:2922–2928. https://doi.org/10.1021/acs.biomac.0c00730

118. Jung HC, Park JH, Park SH, et al (1998) Expression of carboxymethylcellulase on the surface of *Escherichia coli* using *Pseudomonas syringae* ice nucleation protein. Enzyme Microb Technol 22:348–354. https://doi.org/10.1016/S0141-0229(97)00224-X

119. Kamathewatta NJB, Deay DO, Karaca BT, et al (2020) Self-Immobilized Putrescine Oxidase Biocatalyst System Engineered with a Metal Binding Peptide. Langmuir 36:11908–11917. https://doi.org/10.1021/acs.langmuir.0c01986

120. Cowan DA, Fernandez-Lafuente R (2011) Enhancing the functional properties of thermophilic enzymes by chemical modification and immobilization. Enzyme Microb Technol 49:326–346. https://doi.org/10.1016/j.enzmictec.2011.06.023

121. Wohlgemuth R (2010) Biocatalysis—key to sustainable industrial chemistry. Curr Opin Biotechnol 21:713–724. https://doi.org/10.1016/j.copbio.2010.09.016

122. Jesionowski T, Zdarta J, Krajewska B (2014) Enzyme immobilization by adsorption: a review. Adsorption 20:801–821. https://doi.org/10.1007/s10450-014-9623-y

123. Zhang Y, Ge J, Liu Z (2015) Enhanced Activity of Immobilized or Chemically Modified Enzymes. ACS Catal 5:4503–4513. https://doi.org/10.1021/acscatal.5b00996

124. Marzadori C, Miletti S, Gessa C, Ciurli S (1998) Immobilization of jack bean urease on hydroxyapatite: urease immobilization in alkaline soils. Soil Biol Biochem 30:1485–1490. https://doi.org/10.1016/S0038-0717(98)00051-0

125. Mateo C, Palomo JM, Fernandez-Lorente G, et al (2007) Improvement of enzyme activity, stability and selectivity via immobilization techniques. Enzyme Microb Technol 40:1451–1463. https://doi.org/10.1016/j.enzmictec.2007.01.018

126. Pellá MCG, Lima-Tenório MK, Tenório-Neto ET, et al (2018) Chitosan-based hydrogels: From preparation to biomedical applications. Carbohydr Polym 196:233–245. https://doi.org/10.1016/j.carbpol.2018.05.033

127. Grainger DW (2013) Connecting drug delivery reality to smart materials design. Int J Pharm 454:521–524. https://doi.org/10.1016/j.ijpharm.2013.04.061

128. Kakkar P, Madhan B (2016) Fabrication of keratin-silica hydrogel for biomedical applications. Mater Sci Eng C 66:178–184. https://doi.org/10.1016/j.msec.2016.04.067

129. Lima-Tenório MK, Gómez Pineda EA, Ahmad NM, et al (2015) Magnetic

nanoparticles: In vivo cancer diagnosis and therapy. Int J Pharm 493:313–327. https://doi.org/10.1016/j.ijpharm.2015.07.059

130. Soares PAG, Bourbon AI, Vicente AA, et al (2014) Development and characterization of hydrogels based on natural polysaccharides: Policaju and chitosan. Mater Sci Eng C 42:219–226. https://doi.org/10.1016/j.msec.2014.05.009

131. Ullah F, Othman MBH, Javed F, et al (2015) Classification, processing and application of hydrogels: A review. Mater Sci Eng C 57:414–433. https://doi.org/10.1016/j.msec.2015.07.053

132. Lima-Tenório MK, Tenório-Neto ET, Guilherme MR, et al (2015) Water transport properties through starch-based hydrogel nanocomposites responding to both pH and a remote magnetic field. Chem Eng J 259:620–629. https://doi.org/10.1016/j.cej.2014.08.045

133. Arteche Pujana M, Pérez-Álvarez L, Cesteros Iturbe LC, Katime I (2013) Biodegradable chitosan nanogels crosslinked with genipin. Carbohydr Polym 94:836–842. https://doi.org/10.1016/j.carbpol.2013.01.082

134. Xu J, Ma L, Liu Y, et al (2012) Design and characterization of antitumor drug paclitaxel-loaded chitosan nanoparticles by W/O emulsions. Int J Biol Macromol 50:438–443. https://doi.org/10.1016/j.ijbiomac.2011.12.034

135. Yan E, Fu Y, Wang X, et al (2011) Hollow chitosan-silica nanospheres for doxorubicin delivery to cancer cells with enhanced antitumor effect in vivo. J Mater Chem 21:3147–3155. https://doi.org/10.1039/c0jm03234d

136. Park J-U, Jeong S-H, Song E-H, et al (2018) Acceleration of the healing

process of full-thickness wounds using hydrophilic chitosan–silica hybrid sponge in a porcine model. J Biomater Appl 32:1011–1023. https://doi.org/10.1177/0885328217751246

137. Mousavi SJ, Parvini M, Ghorbani M (2018) Experimental design data for the zinc ions adsorption based on mesoporous modified chitosan using central composite design method. Carbohydr Polym 188:197–212. https://doi.org/10.1016/j.carbpol.2018.01.105

138. Pipattanawarothai A, Suksai C, Srisook K, Trakulsujaritchok T (2017) Non-cytotoxic hybrid bioscaffolds of chitosan-silica: Sol-gel synthesis, characterization and proposed application. Carbohydr Polym 178:190–199. https://doi.org/10.1016/j.carbpol.2017.09.047

139. Budnyak TM, Pylypchuk I V., Tertykh VA, et al (2015) Synthesis and adsorption properties of chitosan-silica nanocomposite prepared by sol-gel method. Nanoscale Res Lett 10:1–10. https://doi.org/10.1186/s11671-014-0722-1

140. Pandis C, Madeira S, Matos J, et al (2014) Chitosan-silica hybrid porous membranes. Mater Sci Eng C 42:553–561. https://doi.org/10.1016/j.msec.2014.05.073

141. Wang D, Liu W, Feng Q, et al (2017) Effect of inorganic/organic ratio and chemical coupling on the performance of porous silica/chitosan hybrid scaffolds. Mater Sci Eng C 70:969–975. https://doi.org/10.1016/j.msec.2016.04.010

142. Luan PP, Jiang YJ, Zhang SP, et al (2014) Chitosan-mediated formation of biomimetic silica nanoparticles: An effective method for manganese peroxidase

immobilization and stabilization. J Biosci Bioeng 118:575–582. https://doi.org/10.1016/j.jbiosc.2014.05.003

143. Popat A, Liu J, Lu GQ, Qiao SZ (2012) A pH-responsive drug delivery system based on chitosan coated mesoporous silica nanoparticles. J Mater Chem 22:11173–11178. https://doi.org/10.1039/c2jm30501a

144. Nhavene EPF, da Silva WM, Trivelato Junior RR, et al (2018) Chitosan grafted into mesoporous silica nanoparticles as benznidazol carrier for Chagas diseases treatment. Microporous Mesoporous Mater 272:265–275. https://doi.org/10.1016/j.micromeso.2018.06.035

145. Liu Q, Xu M, Wang Y, et al (2017) Co-immobilization of Pd and Zn nanoparticles in chitosan/silica membranes for efficient, recyclable catalysts used in ullmann reaction. Int J Biol Macromol 105:575–583. https://doi.org/10.1016/j.ijbiomac.2017.07.081

146. Wu M, Li W, Zhang M, Tao K (2007) Preparation and Catalytic Performance of Ni-B Amorphous Alloy Supported by Chitosan/SiO_2. Acta Phys - Chim Sin 23:1311–1315. https://doi.org/10.1016/S1872-1508(07)60064-3

147. Mitra D, Li M, Kang ET, Neoh KG (2017) Transparent Copper-Loaded Chitosan/Silica Antibacterial Coatings with Long-Term Efficacy. ACS Appl Mater Interfaces 9:29515–29525. https://doi.org/10.1021/acsami.7b07700

148. Kadnikova EN, Kostić NM (2002) Oxidation of ABTS by hydrogen peroxide catalyzed by horseradish peroxidase encapsulated into sol–gel glass. J Mol Catal B Enzym 18:39–48. https://doi.org/10.1016/S1381-1177(02)00057-7

149. Córdoba A, Alasino N, Asteasuain M, et al (2015) Mechanistic evaluation of

hematin action as a horseradish peroxidase biomimetic on the 4-aminoantipyrine/phenol oxidation reaction. Chem Eng Sci 129:249–259. https://doi.org/10.1016/j.ces.2015.02.031

150. Olucha F, Martínez-García F, López-García C (1985) A new stabilizing agent for the tetramethyl benzidine (TMB) reaction product in the histochemical detection of horseradish peroxidase (HRP). J Neurosci Methods 13:131–138. https://doi.org/10.1016/0165-0270(85)90025-1

151. Shaner NC, Campbell RE, Steinbach PA, et al (2004) Improved monomeric red, orange and yellow fluorescent proteins derived from *Discosoma* sp. red fluorescent protein. Nat Biotechnol 22:1567–1572. https://doi.org/10.1038/nbt1037

152. Fiamingo A, Montembault A, Boitard S-E, et al (2016) Chitosan Hydrogels for the Regeneration of Infarcted Myocardium: Preparation, Physicochemical Characterization, and Biological Evaluation. Biomacromolecules 17:1662–1672. https://doi.org/10.1021/acs.biomac.6b00075

153. Qu B, Luo Y (2020) Chitosan-based hydrogel beads: Preparations, modifications and applications in food and agriculture sectors – A review. Int J Biol Macromol 152:437–448. https://doi.org/10.1016/j.ijbiomac.2020.02.240

154. Zhao H, Xu J, Lan W, et al (2013) Microfluidic production of porous chitosan/silica hybrid microspheres and its Cu(II) adsorption performance. Chem Eng J 229:82–89. https://doi.org/10.1016/j.cej.2013.05.093

155. Li W, Yuan R, Chai Y, et al (2008) Immobilization of horseradish peroxidase on chitosan/silica sol–gel hybrid membranes for the preparation of hydrogen peroxide biosensor. J Biochem Biophys Methods 70:830–837.

https://doi.org/10.1016/j.jprot.2007.11.010

156. Zhang D, Sun P, Li P, et al (2013) A magnetic chitosan hydrogel for sustained and prolonged delivery of *Bacillus calmette*–Guérin in the treatment of bladder cancer. Biomaterials 34:10258–10266. https://doi.org/10.1016/j.biomaterials.2013.09.027

157. Yagar H, Balkan U (2017) Entrapment of laurel lipase in chitosan hydrogel beads. Artif Cells, Nanomedicine, Biotechnol 45:864–870. https://doi.org/10.1080/21691401.2016.1182920

158. Dwamena AK, Woo SH, Kim CS (2020) Enzyme immobilization on porous chitosan hydrogel capsules formed by anionic surfactant gelation. Biotechnol Lett 42:845–852. https://doi.org/10.1007/s10529-020-02829-w

159. Bilal M, Rasheed T, Zhao Y, Iqbal HMN (2019) Agarose-chitosan hydrogel-immobilized horseradish peroxidase with sustainable bio-catalytic and dye degradation properties. Int J Biol Macromol 124:742–749. https://doi.org/10.1016/j.ijbiomac.2018.11.220

160. Manrich A, Galvão CMA, Jesus CDF, et al (2008) Immobilization of trypsin on chitosan gels: Use of different activation protocols and comparison with other supports. Int J Biol Macromol 43:54–61. https://doi.org/10.1016/j.ijbiomac.2007.11.007

161. Shimomura O, Johnson FH, Saiga Y (1962) Extraction, Purification and Properties of Aequorin, a Bioluminescent Protein from the *Luminous hydromedusan,*Aequorea. J Cell Comp Physiol 59:223–239. https://doi.org/10.1002/jcp.1030590302

162. Taniguchi K, Nomura K, Hata Y, et al (2007) The Si-tag for immobilizing proteins on a silica surface. Biotechnol Bioeng 96:1023–1029. https://doi.org/10.1002/bit.21208

163. Wang H, Wang Z, Liu G, et al (2020) Genetical Surface Display of Silicatein on *Yarrowia lipolytica* Confers Living and Renewable Biosilica-Yeast Hybrid Materials. ACS omega 5:7555–7566. https://doi.org/10.1021/acsomega.0c00393

164. Taniguchi K, Nomura K, Hata Y, et al (2007) The Si-tag for immobilizing proteins on a silica surface. Biotechnol Bioeng 96:1023–1029. https://doi.org/10.1002/bit.21208

APPENDIX I

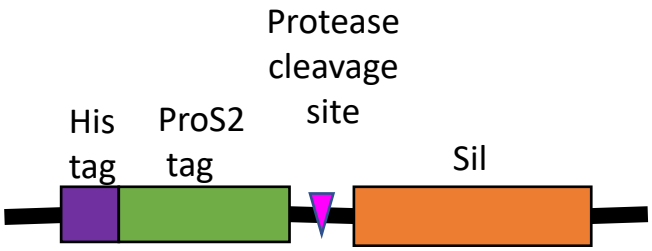

Silicatein

(His tag)-(ProS2 tag)-(protease cleavage site)-DYPEAVDWRTKGAVTAVKDQGDCGAS

YAFSAMGALEGANALAKGNAVSLSEQNIIDCSIPYGNHGCHGGNMYDAFLYVIANE

GVDQDSAYPFVGKQSSCNYNSKYKGTSMSGMVSIKSGSESDLQAAVSNVGPVSVAI

DGANSAFRFYYSGVYDSSRCSSSSLNHAMVVTGYGSYNGKKYWLAKNSWGTNWG

NSGYVMMARNKYNQCGIATDASYPTL-

Figure S 1: Schematic diagram and amino acid sequence of ProS2-Sil.

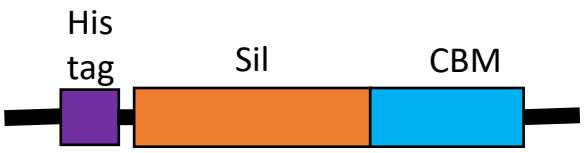

Silicatein
(His tag)-DYPEAVDWRTKGAVTAVKDQGDCGASYAFSAMGALEGANALAKGNAVS

LSEQNIIDCSIPYGNHGCHGGNMYDAFLYVIANEGVDQDSAYPFVGKQSSCNYNSKY

KGTSMSGMVSIKSGSESDLQAAVSNVGPVSVAIDGANSAFRFYYSGVYDSSRCSSSSL

NHAMVVTGYGSYNGKKYWLAKNSWGTNWGNSGYVMMARNKYNQCGIATDASYP

CBM
TLTPTKGATPTNTATPTKSATATPTRPSVPTNTPTNTPANTPVSGNLKVEFYNSNPSDT

TNSINPQFKVTNTGSSAIDLSKLTLRYYYTVDGQKDQTFWCDHAAIIGSNGSYNGITS

NVKGTFVKMSSSTNNADTYLEISFTGGTLEPGAHVQIQGRFAKNDWSNYTQSNDYSF

KSASQFVEWDQVTAYLNGVLVWGKEPGG-

Figure S 2: Schematic diagram and amino acid sequence of Sil-CBM.

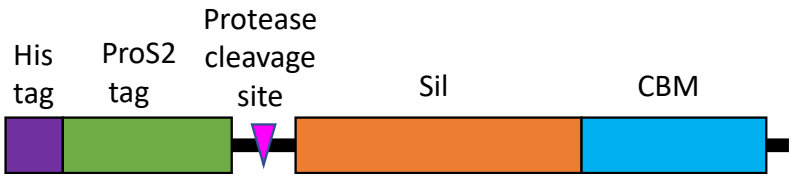

(His tag)-(ProS2 tag)-(protease cleavage site)-DYPEAVDWRTKGAVTAVKDQGDCGAS

Silicatein

YAFSAMGALEGANALAKGNAVSLSEQNIIDCSIPYGNHGCHGGNMYDAFLYVIANE

GVDQDSAYPFVGKQSSCNYNSKYKGTSMSGMVSIKSGSESDLQAAVSNVGPVSVAI

DGANSAFRFYYSGVYDSSRCSSSSLNHAMVVTGYGSYNGKKYWLAKNSWGTNWG

CBM

NSGYVMMARNKYNQCGIATDASYPTLTPTKGATPTNTATPTKSATATPTRPSVPTN

TPTNTPANTPVSGNLKVEFYNSNPSDTTNSINPQFKVTNTGSSAIDLSKLTLRYYYTV

DGQKDQTFWCDHAAIIGSNGSYNGITSNVKGTFVKMSSSTNNADTYLEISFTGGTLE

PGAHVQIQGRFAKNDWSNYTQSNDYSFKSASQFVEWDQVTAYLNGVLVWGKEPG

G-

Figure S 3: Schematic diagram and amino acid sequence of ProS2-Sil-CBM.

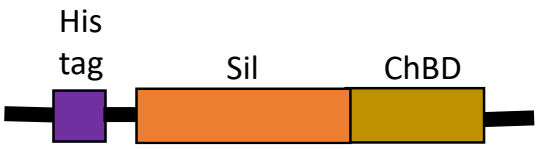

Silicatein

(His tag)-DYPEAVDWRTKGAVTAVKDQGDCGASYAFSAMGALEGANALAK

GNAVSLSEQNIIDCSIPYGNHGCHGGNMYDAFLYVIANEGVDQDSAYPFVGK

QSSCNYNSKYKGTSMSGMVSIKSGSESDLQAAVSNVGPVSVAIDGANSAFRF

YYSGVYDSSRCSSSSLNHAMVVTGYGSYNGKKYWLAKNSWGTNWGNSGY

ChBD

VMMARNKYNQCGIATDASYPTLAWQVNTAYTAGQLVTYNGKTYKCLQPHT

SLAGWEPSNVPALWQLQ

Figure S 4: Schematic diagram and amino acid sequence of Sil-ChBD.

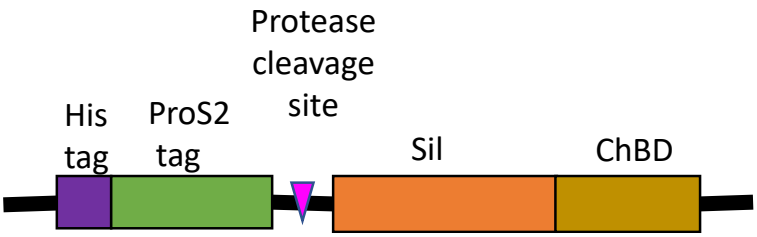

(His tag)-(ProS2 tag)-(protease cleavage site)-DYPEAVDWRTKGAVTAVKDQGDCGAS
Silicatein

YAFSAMGALEGANALAKGNAVSLSEQNIIDCSIPYGNHGCHGGNMYDAFLYVIANE

GVDQDSAYPFVGKQSSCNYNSKYKGTSMSGMVSIKSGSESDLQAAVSNVGPVSVAI

DGANSAFRFYYSGVYDSSRCSSSSLNHAMVVTGYGSYNGKKYWLAKNSWGTNWG

NSGYVMMARNKYNQCGIATDASYPTLAWQVNTAYTAGQLVTYNGKTYKCLQP
ChBD

HTSLAGWEPSNVPALWQLQ-

Figure S 5: Schematic diagram and amino acid sequence of ProS2-Sil-ChBD.

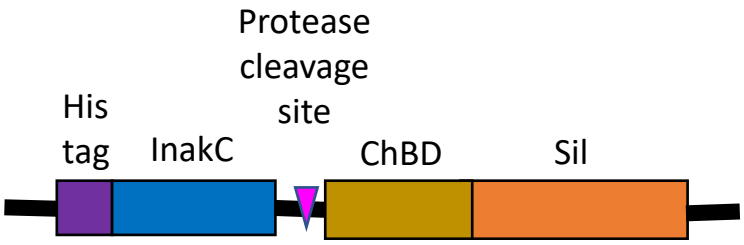

InakC

(His tag)-FRLWDGKRYRQLVARTGENGVEADIPYYVNEDDDIVDKPDEDDD

ChBD

WIEVKVSSIRVISVPVQPR-(protease cleavage site)-AWQVNTAYTAGQLVTYNGK

Silcatein

TYKCLQPHTSLAGWEPSNVPALWQLQDYPEAVDWRTKGAVTAVKDQGDCG

ASYAFSAMGALEGANALAKGNAVSLSEQNIIDCSIPYGNHGCHGGNMYDAF

LYVIANEGVDQDSAYPFVGKQSSCNYNSKYKGTSMSGMVSIKSGSESDLQAA

VSNVGPVSVAIDGANSAFRFYYSGVYDSSRCSSSSLNHAMVVTGYGSYNGK

KYWLAKNSWGTNWGNSGYVMMARNKYNQCGIATDASYPTL-

Figure S 6: Schematic diagram and amino acid sequence of InakC-ChBD-Sil.

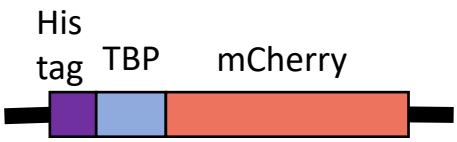

TBP mCherry

-(His tag)-RKLPDAPGMHTWVSKGEEDNMAIIKEFMRFKVHMEGSVNGHEFEIEGEGE

GRPYEGTQTAKLKVTKGGPLPFAWDILSPQFMYGSKAYVKHPADIPDYLKLSFPEGF

KWERVMNFEDGGVVTVTQDSSLQDGEFIYKVKLRGTNFPSDGPVMQKKTMGWEAS

SERMYPEDGALKGEIKQRLKLKDGGHYDAEVKTTYKAKKPVQLPGAYNVNIKLDIT

SHNEDYTIVEQYERAEGRHSTGGMDELYK

Figure S 7: Schematic diagram and amino acid sequence of TBP-mCherry.

APPENDIX II

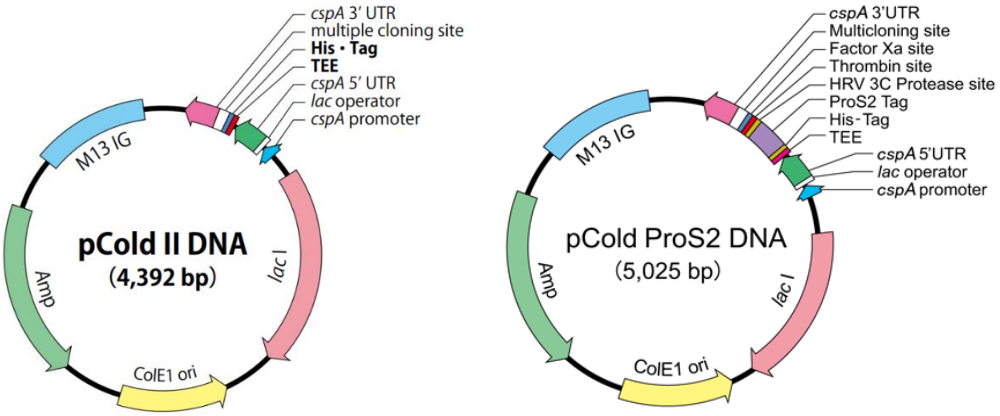

Figure S 8: Vectro map of pCold II and pCold ProS2 expesion vecters (images were tacken from Takarabio Inc.)

Source: https://catalog.takara-bio.co.jp/PDFS/3362_DS_j.pdf, https://www.takarabio.com/products/protein-research/expression-vectors-and-systems/protein-folding-kits/pcold-pros2-dna

M13 IG : Required during sequencing

Amp : Ampicillin resistance function

ColE1 ori : Starting point for replication

Lac I : Lac repressor

cspA promoter : Beginning of transcription

cspA 5'UTA : Function with structural stability at low temperature

cspA3'UTA : Function to induce ribosome trapping phenomenon

TEE : Function to promote translation

His-Tag : Used for purification of expressed proteins